พิร์โรลิดินิลเพปไทด์นิวคลีอิกแอซิดโพรบที่ติดฉลากไพรีนคู่

นายณัฐพล มณีลุน

วิทยานิพนธ์นี้เป็นส่วนหนึ่งของการศึกษาตามหลักสูตรปริญญาวิทยาศาสตรมหาบัณฑิต
สาขาวิชาเคมี ภาควิชาเคมี
คณะวิทยาศาสตร์ จุฬาลงกรณ์มหาวิทยาลัย
ปีการศึกษา 2556

DUAL-PYRENE-LABELED PYRROLIDINYL PEPTIDE NUCLEIC ACID PROBES

Mr. Nattapon Maneelun

A Dissertation Submitted in Partial Fulfillment of the Requirements

for the Degree of Master of Science Program in Chemistry

Department of Chemistry

Faculty of Science

Chulalongkorn University

Academic Year 2013

Thesis Title	DUAL-PYRENE-LABELED PYRROLIDINYL PEPTIDE NUCLEIC ACID PROBES
By	Mr. Nattapon Maneelun
Field of study	Chemistry
Thesis Advisor	Professor Tirayut Vilaivan, D.Phil.

Accepted by the Faculty of Science, Chulalongkorn University in Partial Fulfillment of the Requirements for the Master Degree

……...…....Dean of the Faculty of Science
(Professor Supot Hannongbua, Dr.rer.nat.)

THESIS COMMITTEE

…….……...Chairman
(Assistant Professor Warinthorn Chavasiri, Ph.D.)

…….…….....Thesis Advisor
(Professor Tirayut Vilaivan, D.Phil.)

……Examiner
(Associate Professor Mongkol Sukwattanasinitt, Ph.D.)

……External Examiner
(Chaturong Suparpprom, Ph.D.)

ณัฐพล มณีลุน: พิร์โรลิดินิลเพปไทด์นิวคลีอิกแอซิดโพรบที่ติดฉลากไพรีนคู่ (DUAL-PYRENE-LABELED PYRROLIDINYL PEPTIDE NUCLEIC ACID PROBES) อ.ที่ปรึกษาวิทยานิพนธ์หลัก: ศ. ดร. ธีรยุทธ วิไลวัลย์, 83 หน้า.

ในงานวิจัยนี้มีจุดมุ่งหมายในการออกแบบพีเอ็นเอโพรบชนิดใหม่ที่สามารถเปลี่ยนการเรืองแสงจากเอกซิเมอร์เป็นมอนอเมอร์เพื่อใช้ในการตรวจสอบลำดับเบสของดีเอ็นเอ โดยได้สังเคราะห์พิร์โรลิดินิลเพปไทด์นิวคลีอิกแอซิดที่มีโครงสร้างหลักเป็น α,β-ไดเพปไทด์ (acpcPNA) และติดฉลากไพรีน 2 โมเลกุลเข้าที่โครงสร้างหลักในตำแหน่งที่จำเพาะเจาะจง ในสภาวะสายเดี่ยว acpcPNA โพรบที่ติดฉลากไพรีนคู่จะพับตัวเพื่อให้ส่วนของไพรีนหลีกหนีจากสิ่งแวดล้อมที่มีขั้วของสารละลาย ทำให้เกิดสัญญาณฟลูออเรสเซนส์ของไพรีนเอกซิเมอร์ที่ 470 นาโนเมตร เมื่อเกิดการเข้าคู่กับดีเอ็นเอเป้าหมาย ทำให้เกิดโมเลกุลเกลียวคู่ของพีเอ็นเอ·ดีเอ็นเอ ทำให้ไพรีนทั้งสองถูกแยกออกจากกันส่งผลให้เกิดสัญญาณฟลูออเรสเซนส์ของไพรีนมอนอเมอร์ที่ 380 นาโนเมตร ค่าอัตราส่วนการสวิตซ์ได้ถูกนำเสนอเพื่อวัดประสิทธิภาพของ acpcPNA โพรบที่ติดฉลากไพรีนคู่ โดยสามารถหาค่านี้ได้จากอัตราส่วนมอนอเมอร์ต่อเอกซิเมอร์ของพีเอ็นเอที่เข้าคู่กับดีเอ็นเอ [F_{380}/F_{470}(ds)] หารกับอัตราส่วนดังกล่าวของพีเอ็นเอสายเดี่ยว [F_{380}/F_{470}(ss)] โพรบที่มีค่าอัตราส่วนการสวิตซ์มากแสดงว่ามีประสิทธิภาพมาก ซึ่งอัตราส่วนการสวิตซ์ของโพรบทั้งหมดที่สังเคราะห์ได้มีค่าอยู่ระหว่าง ~5-30 โดยค่าอัตราส่วนที่มากที่สุด ~30 เป็นของลำดับเบสไทมีนล้วนที่ติดฉลากด้วยไพรีนบิวทิลในระยะห่าง 5 เบส พีเอ็นเอลำดับเบสผสมจะให้อัตราส่วนที่ต่ำอยู่ในช่วง ~5-8 โดยโพรบเหล่านี้สามารถจำแนกความต่างแตกระหว่างดีเอ็นเอคู่สมกับดีเอ็นเอที่มีลำดับเบสผิดไป 1 ตำแหน่งได้อย่างดี ผลการทดลองแสดงว่าพิร์โรลิดินิลเพปไทด์นิวคลีอิกแอซิดโพรบที่ติดฉลากไพรีนคู่นี้มีศักยภาพในการตรวจลำดับเบสดีเอ็นเอได้ นอกจากนี้ยังได้นำไปประยุกต์ใช้เป็นโพรบในการติดตามการแทรกตัวของพีเอ็นเอเข้าไปในดีเอ็นเอสายคู่

ภาควิชา เคมี ลายมือชื่อนิสิต.....

สาขาวิชา เคมี ลายมือชื่อ อ.ที่ปรึกษาวิทยานิพนธ์หลัก.....

ปีการศึกษา 2556

##5372242023: MAJOR CHEMISTRY
KEYWORDS: acpcPNA / PYRENE / EXCIMER / PROBE / DNA DETECTION

NATTAPON MANEELUN: DUAL-PYRENE-LABELED PYRROLIDINYL PEPTIDE NUCLEIC ACID PROBES. ADVISOR: PROF. TIRAYUT VILAIVAN, D.Phil., 83 pp.

The main objective of this research is to design a new excimer-monomer switching fluorescence PNA probe for DNA sequence detection. Pyrrolidinyl peptide nucleic acid bearing an α,β-dipeptide backbone (acpcPNA) deriving from D-prolyl-2-aminocyclopetane carboxylic acid was synthesized and site-specifically labeled at the backbone with two pyrene units. In single stranded form, the dual pyrene-labeled acpcPNA probe folded itself to bury the pyrene labels from the hydrophilic aqueous environment, resulting in the excimer emission at 470 nm. After hybridization with target DNA, the PNA·DNA duplex formed and the pyrene labels were forced away from each other, resulting in the monomer emission at 380 nm. To evaluate the efficiency of dual pyrene-labeled acpcPNA probe, the switching ratio was introduced. This was defined as a ratio of the monomer to excimer emissions in the double strand [F_{380}/F_{470}(ds)] divided by the single strand [F_{380}/F_{470}(ss)] forms. The higher the switching ration, the more efficient is the probe. The switching ratios of ~5-30 were observed for all acpcPNA probes. The best ratio of ~30 was obtained in a homothymine sequence with the pyrenebutyl labels located 5-base apart of pyrenes. Lower switching ratios ~5–8 were observed with mix-base DNA sequences. Excellent discrimination between complementary and single mismatched DNA targets was achieved for all probes. The results showed that these dual pyrene-labeled acpcPNA probes are potentially useful for DNA sequence determination. An application of the probe in monitoring the DNA duplex invasion by acpcPNA was also demonstrated.

Department: Chemistry Student's Signature.....

Field of Study: Chemistry Advisor's Signature.....

Academic Year: 2013

ACKNOWLEDGEMENTS

I would like to initially thank to my master thesis advisor, Prof. Dr. Tirayut Vilaivan, for his guidance throughout the master studying, and all the tremendous work involved in supervising me. In addition, he served as undergraduate research mentor to me to introduce me into a research setting. He has always expressed an enthusiastic approach to chemistry, and I owe any future successful to his influence. Moreover, I would like to thank Assist. Prof. Dr. Warinthorn Chavasiri, Assoc. Prof. Dr. Mongkol Sukwattanasinitt, and Dr. Chaturong Suparpprom for their interest, value suggestions, comments as committee members, and thesis examiners.

The Organic Synthesis Research Unit has been pivotal in complete my master, especially, Miss Chalothorn Boonlua, who had been my trainer and spent many hours in my research. Moreover, I would like to thank the members of the Organic Synthesis Research Unit at the Department of Chemistry, Chulalongkorn University for all helps and their encouragement me. In addition, I would like to acknowledge the Thailand Research Fund (RTA5280002) for financial support.

I would like to express my deepest gratitude to my parents and family for their love, kindness, encouragement, and financial support throughout my life. Finally, I would like to fully thank the Development and Promotion of Science and Technology Project (DPST) for financial support and inspiration for the scientific pathway.

CONTENTS

Page

LIST OF TABLES

LIST OF FIGURES

Page

Page

Page

Page

Page

Page

LIST OF SCHEME

LIST OF ABBREVIATIONS AND SYMBOLS

γCD	Gamma cyclodextrin
^{o}C	Degree celcius
μL	Microliter
μM	Micromolar
A	Adenine
A^{Bz}	N^6-benzoyladenine
Ac	Acetyl
Ac_2O	Acetic anhydride
Boc	*tert*-butoxycarbonyl
Bz	Benzoyl
C	Cytosine
calcd	Calculated
C^{Bz}	N^4-benzoylcytosine
CCA	α-cyano-4-hydroxy cinnamic acid
DBU	1,8-diazabicyclo[5.4.0]undec-7-ene
DIAD	Diisopropylazodicarboxylate
DIEA	Diisopropylethylamine
DMF	*N,N'*-dimethylformamide
DNA	Deoxyribonucleic acid
[DNA]	Concentration of DNA
ds	double strand
equiv	equivalent (s)
expt	experiment
excit	excitation
Fmoc	9-fluorenylmethoxycarbonyl
FRET	fluorescence resonance energy transfer
G	Guanine
G^{Ibu}	N^2-isobutyrylguanine
HATU	*O*-(7-azabenzotriazol-1-yl)-*N,N,N',N'*-tetramethyluronium hexafluorophosphate
HOAt	1-hydroxy-7-azabenzotriazol

HPLC	high performance liquid chromatography
Ibu	Isobutyryl
Lys	Lysine
MALDI-TOF	matrix-assisted laser desorption/ionization-time of flight
MeOH	Methanol
mg	Milligram
mL	Milliliter
mM	Millimolar
MS	mass spectrometry
m/z	mass to charge ratio
nm	Nanometer
Pfp	Pentafluorophenyl
PNA	Peptide nucleic acid
[PNA]	Concentration of PNA
TFA	trifluoroacetic acid
T_m	melting temperature
t_R	retention time

CHAPTER I

INTRODUCTION

Deoxyribonucleic acid (DNA), first discovered in 1869 by Friedrich Miescher, is a kind of macromolecule in living organisms which plays extremely important roles in the storage of genetic information. The smallest subunits of DNA are called nucleotides. It consists of three parts: sugar (deoxyribose), phosphate and nucleobase. The backbone of DNA consists of a deoxyribose phosphate ester (shown in black in **Figure 1.1**). The nucleobase is the important part for encoding the genetic information (blue in **Figure 1.1**). The genetic information is encoded in the base sequence of the DNA. DNA consists of four nucleotide bases: adenine (A), thymine (T), cytosine (C) and guanine (G). Certain pairs of bases can interact to each other in a complementary fashion *via* specific hydrogen bondings according to the famous Watson-Crick's base-pairing rules (red dashed line in **Figure 1.1**). Adenine (A) pairs with thymine (T) through two hydrogen bondings while cytosine (C) and guanine (G) pairs to each other via three hydrogen bondings. Accordingly, DNA exists in nature as a duplex consisting of two strands with "complementary" base sequences.

A small change in the base sequence can totally change the structure of proteins deriving from the gene. The change is called "mutation". While mutation is important in evolution, it may also result in malfunctioned proteins which cause genetically-related diseases. As a result, the ability to accurately determine the DNA sequence is very important. The ability of DNA to specifically pair with the other strand in a complementary fashion allows the determination of its sequence by the use of a hybridization probe. To detect the hybridization event, some mechanisms for signal transduction must be incorporated to allow measurement. Examples of measurable signals include electrochemical signal, fluorescence, surface plasmon resonance etc. This is often achieved by incorporating a suitable label to the probe. A good detection process must be able to differentiate between the complementary and mismatched DNA with high sensitivity and specificity.

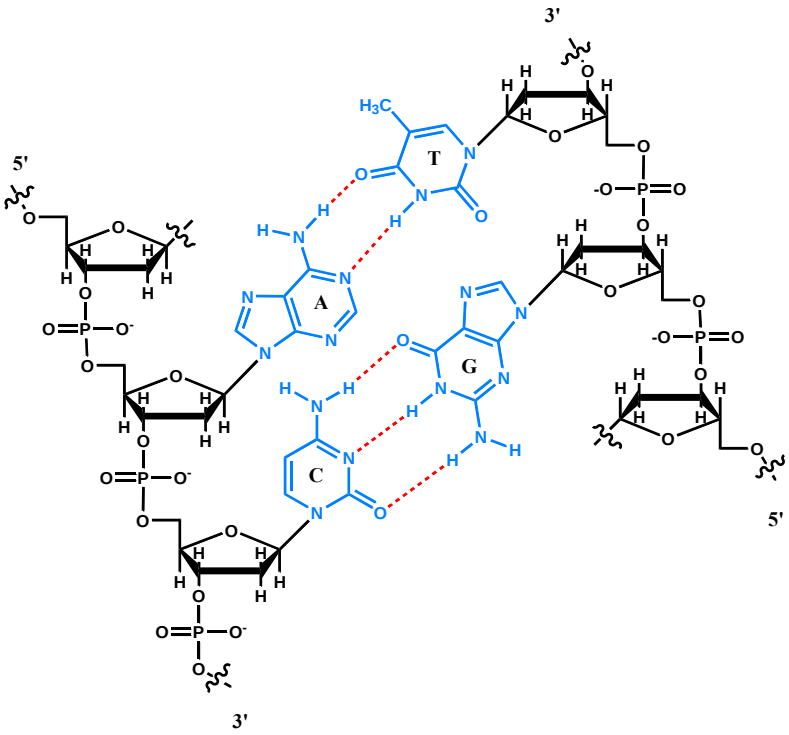

Figure 1.1 Structure and base pairing of DNA.

Peptide nucleic acid (PNA) is a structural mimic of DNA obtained by replacing the deoxyribosephosphate backbone with polyamide. In 1991, the first PNA with *N*-(2-aminoethyl)-glycine backbone was introduced by Neilsen et al [1, 2]. Four nucleotide bases were attached to the PNA backbone through methylene carbonyl linkages (**Figure 1.2**). Instead of 5'- and 3'- termini, PNA has an amino (*N*-) and carboxyl (*C*-) termini instead. PNA can hybridize to complementary DNA following the Watson-Crick's rule. Not only PNA can bind with complementary DNA to form a stable hybrid, but it also binds with higher selectivity than DNA itself. Because PNA has no negative charge in the backbone, the unfavorable Coulombic repulsion is absent in PNA·DNA hybrids (**Figure 1.3**). The high selectivity means that complementary PNA·DNA hybrids are much more stable than the mismatched PNA·DNA hybrids [2].

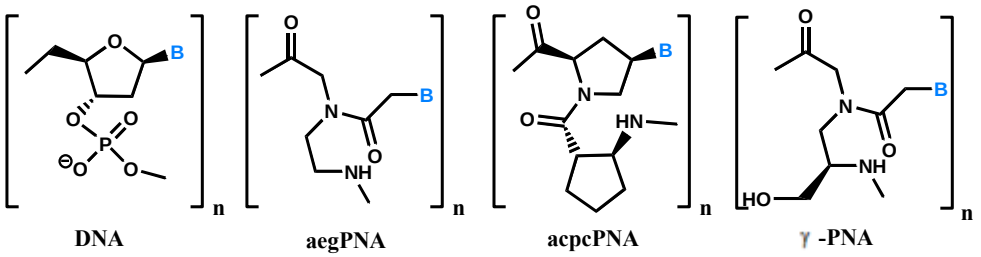

Figure 1.2 Structures of DNA and some PNA.

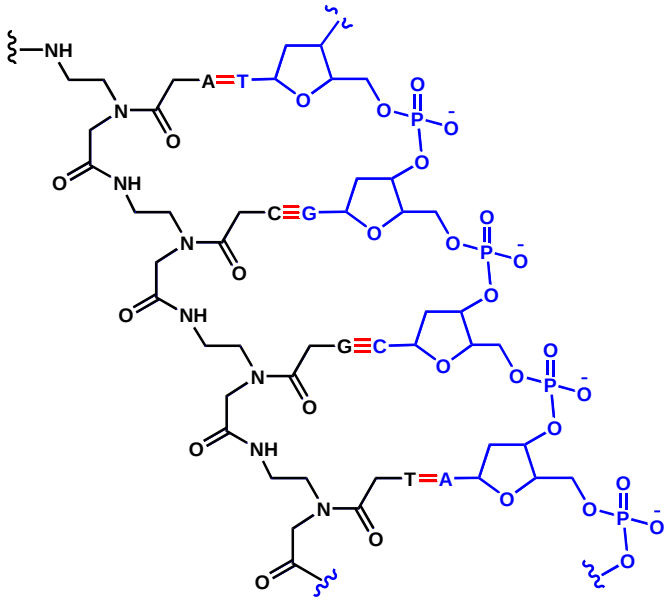

Figure 1.3 Hybridization between aegPNA and DNA.

In addition to the charge, PNA exhibits many different properties from DNA. It is completely resistant to nucleases and proteases. The stability of PNA·DNA hybrids is much less dependent to salt concentration than DNA·DNA hybrids. From these advantages, PNA can have applications in several areas including therapeutic, diagnostic and as molecular tools for DNA manipulation. In 2005, Vilaivan et al have studied the new conformationally constrained pyrrolidinyl PNA system based on a D-

prolyl-2-aminocyclopentanecarboxylic acid backbone (**Figure 1.2**). This new system, which is known as acpcPNA, hybridizes to complementary DNA with higher affinity and specificity than the original aegPNA [3,4]. It also strongly prefers binding to DNA in antiparallel fashion (**Figure 1.4**). Another example of new PNA includes γ-PNA developed by Ly et al (**Figure 1.2**) [5,6]. The substituent at the γ-position of aegPNA backbone strongly pre-organizes the PNA structure in such a way that the binding affinity to DNA is significantly improved. These new PNA have potentials for much wider range of applications than the original aegPNA.

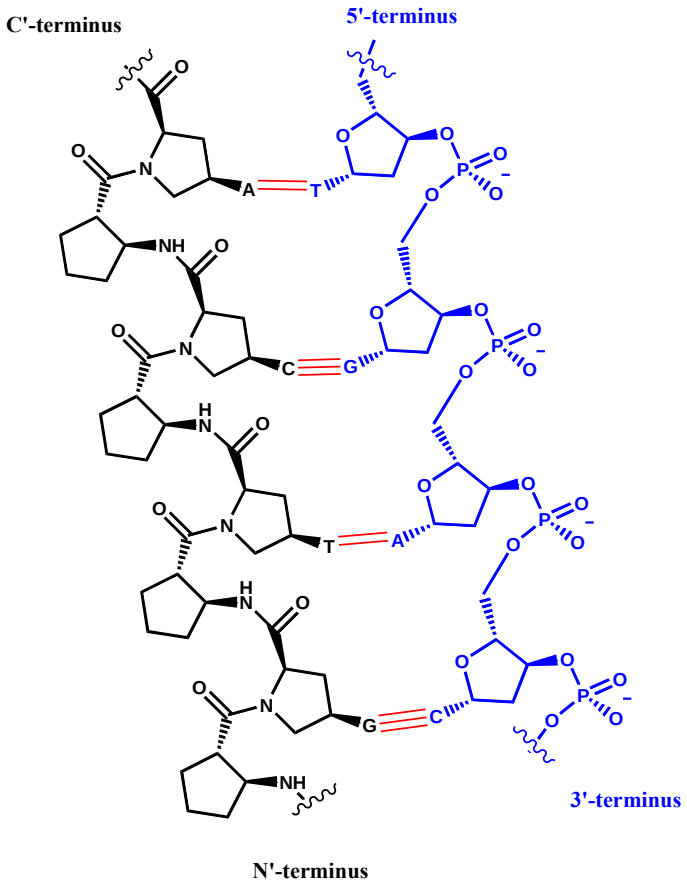

Figure 1.4 Hybridization between acpcPNA and DNA in antiparallel fashion.

DNA and analogues like LNA and PNA have found widespread uses as probes for DNA sequence detection. Fluorescence is among the most popular techniques for signal transduction. To report the hybridization event, the probe must show distinct signals in response to the binding with the DNA target. An example is a self-reporting probe that can yield different fluorescent signals as the free probe and after binding with the DNA target. One popular of such self-reporting probe is a molecular beacon (MB) that it is obtained by attaching a fluorophore and a quencher at opposite ends of an oligonucleotide strand (**Figure 1.5**) [7,8]. Each termini of the probe was designed to have a partial complementary sequence so that it can form a "stem" structure. The middle part of the MB contains the recognition sequence that can specifically bind to the DNA target. Consequently, in the absence of a DNA target, MB forms a stem-loop structure through base pairing between the two ends. This conformation forces the fluorophore and the quencher in close contact and the fluorescent signal is quenched by energy transfers from donor molecule (fluorophore) to acceptor molecule (quencher) by various mechanisms including static quenching and/or fluorescence resonance energy transfer (FRET). The FRET efficiency depends on the distance between the two fluorophores/chromophores [9-11]. Hence, MB in the free-state exhibits a low fluorescence. Hybridization of the MB and a complementary DNA target results in separation of the fluorophore and quencher. Since the distance between the fluorophore and the quencher is now large, no quenching or FRET is possible. This will result in fluorescence increase.

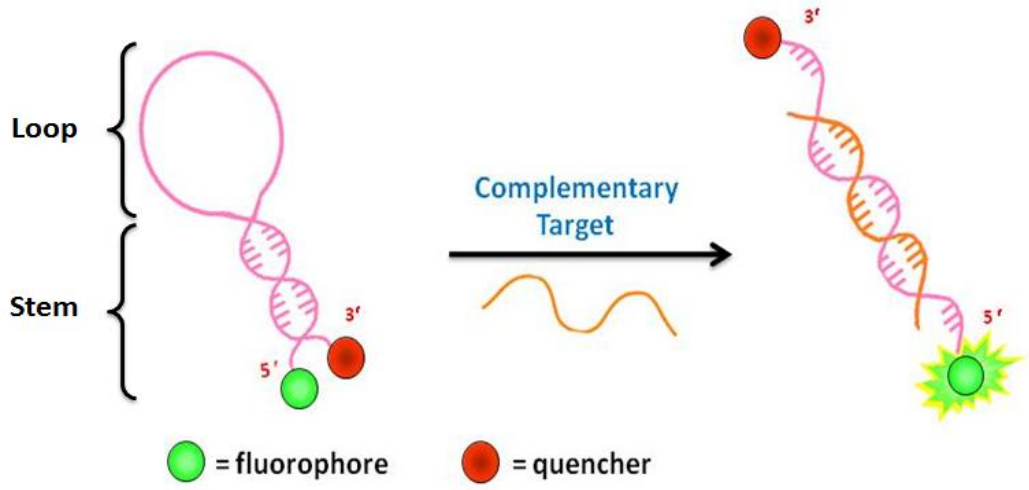

Figure 1.5 The principle of molecular beacon (MB).

In more recent examples, guanine or other nucleobases may act as a quencher and thus a quencher is not required, which simplifies the design and synthesis of the MB further [12,13]. In addition to molecular beacon, binary probes (BP) have been designed for DNA sequence detection. BP consists of two oligonucleotide probes, each labeled with a fluorophore at the end of the molecule (**Figure 1.6**) [14]. The two probes must be complementary to the adjacent positions of the DNA target. Upon binding to form a ternary complex, the two fluorophores are interacting with each other to give a detectable signal. For instance, Shimadzu et al designed a binary probe based on a FRET between pyrene and perylene. After two probes binds with complementary DNA, exciting the pyrene donor result in emission of the perylene acceptor via FRET and thus the perylene fluorescence was observed instead of the pyrene [15].

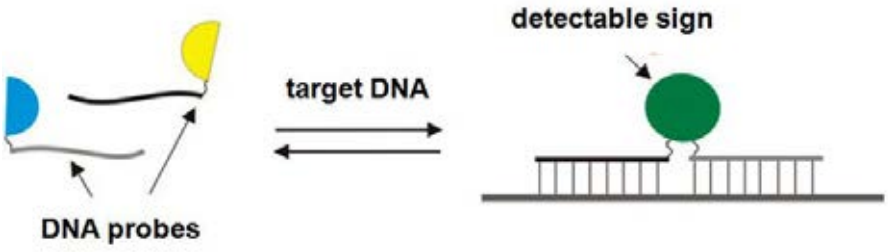

Figure 1.6 The principle of binary probe (BP).

The principle of FRET can be used to create MB that can change fluorescence color in addition to intensity. In 2010, Wagenknect et al. had introduced pyrene and nile red as fluorophores into the stem of a DNA molecular beacon via an ethynyl liker at the position 5 of 2'-deoxyuridine [16]. In free MB, excitation at the pyrene wavelength result in energy transfer to the nile red, thus red fluorescence was observed. After adding the target DNA in sub-stoichiometric quantities, the white or blue fluorescence were observed due to a mix fluorescence of free pyrene (blue) and FRET from pyrene to nile red (red). Pure blue pyrene fluorescence was observed after complete hybridization (**Figure 1.7**).

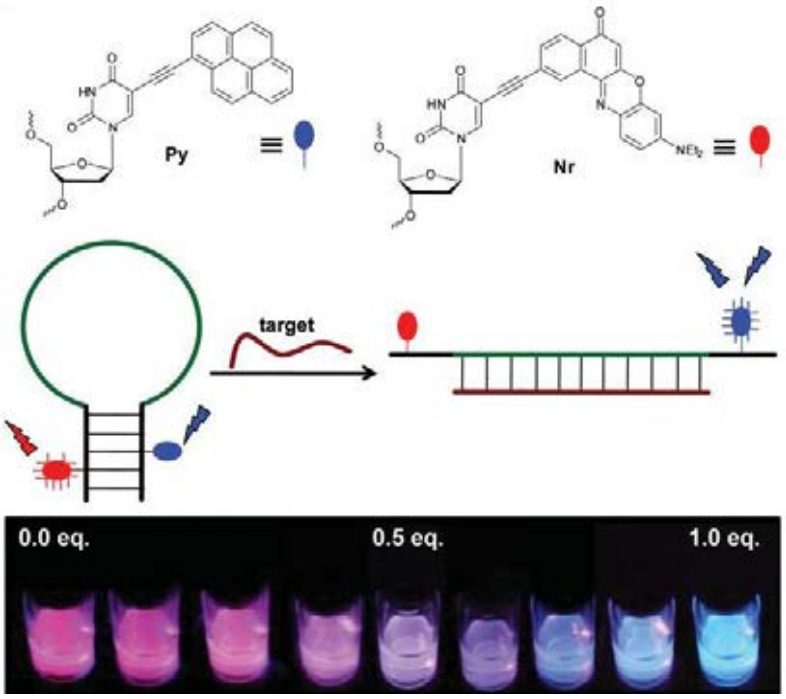

Figure 1.7 The red-white-blue fluorescence of Wagenknect's MB [16].

In addition to quenching and FRET, other popular types of interactions between fluorophores that had been employed for DNA sequence detection is on the formation of excimer or exciplex. Fluorophore dimer can form via dipole-dipole or pi-stacking, which results in a smaller gap between highest occupied molecular orbital (HOMO) and lowest unoccupied molecular orbital (LUMO) and thus emission at longer wavelength. [17] Pyrene is the most frequently studied system for excimer formation [18]. Pyrene excimer emission appears as a broad, featureless band at 480 nm (green light) which is very different from the monomer emission at 370 nm (blue light). The large difference together with the extremely long fluorescence lifetime of pyrene excimer makes excimer-monomer switching an attractive means for signaling the hybridization. Consequently, there are many reports about hybridization probes and molecular beacons based on this principle [19-25]. For example, DNA probe with two pyrenes attached can form excimer as the free probe or in the presence of

mismatched DNA targets. But hybridization with the target DNA resulted in pyrene monomer emission or total quenching due to intercalation of the pyrene into the DNA duplex (**Figure 1.8**) [19].

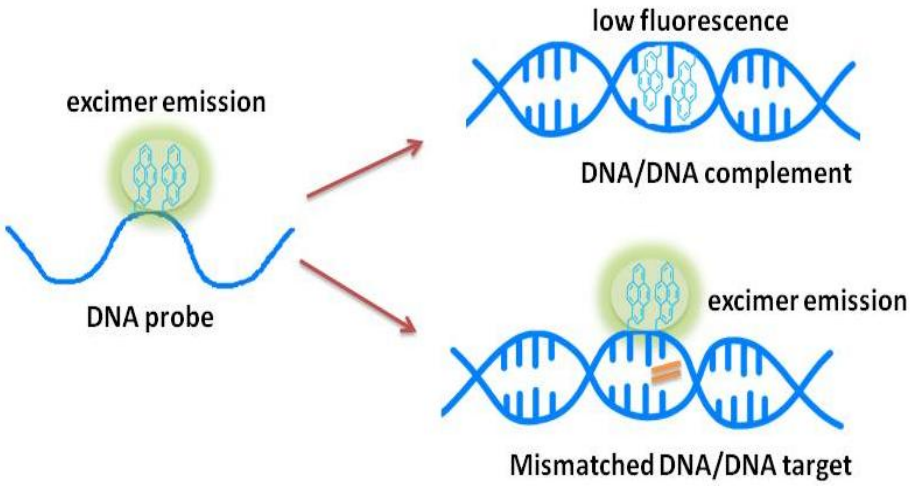

Figure 1.8 The dual pyrene labeled on DNA probe.

In another related work, a DNA beacon with two pyrene labels at each terminus was reported by **Inouye** [20]. In the stem-loop conformation, the pyrene excimer emission was observed because the two pyrenes could interact with each other to form the excimer. After binding with the target DNA, the two pyrene moieties were separated by the duplex formation. As a result, the monomer fluorescence was detected (**Figure 1.9**). As a binary probe example, Kool et al. had labeled an oligonucleotide probe with pyrene at 5'-end and the other with pyrene at 3'end (**Figure 1.10**). Upon binding to the adjacent positions on the DNA target, blue-to-green fluorescence was observed due to the excimer formation.[21].

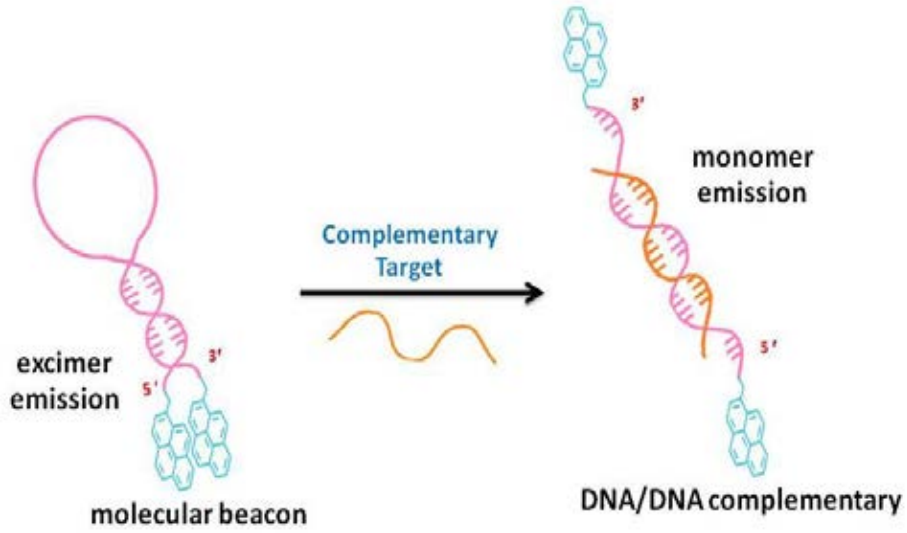

Figure 1.9 DNA MB based on pyrene excimer.

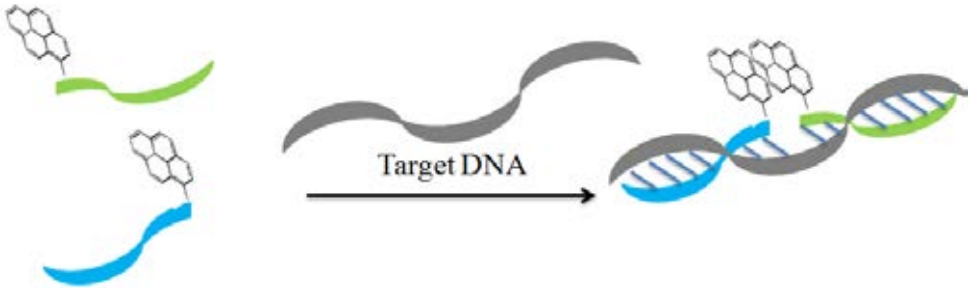

Figure 1.10 Binary probes based on pyrene excimer.

In another work involving pyrene-labeled oligonucletide probe, Haralambidis et al had designed pyrene polyamide-modified oligonucleotide as a probe to detect DNA in 1995 [22]. In 2002, Nokano et al. had studied a hybridization probe labeled with two pyrene units at the 5'-end and at an internal position of oligonucleotide probes. They found that the terminally-labeled probe gave a better monomer/excimer switching than the internally-labeled probe after hybridization with DNA. In the internally-labeled probe, the pyrenes interacted with the nucleobases, which resulted in increasing monomer and decreasing excimer fluorescence [23]. In 2007, Tan et al had designed molecular beacon containing two pyrene units at the 5' terminus and 3'

terminus labeled with DABCYL as a quencher. In stem-loop conformation, no fluorescence signal was observed because of the quenching by DABCYL. After hybridization with target DNA, the stem-loop form was opened and the two pyrene units were separated from the quencher, resulting in an increased pyrene excimer fluorescence [24].

PNA is very interesting as a probe for DNA diagnosis because of its higher affinity and selectivity than DNA. In recent years, PNA probes labeled with two fluorophore/quencher or two different fluorophores have been developed into MB [25]. The stem-loop structure is not required for PNA-based because PNA probe usually folds itself into a compact shape in the aqueous environment. This folding forces the fluorophore and the quencher to be in close proximity. In this dissertation, we are interested in developing a fluorescence PNA probe that can exhibit distinctive fluorescence change upon binding to the correct DNA target and free probe based on the pyrene excimer-monomer switching principle. Such probes should be useful for DNA sequence detection. To the best of our knowledge, no PNA-based pyrene excimer probe had been reported.

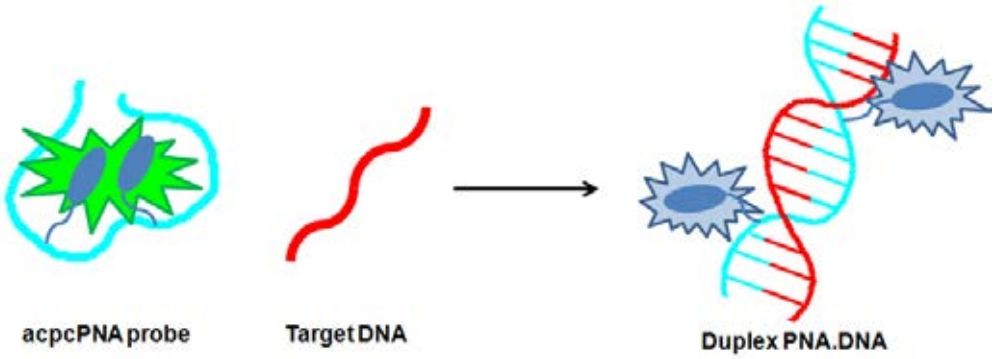

Figure 1.11 The hypothesis of dual pyrene-labeled acpcPNA probe.

In our design, dual pyrene-labeled acpcPNA will be developed as an excimer-monomer switching probe. In the single stranded form, the probe should adopt a

compact structure that allows close contact between the two pyrene chromophores resulting in excimer emission. After hybridization with the target DNA, the two pyrene labels will be forced apart, resulting in the decrease in excimer and increase in monomer emissions (**Figure 1.11**). Stability and selectivity of the probe will be investigated by melting temperature (T_m), UV-Vis and fluorescence studies. The effects of the type of the linker between the pyrene and the acpcPNA backbone, as well as the distance between the two pyrene labels will be studied. The generality of the design will be evaluated in different sequence contexts.

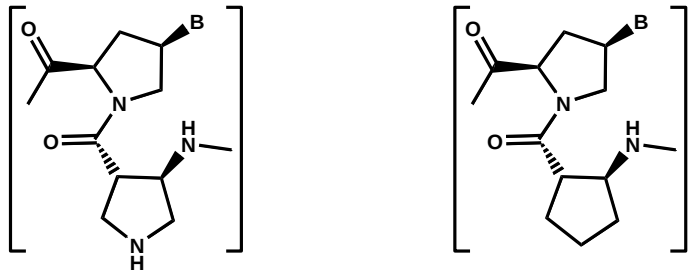

Figure 1.12 APC-modified acpcPNA and acpcPNA.

The method developed by Suparprom et al. will be used for attachment of the pyrene labels [26]. According to this method, the acpcPNA should be first modified by replacement of ACPC spacer with (3*R*,4*S*)-3-aminopyrrolidine-4-carboxylic acid (APC) to form the APC-modified acpcPNA (**Figure 1.12**). The pyrene labels can then be attached to the pyrrolidine nitrogen atom of the APC spacer by acylation or reduction alkylation [27].

CHAPTER II
EXPERIMENTAL

2.1 Chemicals

AR grade solvents were used for all reactions unless specified otherwise. 1-Pyrenebutyric acid was obtained from Fluka, 1-pyreneacetic acid and 1-pyrenecarboxylic acid were purchased from Aldrich. 1-Pyrenebutyraldehyde was supplied by Dr. Tirayut Vilaivan. TentaGel S RAM Fmoc resin (Fluka) was used as solid support for manually peptide synthesis. Anhydrous *N*,*N*-dimethyl formamide (DMF) for solid phase peptide synthesis was obtained from RCI Labscan (Thailand) and dried over 4A molecular sieves before use. The protected amino acid Fmoc-L-Lys(Boc)-OPfp was obtained from Calbiochem Novabiochem (USA). Piperidine, trifluoroacetic acid (TFA), 1,8-diazabicyclo[5.4.0]undec-7-ene (DBU), sodium cyanoborohydride ($NaBH_3CN$), *O*-(7-azabenzotriazol-1-yl)-*N,N,N',N'*-tetramethyluronium hexafluoro-phosphate (HATU) and *N,N*-diisopropylethylamine (DIEA) were obtained from Fluka. 1-Hydroxy-7-azabenzotriazole (HOAt) was purchased from GLBiochem (China). Nitrogen gas (99.9%) was obtained from Thai Industrial Gas (Thailand). MilliQ water was obtained from ultrapure water system with Millipak® 40 filter unit 0.2 μm Millipore (USA). α-Cyano-4-hydroxy cinnamic acid (CCA) used as a matrix for MALDI-TOF mass spectrometry was obtained from Fluka. Oligonucleotides were purchased from Pacific Science Co.,Ltd. (Thailand) or BioDesign Co.,Ltd. (Thailand).

2.2 Synthesis of pyrrolidinyl peptide nucleic acid (acpcPNA)

2.2.1 Pyrrolidynyl PNA monomers, ACPC spacer and APC spacer

The four Fmoc-protected, Pfp-activated pyrroldinyl PNA monomers (Fmoc-A^{Bz}-OPfp, Fmoc-C^{Bz}-OPfp, Fmoc-G^{Ibu}-OH, Fmoc-C^{Bz}-OPfp and Fmoc-T-OPfp) and ACPC spacer were synthesized by Dr. Chalotorn Boonlua, Dr. Woraluk Mansawat and Ms. Boonsong Ditmangklo according to the literature protocol [3,4]. The

Fmoc/Tfa-protected APC spacer (3*R*,4*S*)-1-(2,2,2-trifluoroacetyl)-3-(9*H*-fluoren-9-yl-methoxycarbonyl amino)-pyrrolidine-4-carboxylic acid pentafluorophenyl ester for PNA modification was synthesized as described by Suparpprom and co-workers [26]. The structures of all monomers are shown in **Figure 2.1**.

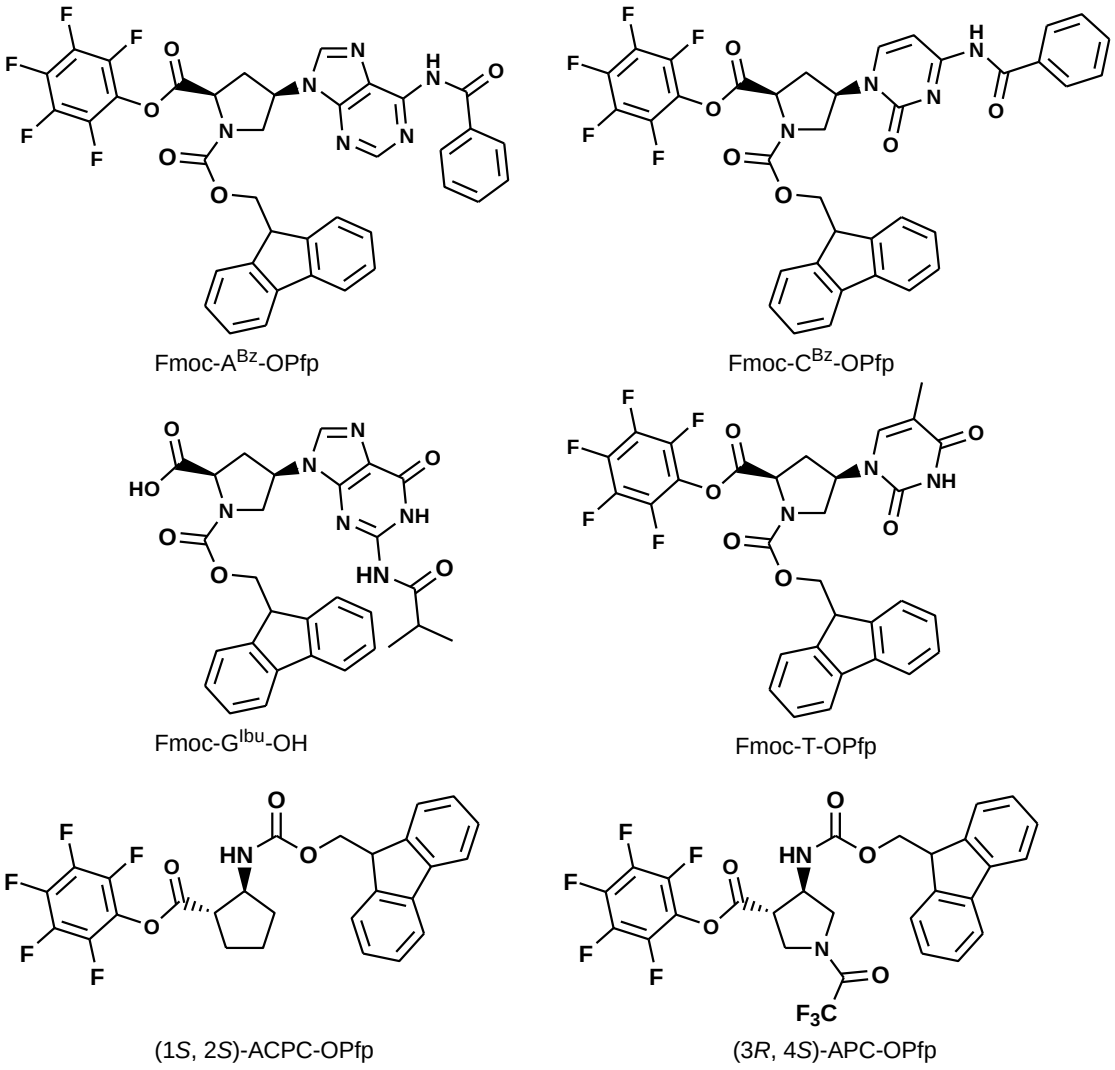

Figure 2.1 Structures of pyrrolidinyl PNA monomers and spacers used for the solid phase peptide synthesis.

2.2.2 Solid phase synthesis of APC-modified acpcPNA

All APC-modified PNAs were synthesized by Fmoc-solid phase peptide synthesis on a Tentagel S-RAM resin at 1.5 μmol scale exactly as described in the literature [26, 28, 29]. One lysine residue was included at each of the *C*- and *N*-terminus for increasing the solubility of the PNA in water.

2.2.3 Modification at nitrogen atom of APC spacer with pyrene derivatives

Tha APC-modified PNA was divided to 3 parts (each part is 0.5 μmol) while it was still on the solid support and have all protecting groups attached. The Fmoc group on the *N*-terminal lysine residue was removed and the free amino group was acetylated (details). The nucleobase protecting groups (Bz for A and C, Ibu for G) and APC spacer protecting group (Tfa) were simultaneously removed by heating with 1:1 aqueous ammonia/dioxane in a screw cap test tube at 60 ^{o}C for 12 hours.

- coupling with pyrene carboxylic derivatives

Pyrene carboxylic acid derivatives (1-pyrenebutyric acid, 1-pyreneacetic acid and 1-pyrenecarboxylic acid) were coupled to the deprotected pyrrolidine nitrogen atom of the APC spacer via an amide bond formation reaction. The deprotected PNA resin (0.5 μmol) was pre-swollen in DMF for 5 min and with a mixture of the pyrene carboxylic acid (6 μmol, 12 equiv.), HATU (2.2 mg, 6 μmol) and 30 μL of coupling solution (7% DIEA in anhydrous DMF) for 1 h at room temperature. The coupling was repeated twice and the progress was monitored by MALDI-TOF MS after cleavage of some PNA samples from the solid support using trifluoroacetic acid (TFA).

- coupling with pyrene aldehyde derivatives

Pyrene aldehyde derivatives (1-pyrenebutyraldehyde and 1-pyrencarboxaldehyde) were coupled to the deprotected pyrrolidine nitrogen atom of the APC spacer by reductive alkylation [27]. The deprotected PNA resin (0.5 μmol) was treated with a mixture of the pyrenealdehydes (15 μmol, 30 equiv.), HOAc (2 μL, 30 μmol, 60 equiv.), $NaBH_3CN$ (1.8 mg, 30 μmol, 60 equiv.) and methanol (100 μL)

for 12 h at room temperature at least 12 h. The coupling was repeated twice and the progress was monitored by MALDI-TOF MS as above.

2.2.4 Cleavage and purification of PNA oligomers

The PNA was cleaved from the resin by trifluoroacetic acid containing 10% triisopropylsilane as previously described [30]. HPLC experiments were carried out on Water Delta 600^{TM} system equipped with gradient pump and Water 996^{TM} photodiode array detector. An ACE M8-AR HPLC column (4.6 x 150 mm, 5 μ particle size) was used for both analytical and preparative purposes. The crude PNA was dissolved in 120 μL MilliQ water and centrifuged to remove any precipitate before HPLC purification. The HPLC purification and analysis were performed in a reverse phase mode, eluting with a gradient system of 0.1% trifluoroacetic acid in methanol and MilliQ water. The gradient system consisted of two solution systems that are solvent A (0.1% trifluoroacetic acid in MilliQ water) and solvent B (0.1% trifluoroacetic acid in methanol). The gradient started from A:B at 90:10 for the first 5 min and then increased linearly to 10:90 over 60 min. The peaks were monitored at by UV absorbance at 260 nm. Fractions containing the pure PNA (according to MALDI-TOF MS analysis) were combined and freeze dried to obtain the purified PNA.

2.2.5 Characterization of PNA by MALDI-TOF MS analysis

All PNA oligomers were characterized by MALDI-TOF mass spectrometry. All samples were prepared by mixing around 1 μL of PNA samples with 10 μL of matrix solution containing CCA in 0.1% trifluoroacetic acid in acetonitile:water (1:2) solution and deposited on MALDI target. The acpcPNA mass spectra were performed on Microflex MALDI-TOF mass spectrometry (Bruker Daltonics) and recorded in a linear positive ion mode with accelerating voltage 25 kV. The observed masses were compared with the calculated mass obtained from an in-house PNA molecular weight calculator web application developed by Dr. Tirayut Vilaivan (http://www.chemistry.sc.chula.ac.th/pna).

2.2.6 Determination of PNA concentration

The concentration of the modified PNA was measured on a CARY 100 UV-Visible spectrophotometer (Varian, Australia). The stock PNA was diluted with 10 mM phosphate buffer pH 7.0 to give a measurable absorbance at 260 nm. The absorbance of the original stock was then calculated and the concentration was obtained from Beer's Law. Extinction coefficients (ε) of PNAs were calculated from sum of individual extinction coefficients (ε) that directly corresponded from nucleobase and fluorophore. The individual extinction coefficients at 260 nm used in the calculation were ε(A) = 10.8 $mM^{-1}.cm^{-1}$, ε(C) = 7.4 $mM^{-1}.cm^{-1}$, ε(G) = 11.5 $mM^{-1}.cm^{-1}$, ε(T) = 8.8 $mM^{-1}.cm^{-1}$, ε(pyrene) = 13.3 $mM^{-1}.cm^{-1}$. In practice, the extinction coefficients were calculated using the in-house web application developed by Dr. Tirayut Vilaivan (http://www.chemistry.sc.chula.ac.th/pna).

2.3 Studies of PNA·DNA hybridization

2.3.1 Sample preparation

The sample was prepared in a 10 mm quartz cell with a Teflon stopper by mixing calculated amount of stock PNA and DNA with the phosphate buffer stock (pH 7.0) to give the final concentration of the buffer = 10 mM after adjusting the volume to 1000 μL with degassed MilliQ water.

2.3.2 T_m experiments

Melting temperature (T_m) was measured on a CARY 100 UV-Visible spectrophotometer (Varian, Australia) equipped with a thermal melt system. The sample was equilibrated at the stating temperature for 10 min. The absorbance at 260 nm (A_{260}) was measured from 20 to 90 ^oC (block temperature) with a temperature ramp of 1^oC/min. The recorded temperature was corrected by an equation obtained

from comparison of the block temperature with the true temperature according to the built-in temperature probe.

Corrected temperature and normalized absorbance are defined as follows.

$$\text{Corrected Temp.} = (0.9696 \times T_{block}) - 0.8396$$

$$\text{Normalized Abs} = Abs_{obs} / Abs_{init}$$

The absorbance was normalized by dividing the value each temperature with the initial absorbance. The melting temperature was carried out from first derivative plot after smoothing with KaliedaGraph 3.6 (Synergy Software). Data analysis was performed on a computer using Microsoft Excel XP (Microsoft Corp.).

2.3.3 UV-Vis experiments

All UV-Vis experiments were carried out on a CARY 100 UV-Visible spectrophotometer (Varian, Australia) equipped with a thermal melt system. Unless otherwise specified, the temperature was not controlled.

2.3.3 Fluorescence experiments

Fluorescence spectra were measured on a Cary Eclipse Fluorescence Spectrophotometer (Varian, Australia). The excitation and emission slit were set to 5 nm and the photomultiplier (PMP) tube voltage were set to an appropriate value that will give a response in the range of 100–1000 unit. The excitation wavelength was fixed at 350 nm. Unless otherwise specified, the temperature was not controlled.

2.3.4 Circular dichroism (CD) spectroscopy

CD spectra were recorded on a JASCO Model J-815 spectrometer (Japan). The spectra were collected at 20 ^{o}C from 200 nm to 500 nm with scanning speed 200 nm/min and averaged 4 times then subtracted from a spectrum of the blank under the same condition.

2.3.5 Photographing

The samples were prepared by mixing the PNA and the DNA stock and buffer to give in the required final concentration (typically 10 μM for PNA and 12 μM for DNA) in 10 mM phosphate buffer (pH 7.0) with a total volume of 10 μL. The photograph was taken under black light (405 nm) in a dark room by a digital camera (Canon PowerShot SX110 IS) in manual mode (ISO 80, F4.0, shutter speed 1 sec.).

CHAPTER III
RESULTS AND DISCUSSION

The original peptide nucleic acid (PNA) was first introduced by Nielsen *et al* in 1991 [1,2]. In the structure of PNA, the DNA backbone was replaced with *N*-(2-aminoethyl)-glycine unit, hence it was named as "aegPNA". PNA hybridizes with DNA following Watson-Crick base pairing rule. Many advantages of PNA over DNA such as the abilities to form hybrids with higher stability, selectivity, specificfity and resistance to enzymes attracted interests from many scientists to move into PNA field and began contributing innovation to this research area. One of the most widespread applications of PNA is in the area of DNA sequence diagnosis. This dissertation focused on designing a new fluorescent PNA probe which can provide distinguishable fluorescence in the presence of target DNA and non-target DNA. This kind of probe should be useful for DNA sequence detection in homogeneous format. Most of fluorescence PNA probes reported to date was based on the original aegPNA of Nielsen. In recent years, the chiral PNA with prolyl-2-aminocyclopentane-carboxylic acid alpha/beta-dipeptide backbone (acpcPNA) have been introduced by Vilaivan *et al* [3]. This PNA system showed superior properties than aegPNA in many aspects, for instance thermal stability, specificity and non self-pairing ability [4]. Fluorescent acpcPNA probes have been actively studied by Vilaivan's group in the past few years [30]. All works focused on singly labeled acpcPNA probes including quencher free PNA beacon and base discrimination fluorescent PNA probes. No excimer forming probes based on acpcPNA and other PNA systems had been described before. Accordingly, this dissertation was dedicated to the design and performance evaluation of excimer forming probe based on acpcPNA. Pyrene was selected as the excimer forming fluorophores because pyrene excimer exhibits a large Stoke's shift and long fluorescence lifetime. Two pyrene moieties were covalently incorporated onto the backbone of pyrrolidinyl acpcPNA previously modified at pre-determined positions with 3-aminopyrrolidine-4-carboxylic acid (APC-spacer) following the strategy introduced by Suparpprom *et al* [26]. The dual-pyrene labeled acpcPNAs were

expected to form excimer in single strand state due to hydrophobic folding that forced the two pyrene molecules to be in close proximity. In the presence of the correct DNA target, the base pairing forced the two pyrene labels away from each other, resulting in emission of the fluorescence signal due to pyrene monomers.

3.1 Synthesis of pyrene-modified acpcPNA

The excimer forming acpcPNA probes were designed by incorporating two pyrene fluorophores onto the backbone of acpcPNA previously modified with two APC spacers. The two APC spacers substituted the usual ACPC-spacers at various positions in the PNA backbone to provide different distances between the two pyrene labels (1-6 and 9 bases). The pyrene molecules were covalently attached at the two APC spacer positions via acylation or reductive alkylation chemistry that had been previously reported by Ditmangklo et al [27]. Various pyrene labels with different linker length and type of modification were chosen to investigate the behavior of different pyrene labels in excimer formation. The effects of distance between the two pyrenes were examined with the aim to maximize the excimer/monomer switching. The pyrene amide derivatives (PyCO, PyAc and PyBtr) were made by coupling of the pyrene labels to the APC spacer via acylation with an appropriate pyrenecarboxylic acid to form the amide linkage. The alkyl derivative (PyBtl) were introduced onto the acpcPNA through reductive alkylation

3.1.1 Modification of pyrene carboxylic acid and aldehyde derivatives onto acpcPNA.

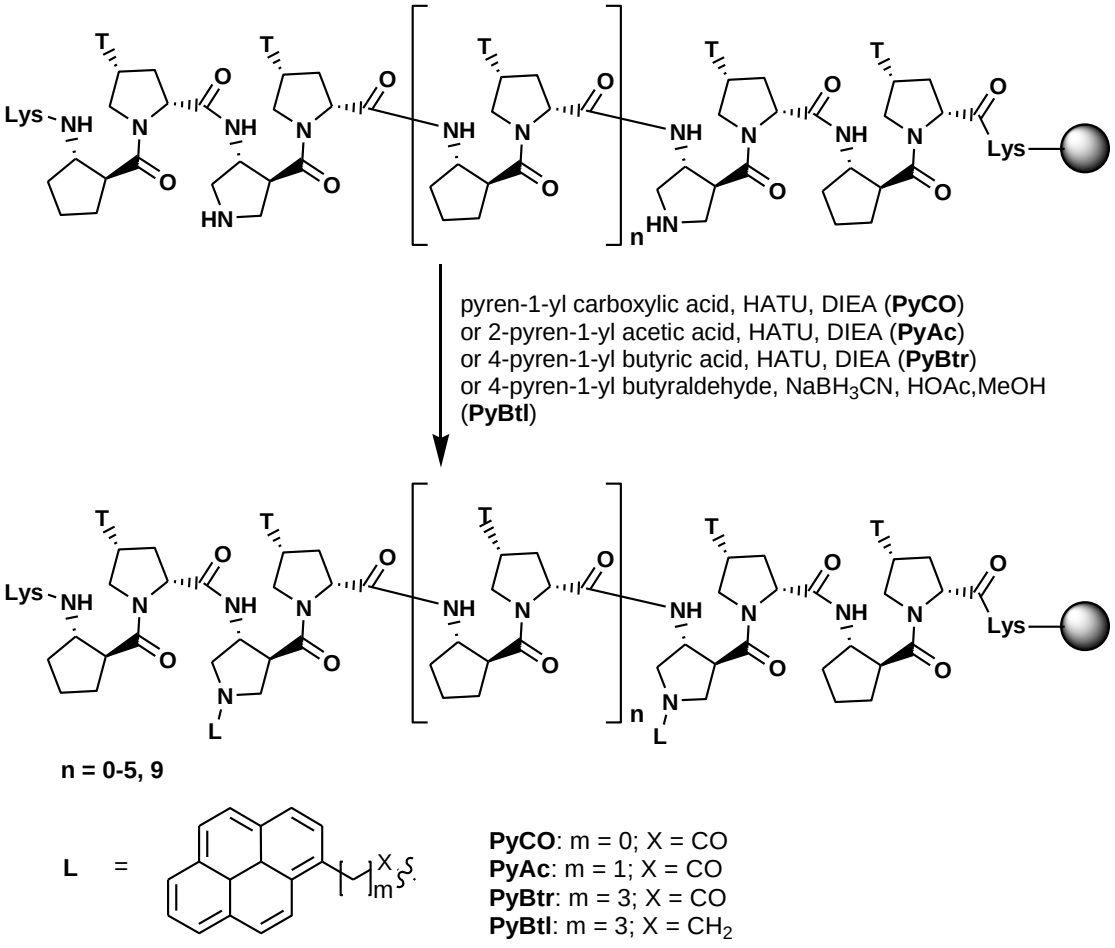

Scheme 1. Synthesis of doubly-pyrene-functionalized acpcPNA.

All dual pyrene-labeled acpcPNA were modified with two lysines at each terminal to provide sufficient solubility in water. The strategy for labeling pyrene at the internal position of acpcPNA backbone started with substitution of the conventional ACPC-spacer with two 3-aminopyrrolidinyl-4-carboxylic acid (APC) monomers bearing a trifluoroacetyl protecting group at the pyrrolidine nitrogen atom [26,27]. After the synthesis of the acpcPNA carrying the two APC spacers was achieved, the Fmoc protecting group on the last lysine was deprotected and the free

amino terminus was capped with acetic anhydride. Subsequently, all nucleobase protecting groups as well as the trifluoroacetyl group at the APC spacer were removed by treatment with 1:1 aqueous ammonia:dioxane at 60^{o}C overnight to give the free 2^{o}-amino group of the APC spacers. Pyrene carboxylic acid derivatives were further reacted with the deprotected PNA via acylation to give an amide linkage by using HATU/DIEA as activators. The reaction progress was monitored by MALDI-TOF mass spectrometry. Three derivatives of pyrene carboxylic acid were used in this study to examine how the flexibility of the linker affected the excimer forming capability. These include 1-pyrenebutyric acid (PyBtr), 1-pyreneacetic acid (PyAc) and 1-pyrenecarboxylic acid (PyCO).

In addition to the pyrenecarboxylic derivative, two pyrenealdehydes namely 1-pyrenecarboxaldehyde and 1-pyrenebutyraldehyde were also selected to functionalize the acpcPNA backbone. These pyreneadehydes were incorporated onto the acpcPNA through reductive alkylation at the deprotected 2^{O} nitrogen atom of the APC spacer by using $NaBH_3CN$ and acetic acid in methanol following the reported procedure [27]. Its progress was also monitored with MALDI-TOF mass spectrometry.

3.1.2 Cleavage, purification and identification of all synthesized acpcPNA

When the coupling reactions were completed, the labeled acpcPNA probes were cleaved from the solid support (Tenta Gel S-RAM resin) using 10% triisopropylsilane (TIS) in trifluoroacetic acid. The synthesized acpcPNA probes were purified by reverse phase HPLC. The purified probes were characterized by MALDI-TOF mass spectrometry and the purity as certained by reverse phase HPLC analysis. In all cases, the PNA were obtained in purity >90% except for the case of 1-pyrenemethyl obtained from the reaction of 1-pyrenecarboxaldehyde, which could not be purified from the incompletely labeled products. The sequence, retention time, calculated mass, observed mass and isolated yield of all dual pyrene-labeled acpcPNA probes successfully synthesized are shown in **Table 3.1**.

Table 3.1 Sequences and yield of modified PNA obtained after HPLC purification.

PNA	Sequence N → C	t_R (min)	*m/z* (calcd)	*m/z* (found)	%yield
1BPBr	Ac-Lys-TTTTT^{PyBtr}T^{PyBtr}TTT-Lys	36.5	3850.24	3848.81	5.53
2BPBr	Ac-Lys-TTTT^{PyBtr}TT^{PyBtr}TTT-Lys	36.3	3850.24	3851.07	2.28
3BPBr	Ac-Lys-TTT^{PyBtr}TTT^{PyBtr}TTT-Lys	37.0	3850.24	3851.36	1.89
4BPBr	Ac-Lys-TT^{PyBtr}TTTT^{PyBtr}TTT-Lys	37.0	3850.24	3851.59	5.82
5BPBr	Ac-Lys-TT^{PyBtr}TTTTT^{PyBtr}TT-Lys	37.0	3850.24	3852.08	1.75
3BPAc	Ac-Lys-TTT^{PyAc}TTT^{PyAc}TTT-Lys	35.7	3794.08	3796.37	1.29
3BPCO	Ac-Lys-TTT^{PyCO}TTT^{PyCO}TTT-Lys	33.6	3766.08	3766.96	5.11
3BPBt	Ac-Lys-TTT^{PyBtl}TTT^{PyBtl}TTT-Lys	35.3	3822.27	3826.54	5.76
4BPBt	Ac-Lys-TT^{PyBtl}TTTT^{PyBtl}TTT-Lys	35.0	3822.27	3823.72	7.94
5BPBt	Ac-Lys-TT^{PyBtl}TTTTT^{PyBtl}TT-Lys	35.5	3822.27	3824.88	4.82
6BPBt	Ac-Lys-T^{PyBtl}TTTTTT^{PyBtl}TT-Lys	36.6	3822.27	3823.94	2.98
9BPBt	Ac-Lys-^{PyBtl}TTTTTTTTT^{PyBtl}-Lys	35.8	3933.27	3935.58	0.54
MBS1	Ac-Lys-AGTC^{PyBtl}ACACA^{PyBtl}CTG-Lys	32.7	4845.37	4847.48	2.90
MBS2	Ac-Lys-AGTT^{PyBtl}ATCCC^{PyBtl}TGC-Lys	33.0	4827.34	4830.55	1.10
MBS3	Ac-Lys-TGAT^{PyBtl}TCACT^{PyBtl}TAT-Lys	33.5	4865.39	4864.28	2.84

3.2 Thermal stability

Thermal stability was studied by measurement of melting temperature (T_m) experiment by UV-Vis spectrophotometry. In this technique, the duplex maximum absorption at 260 nm was monitored at different temperature from 20-90^oC. When the temperature is increased, the duplex oligomer denatures by breaking of the hydrogen bond between the nucleobases. This results in separation of the duplex into two random coiled strands that exhibited around 10-20% hyperchromicity relative to the duplex. The intensity at 260 nm is plotted with temperature to give a sigmoidal curve. The melting temperature is defined as the temperature at which an equilibrium state

between double-stranded and single strand of oligonucleotide take place. The first derivative of the S-curve was carried out to identify the *Tm* value from the maximum of the first derivative plot. T_m values can be used to estimate the binding affinity and specificity of the probe to the target. T_m values of all doubly pyrene-labeled acpcPNA are shown in **Table 3.2**.

Table 3.2 The T_m profile of all acpcPNA.

PNA	DNA sequences 5' → 3'	T_m (°C)
1BPBr	AAAAAAAAA	-
2BPBr	AAAAAAAAA	-
3BPBr	AAAAAAAAA	-
4BPBr	AAAAAAAAA	-
5BPBr	AAAAAAAAA	-
3BPAc	AAAAAAAAA	-
3BPCO	AAAAAAAAA	-
3BPBt	AAAAAAAAA	-
	AAAA<u>C</u>AAAA	-
	AAAA<u>G</u>AAAA	-
	AAAA<u>T</u>AAAA	-
4BPBt	AAAAAAAAA	44.5
	AAAA<u>C</u>AAAA	36.0
	AAAA<u>G</u>AAAA	42.8
	AAAA<u>T</u>AAAA	40.5
5BPBt	AAAAAAAAA	54.7
	AAAA<u>C</u>AAAA	42.0
	AAAA<u>G</u>AAAA	40.0
	AAAA<u>T</u>AAAA	32.0
6BPBt	AAAAAAAAA	46.2
	AAAA<u>C</u>AAAA	43.1
	AAAA<u>G</u>AAAA	42.3
	AAAA<u>T</u>AAAA	42.5
9BPBt	AAAAAAAAA	61.7
MBS1	CAGTGTGTGACT	43.3
	CAGTG<u>A</u>GTGACT	-
	CAGTGTG<u>A</u>GACT	-
MBS2	GCACCCATAACT	53.5
	GCACCC<u>C</u>TAACT	-

Table 3.2 The T_m profile of all acpcPNA (continue).

PNA	DNA sequences 5' → 3'	T_m (^oC)
MBS3	ATAATGTAACTA	57.8
	ATAATCTAACTA	40.6
	ATATTGTAACTA	46.3

3.2.1 Thermal stability of homothymine dual-pyrene-labeled acpcPNA probes

The nine bases homothymine acpcPNA (T_9) was selected as a model system for optimization of the type and distance between the two pyrene labels in all experiments because it is the simplest and shortest sequence that can exhibit a good thermal stability (T_m = 80.0^{o}C) upon hybridization with complementary DNA (dA_9) in comparison with others [27]. All novel excimer forming acpcPNA probes were investigated for the duplex stability and specificity by melting temperature experiments. The results showed that the chemical linkage and distance of the two pyrenes have significant effects on the PNA·DNA duplex stability. In chemical linkage comparison, all amide linkages showed no T_m whereas most of amine linkages exhibited T_m values that were considerably lower than the unmodified homothymine acpcPNA (**Table 3.2**). It meant that pyrene moieties decrease the stability hybrids regardless of the type and length of the linkage. The mixture of *cis*- and *trans*- amide rotamers in case of the amide-type linkers, appeared to decrease the stability of the duplex more than the flexible alkylamino linkage. For the flexible amine bond, no T_m could be observed at three-base separation (and presumably shorter distances too). This could be explained by the π-π stacking that stabilize the two pyrenes chromophores and the single stranded form, but destabilize the duplex form, of acpcPNA. The terminal doubly pyrene labeled acpcPNA probe **9BPBt** showed the highest T_m value, indicating that the terminal pyrene labels had only little affected on the stability of PNA·DNA hybrid.

3.2.2 Thermal stability of mix-bases acpcPNA probes

Three mix-base 12 mers acpcPNA probes were designed for studying of the more general behavior of the acpcPNA-based excimer forming probes. All mix-base acpcPNA probes synthesized carry the two pyrenebutyl labels at five bases distance because this system was shown to be the most effective for the T9 sequence. All results showed that mix-base acpcPNA probes were able to hybridize with their complementary targets as shown by the T_m values of 43.3, 53.5 and 57.8^oC for **MBS1**, **MBS2** and **MBS3** respectively. Single base mismatch PNA·DNA duplexes gave much lower T_m than the complementary PNA·DNA duplexes as shown in **Table 3.2**. The higher T_m of perfectly matched PNA·DNA indicated the high specificity of the dual pyrene-labeled acpcPNA probes.

3.3 Optical properties of excimer forming acpcPNA probes

3.3.1 UV-Vis absorption of excimer forming acpcPNA probes

UV-Vis absorption spectra of all homothymine acpcPNA incorporating two pyrene labels were firstly investigated in both single stranded form and as duplexes with complementary and single base mismatched DNA. The UV-Vis spectra of single stranded doubly pyrene-labeled acpcPNA exhibited a pyrene absorption peak with a λ_{max} at 345 nm and two smaller peaks at 330 and 320 nm. The shape of the pyrene absorption bands are similar to single strand DNA modified with pyrene at the backbone [30]. In the complementary PNA·DNA duplexes, UV-Vis spectra showed a small but noticeable red-shift of λ_{max} by 5 nm with a small hypochromism. The single base mismatch duplexes showed smaller change relative to the complementary duplexes. As an example, UV-Vis spectra of **3BPBtr** are shown in **Figure 3.1**. Raw UV-Vis spectra are included in the appendices.

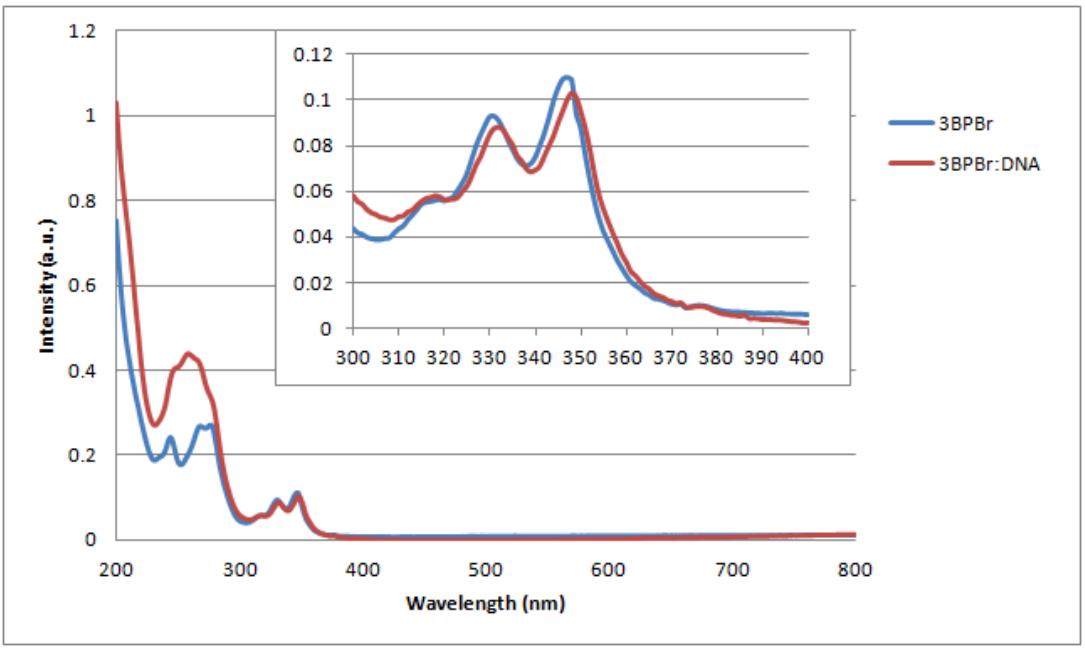

Figure 3.1 UV-Vis spectrum of 3BPBtr in the present of target DNA (red line) and without (blue line), [3BPBr] = 2.5 μM, [DNA] = 3.0 μM and [phosphate buffer] = 10 mM.

3.3.2 Fluorescence property of homothymine acpcPNA probes

Fluorescence spectra of all doubly pyrene-labeled acpcPNA probes and their DNA hybrids were measured in 10 mM sodium phosphate buffer pH 7.0 and excited at 350 nm [31]. The fluorescence spectra of most single stranded doubly pyrene-labeled acpcPNA exhibited monomer bands with vibrational fine structures at 380, 398 and 420 nm and an excimer band at 470 nm [17]. After adding the DNA target, the fluorescence spectra changed as shown by a decrease in the intensity of the excimer and an increase in the intensity of the monomer bands. According to our hypothesis the dual-pyrene labeled acpcPNA probes should display mainly the excimer in the absence of DNA the target due to the folding of the PNA strand that forced the two pyrene units in close proximity. After adding the complementary DNA, the probes would hybridize to form a rigid PNA·DNA duplex that will separate the two pyrene units by exposing them to the surrounding aqueous environment. This

fits nicely with the results. To quantitatively compare the switching behaviors of different probes, the ratio of monomer to excimer (M/E ratio) was calculated by dividing the fluorescence intensity at 380 nm (monomer emission) by the intensity at 470 nm (excimer emission). Only the intensities change at 380 and 470 nm were used for calculation of the excimer-monomer ratio because they were the maxima of monomer and excimer emissions, respectively. The switching ratio of each probe was obtained by dividing the M/E ratio of the probe after hybridization by the M/E ratio of the single stranded probe.

3.3.2.1 Effects of distance between the two pyrene units to fluorescence properties of dual pyrenebutyryl-labeled acpcPNA probes

The two pyrenebutyryl label were successfully incorporated into acpcPNA with a T9 sequence at distances ranging from 1-5 bases following acylation chemistry that generated amide linker as previously reported [26,27]. The M/E ratios of single strand doubly-pyrenebutyryl labeled acpcPNA probes were 0.43, 0.27, 0.43, 0.96 and 1.38 for the distance of 1, 2, 3, 4 and 5 bases respectively. The M/E ratios of the corresponding duplexes were 0.48, 0.62, 1.19, 1.91 and 3.13 respectively. The M/E ratios of the free probes are clearly related to the distance between the two pyrene chromophores. If the distance is large, the two pyrene labels would be far from each other and the monomer emission was predominant. At smaller distance (1-3 bases), the excimer became the major species as shown by the M/E ratios of less than unity. When compared with double-stranded forms, switching ratios of 1.10, 2.26, 2.75, 1.99 and 2.26 were obtained for the distances of 1 to 5 bases, respectively. The **3BPBr** with three-base separation provided the best switching ratio of 2.75. The values are shown in **Figure 3.2** and raw fluorescence spectra are included in the appendices.

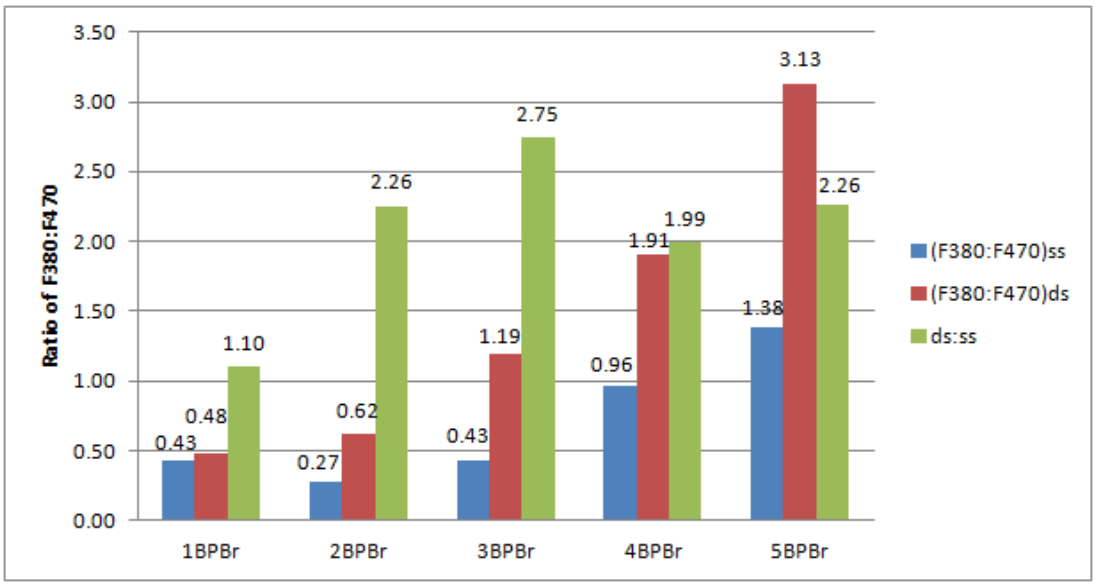

Figure 3.2 M/E ratios, as well as the switching ratio (ds/ss), of various doubly pyrenebutyryl-labeled acpcPNA probes 1BPBr, 2BPBr, 3BPBr, 4BPBr and 5BPBr in single stranded and duplex forms, as well as the switching ratio (ds/ss).

3.3.2.2 Effects of the length and linker to fluorescence properties of dual pyrene-modified acpcPNA probes

To study the effects of the length of the linker between pyrene and the acpcPNA backbone, 1-pyreneacetic acid (C1+CO) and 1-pyrenecarboxylic acid (CO) were attached onto acpcPNA at three-base separation to give the dual pyreneacetyl-labeled acpcPNA (**3BPAc**) and dual pyrenecarboxyl-labeled acpcPNA (**3BPCO**). Their fluorescence properties were compared with **3BPBr** carrying the pyrenebutyryl label (C3+CO) to search for the optimal length of the linker. The M/E ratios of **3BPAc** in single stranded and duplex forms were 1.91 and 9.39 whereas those of **3BPCO** were 3.82 and 6.18, respectively. The switching ratios (ds/ss) of 4.98 and 1.62 were obtained for **3BPAc** and **3BPCO**, respectively. The **3BPAc** with a short linker gave a better switching ratio (4.98) than **3BPBr** (2.75). However, for these dual pyrene-labeled probes with short linkers, the M/E ratios of the single stranded forms were greater than 1. This means that the excimer could not form effectively because

the short linkers did not allow efficient contact between the two pyrene chromophores. The results are summarized in **Figure 3.3**.

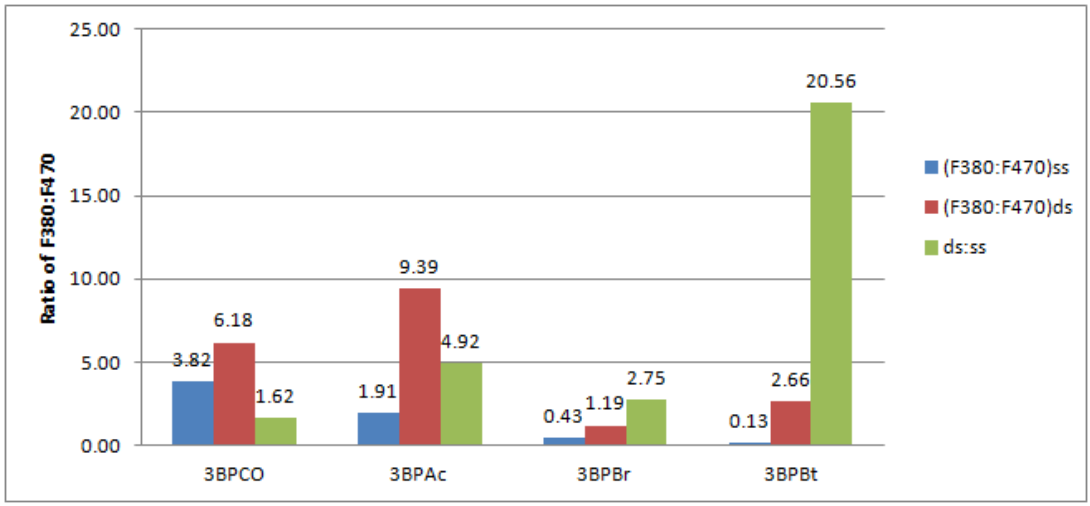

Figure 3.3 M/E ratios, as well as the switching ratio (ds/ss), of various doubly pyrenebutyryl-labeled acpcPNA probes **3BPCO**, **3BPAc**, **3BPBr** and **3BPBt** in single stranded and duplex forms, as well as the switching ratio (ds/ss).

Although excimer/monomer switching behaviors were observed in these pyrene-amide labeled acpcPNA, the amide type linkage may not be ideal because an amide bond possesses two geometric isomers, namely *cis*- and *trans*- forms as a consequence of the slow rotation of the amide C-N bond. Consequently, the alkylamine linkage was proposed to be a better linker candidate because it can freely rotate so there should be no geometrical isomers

1-Pyrenecarboxaldehyde and 1-pyrenebutyraldehyde were chosen to incorporate into acpcPNA via reductive alkylation for making the amine-type linker [27]. The distance between the two labels were still fixed at three bases to compare the fluorescence properties with other systems. The dual pyrenebutyl-modified acpcPNA (**3BPBt**) was successfully synthesized, but not the pyrenemethyl-modified acpcPNA due to the incomplete double alkylation as a result of the low reactivity of the aromatic alhehyde. Therefore only fluorescence properties of **3BPBt** could be

investigated. **3BPBt** showed the M/E ratios in single- and double-stranded forms of 0.13 and 2.66, respectively. The very high switching ratio of 20.56 was then obtained. This is 7.5 times higher than that of **3BPBr** (2.75) (see Figure 3.3). The large switching ratio obtained here suggests that the effective free rotation was a necessary factor to achieve a better excimer/monomer switching acpcPNA probes. Raw fluorescence spectra were shown in appendices. The effects of distance between the two pyrenebutyl lables were next studied.

3.3.2.3 Effects of distance between the two pyrene units to fluorescence properties of dual pyrenebutyl-labeled acpcPNA probes

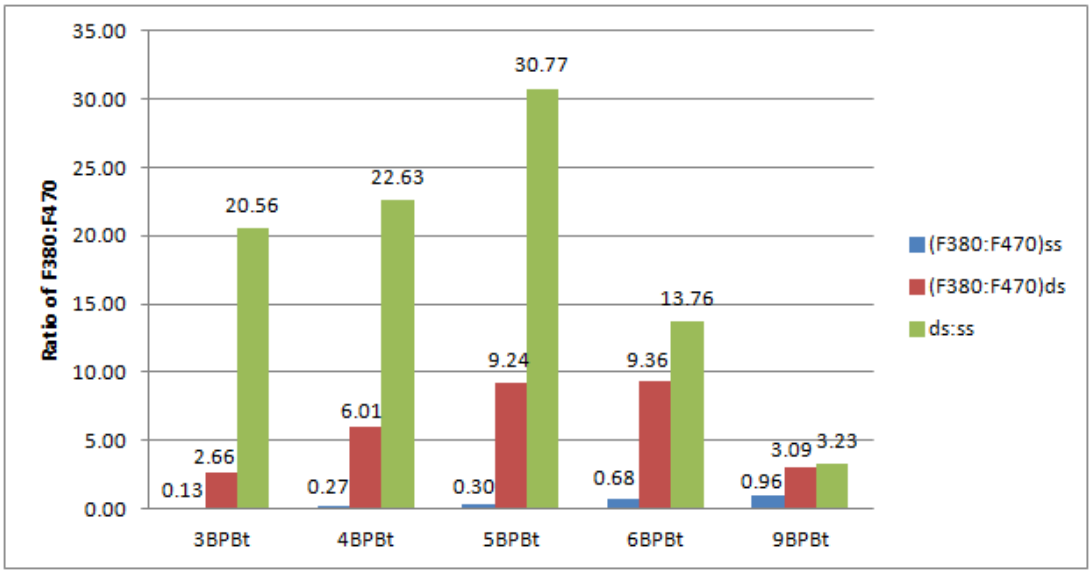

Figure 3.4 M/E ratios, as well as the switching ratio (ds/ss), of various doubly pyrenebutyryl-labeled acpcPNA probes **3BPBt**, **4BPBt**, **5BPBt**, **6BPBt** and **9BPBt** in single stranded and duplex forms.

Dual pyrenebutyl labeled acpcPNA with the distance between the two labels varying from three- to six-bases (**3BPBt**, **4BPBt**, **5BPBt**, **6BPBt**) and nine-base (**9BPBt**) were synthesized. In the case of nine-base separation, the pyrenebutyl labels

were placed at the N- and C-termini of the T_9 PNA. Fluorescence properties of both of single stranded and duplexes with complementary and single mismatched DNA were studied as before. The results showed that the M/E ratios of the free probes were 0.13, 0.27, 0.30, 0.68 and 0.96 for **3BPBt**, **4BPBt**, **5BPBt**, **6BPBt** and **9BPBt** respectively. The M/E ratio of the free probe was increased when the distance was larger. The value gradually increased from **3BPBt** and **9BPBt**. The data suggest that the excimer could better form when the two pyrenebutyl moieties were close to each other. Thus, **3BPBt** had the smallest M/E ratio and **9BPBt** had the largest M/E ratio. The M/E ratios in complementary PNA·DNA duplexes were 2.66, 6.01, 9.24, 9.36 and 3.09 for **3BPBt**, **4BPBt**, **5BPBt**, **6BPBt** and **9BPBt**, respectively. The maximum monomer formation was observed at a distance between 5-6 bases. This value is coincidence with the distance that will make the pyrene locate on the opposite sides of the duplex (assuming the 10-12 base pairs per turn in PNA·DNA duplex like in normal DNA·DNA duplex). From these M/E values, the switching ratios of the dual pyrenebutyl-modified acpcPNA were 20.50, 22.63, 30.77, 13.76 and 3.23 for **3BPBt**, **4BPBt**, **5BPBt**, **6BPBt** and **9BPBt**, respectively (see Figure 3.4). The best switching ratio at 30.77 was observed with **5BPBt**, which was presumably the optimal distance that allows maximum monomer formation in the duplex and yields reasonable excimer formation in the single stranded states. Although the **6BPBt** displayed higher M/E in duplex (9.36), the M/E ratio in the single strand form was 0.68, which was two-fold higher than that of **5BPBt**. Accordingly, a lower switching ratio was observed when compared to **5BPBt**.

In addition to complementary DNA targets, the fluorescence properties of **3BPBt**, **4BPBt**, **5BPBt** and **6BPBt** were also measured in the presence of single base mismatched DNA. In all cases, the switching ratios of these mismatched duplexes were lower than those of the complementary duplexes. The switching ratios with single mismatch C, G and T at the middle of the DNA strand were 4.62, 2.90, 3.36 for **3BPBt**; 6.23, 4.07, 4.46 for **4BPBt**; 3.45, 2.92, 3.24 for **5BPBt** and 1.49, 1.04, 1.36 for **6BPBt**, respectively. The results suggest that the dual pyrenebutyl-labeled acpcPNA can recognize the DNA target with high specificity. The **6BPBt** system exhibited the lowest switching ratio for mismatched duplexes, suggesting the highest

specificity. However, the switching ratio with complementary DNA at 13.76 was much lower than **5BPBt**. Hence, the **5BPBt** was concluded to be the best system of dual pyrene-modified acpcPNA probes. The ratios are shown in **Figure 3.5** and raw fluorescence spectra are shown in appendices.

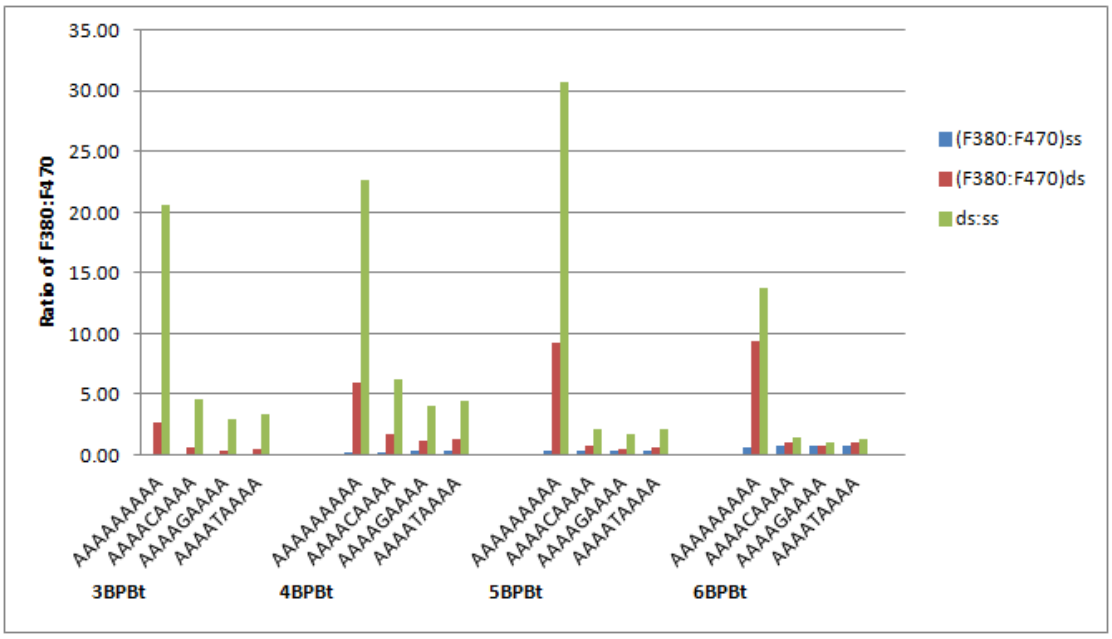

Figure 3.5 M/E ratios, as well as the switching ratio (ds/ss), of various doubly pyrenebutyryl-labeled acpcPNA probes **3BPBt**, **4BPBt**, **5BPBt** and **6BPBt** in single stranded and duplex forms with complementary and mismatched DNA.

3.3.2.4 Fluorescent titration and temperature-dependent fluorescence of 5BPBt with complementary DNA

To find out the stoichiometry of the target DNA that can cause switching of the probe from excimer to monomer, the fluorescent titration experiment was performed. The **5BPBt** was titrated with its complementary DNA by increasing the DNA from 0-1.2 equivalents while keeping the volume change as small as possible. The result showed that at a mole fraction of DNA to acpcPNA of 0.25, the switching from excimer to monomer was evidenced as shown in **Figure 3.6**. The signal of the

excimer was decreased, and that of the monomer was increased until a full equivalent of the DNA was added. After that, both signals remain relatively constant. This experiment showed that the stoichiometry of the binding between **5BPBt** and dA_9 is 1:1 and that the switching behavior can be observed even when sub-stoichiometric amount of DNA target was added.

A)

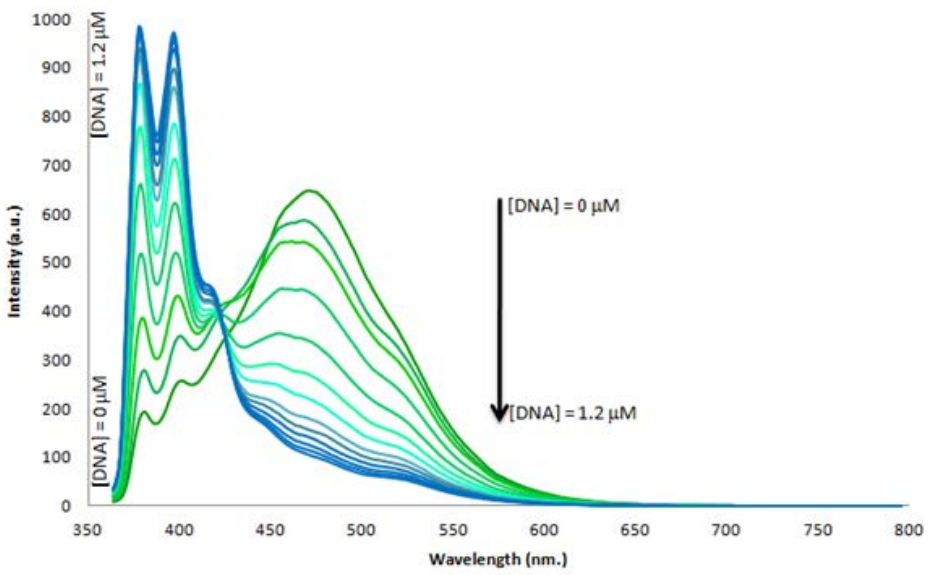

B)

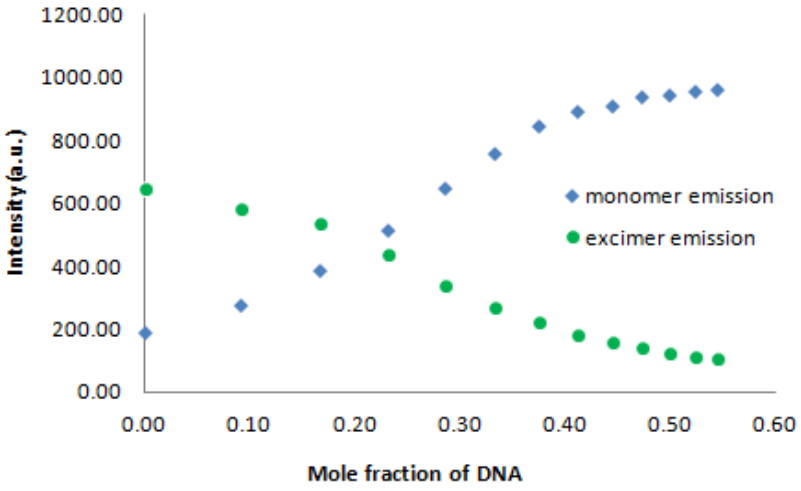

C)

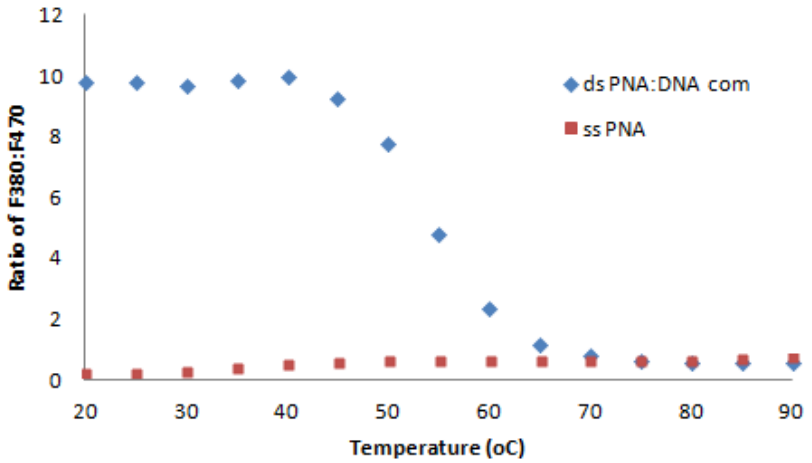

Figure 3.6 A) Fluorescence titration of **5BPBt** with complementary DNA in 10 mM phosphate buffer pH 7.0, [PNA] = 1.0 μM and [DNA] = 0-1.2 μM, λ_{excit} = 350 nm. **B)** Plots of monomer and excimer emissions as a function of mole fraction of DNA in the mixture. **C)** fluorescence melting curves of **5BPBt** and its DNA duplex obtained by plotting the M/E emission ratios as a function of temperature.

Moreover, the fluorescence melting experiment was also performed with this system. Upon heating, the monomer/excimer emissions were significantly decreased for the PNA·DNA duplex, and only slightly change in the case of single stranded **5BPBt**. The plot between F380/F470 against temperature gave a sigmoidal curve like the melting curve obtained from UV-Vis experiments. From the fluorescence melting curve, the melting temperature of **5BPBt** duplex of around 55^{o}C could be deduced. This value is in good agreement with the melting temperature obtained from UV experiment at 54.7^{o}C as shown in **Figure 3.6**.

In addition, circular dichroism (CD) technique was also brought to study the conformation change of PNA·DNA hybrid and the orientation of the pyrene chromophores. The result showed a rather small difference between CD spectrum of the duplex from the sum of CD spectra of each component (**Figure 3.7**). This observation confirms that there were conformational change taken place upon hybridization between complementary DNA and acpcPNA. However, no change in

the pyrene absorption region was observed. This suggests that in the duplex, the pyrenes do not have a fixed position and orientation within the duplex.

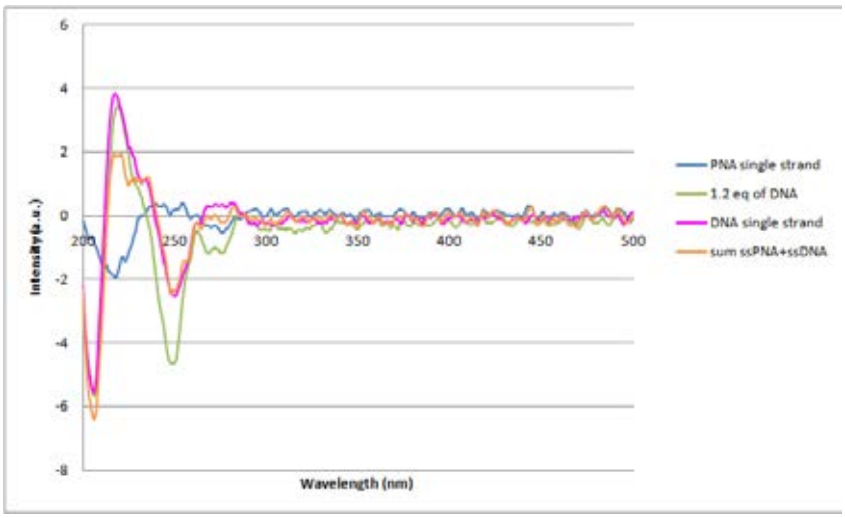

Figure 3.7 CD spectra of **5BPBt** , dA_9, a mixture of both and sum of the CD spectra of **5BPBt** and dA_9 . The spectra were measured in 10 mM phosphate buffer pH 7.0, [PNA] = 1.0 μM and [DNA] = 1.2 μM, λ_{excit} = 350 nm.

3.3.3 Fluorescence property of mixed sequence acpcPNA probes

To examine the generality of the excimer-monomer forming acpcPNA probe, the best design optimized with the T_9 sequence (five-base distance, pyrenebutyl label) was applied to mixed sequence acpcPNA probes. Three 12 mers mix-base acpcPNA sequences were synthesized and labeled with two pyrenebutyl labels at 5-base separation. The sequences studied include AGTCACACACTG (**MBS1**), AGTTAT CCCTGC (**MBS2**) and TAGTTACATTAT (**MBS3**). Fluorescence spectra of all mix-base probes were tested with complementary and single base mismatched DNA (with the mismatch position directly opposite the pyrene label or further away). From the results shown in **Figure 3.8**, the M/E ratios of these three systems were 1.0, 1.1 and 1.3 for single stranded **MBS1**, **MBS2** and **MBS3**, respectively. The relatively large

M/E values suggest that the formation of excimer is not as effective as in the T_9 sequence despite having the same distance and type of label. After hybridization, the complementary PNA·DNA duplexes exhibited M/E ratios of 4.8, 5.4 and 11.1 for **MBS1**, **MBS2** and **MBS3**, respectively. These showed that the probes were able to switch from excimer to monomer upon hybridization with complementary DNA. From these figures, the switching ratios of 4.9, 5.2 and 8.6 were obtained for **MBS1**, **MBS2** and **MBS3**, respectively. These switching ratios were considerably lower than that of **5BPBt**. This may be due to the strong quenching of pyrene monomer by thymine that makes the M/E ratio particularly low in homothymine sequences [27]. Nevertheless, the mixed base probes displayed distinctive switching behavior. In addition, when mismatched bases were introduced in the DNA target, the switching ratios were much lower when compared to the complementary duplexes. The switching ratios were 1.3 and 1.2 for **MBS1** (with the mismatched base in the middle of the DNA strand and opposite to one of the pyrene label, respectively), 1.3 for **MBS2** (with the mismatched base in the middle of the DNA strand) and 4.0 and 4.8 for **MBS3** (with the mismatched base in the middle of the DNA strand). These results suggest that discrimination between complementary and single mismatched DNA targets is possible in these mix-base sequences. However, the efficiency was quite dependent on the sequence, but not on the location of the mismatch base. The fluorescence change of **MBS1** can be clearly observed by naked eyes under black light (Figure 3.9). This means that the switching ratio of ~5 was sufficient to allow discrimination between complementary and mismatched DNA targets by naked eyes.

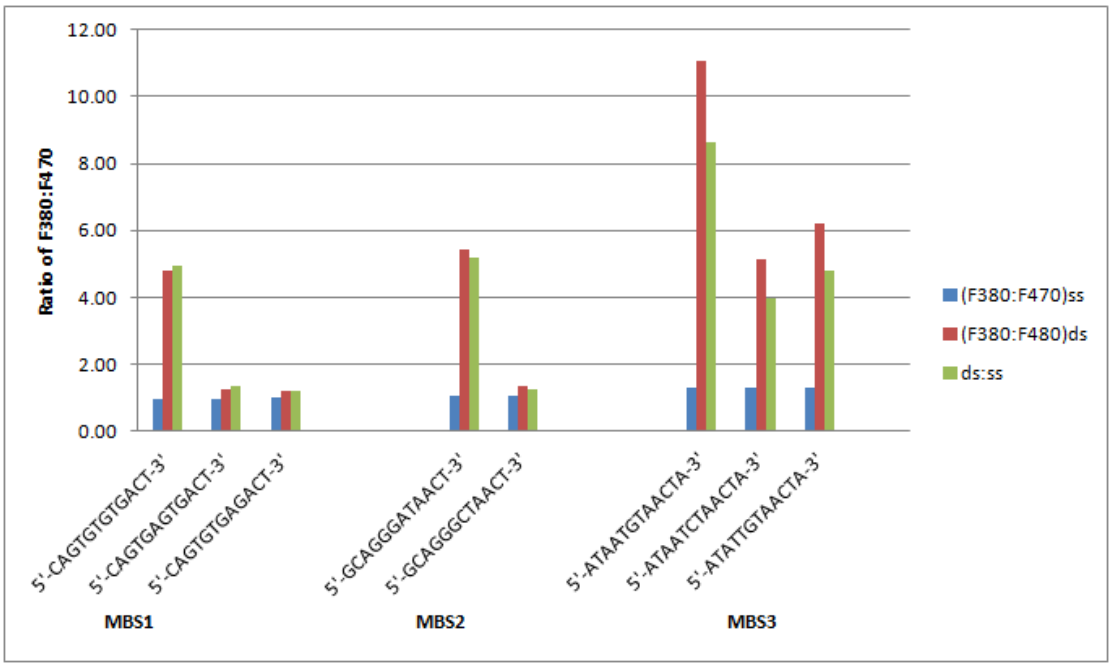

Figure 3.8 M/E ratios, as well as the switching ratio (ds/ss), of various doubly pyrenebutyryl-labeled acpcPNA probes **MBS1**, **MBS2** and **MBS3** in single stranded and duplex forms with complementary and mismatched DNA.

Figure 3.9 Fluorescent MBS1 photographs under black light (405 nm) (left: single stranded, middle: hybrid with complementary DNA, right: hybrid with single-base mismatched DNA). Conditions: 10 mM phosphate buffer pH 7.0, [PNA] = 10 μM and [DNA] = 12 μM.

3.4 Attempts to improve the switching ratio in mix-base PNA probes

As observed in the previous section, the mix-base acpcPNA probes gave lower switching ratios than the model homothymine **5BPBt** system. Examination of the fluorescence spectra of **MBS1** – **MBS3** suggests that the M/E ratios in the single stranded acpcPNA probes are rather high, indicating that the excimer formation was not effective. According to a literature report, γ-cyclodextrin could enhance the pyrene excimer formation in DNA beacons [31] which was explained by the inclusion of the excimer in the hydrophobic cavity of γ-cyclodextrin.

Based on this work, it was thought that γ-cyclodextrin might enhance the formation of the pyrene excimer in the single stranded probe. The fluorescence of the single stranded mix-base acpcPNA probe (**MBS1**) was first measured at 0.1 μM concentration. Excess of γ-cyclodextrin was next added (final concentration = 8.0 mM) and the fluorescence was measured again. Finally, the target DNA was added and the final fluorescence spectrum was measured. The results showed that the addition of γ-cyclodextrin did not improve the excimer formation as shown by a marginal stronger monomer emission, but no significant change was observed in the excimer emission (**Figure 3.10**). Only after addition of the complementary DNA that the monomer emission was increased and the excimer emission decreased. The final M/E ratio was about the same as without cyclodextrin. This suggests that the inclusion of the pyrene excimer could not take place in acpcPNA system and this approach was therefore abandoned.

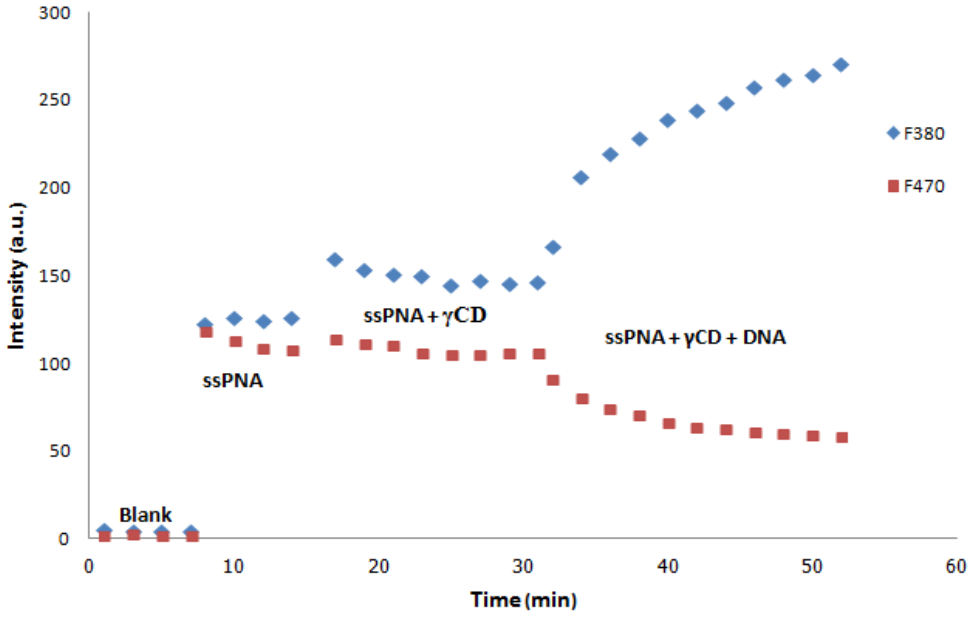

Figure 3.10 Fluorescence signals at 380 nm and 470 nm were measured 10 mM phosphate buffer pH 7.0, [PNA] = 1.0 μM and [DNA] = 1.2 μM, λ_{excit} = 350 nm.

3.5 Applications of dual-pyrene-labeled acpcPNA for monitoring DNA duplex invasion

PNA could hybridize with DNA to form a PNA·DNA duplex that is more stable than a DNA·DNA duplex with the same sequence. Thermodynamically, PNA should be able to spontaneously invade into DNA duplex. There are two modes of invasion of PNA to duplex DNA could divide two types - namely duplex invasion (**Figure 3.11A**) and double duplex invasion (**Figure 3.11B**). The duplex invasion is generated by binding of PNA to a region of DNA duplex, leaving the other DNA strand free to form a ”D-loop” structure. In double duplex invasion, two PNA strands is required, and there is no free DNA strand left [25]. This double duplex invasion mode should yield a more stable complex because the DNA duplex cannot re-form, but it require modification of the base (diaminopurine replacing adenine and 2-thiouracil instanced of thymine) in order to form a “pseudocomplementary” PNA that

can bind to DNA but not to itself. Since acpcPNA is intrinsically pseudocomplementary without having to modify the base, it is an ideal molecule for DNA double duplex invasion.

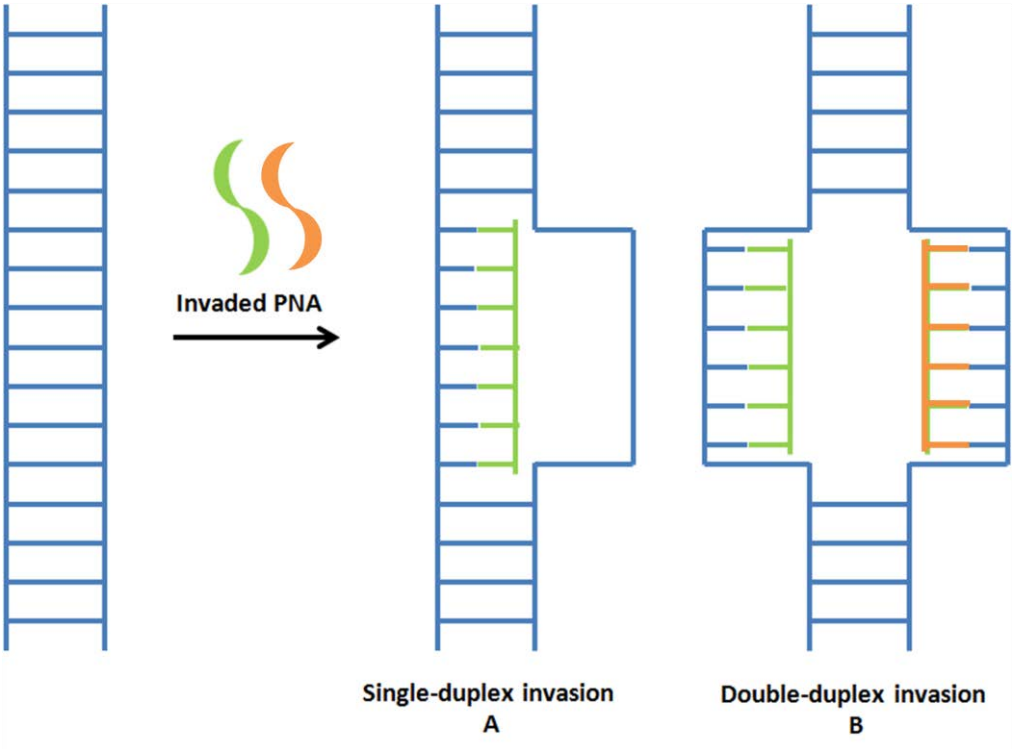

Figure 3.11 Two different DNA duplex invasion modes.

In this experiment, the mix-base acpcPNA probe **MBS1** was selected as self-reporting probe for monitoring the DNA duplex invasion of DNA duplex. The sequences of acpcPNA and DNA target used are as follow:

MBS1: N-AGTC^{PyBtl}ACACA^{PyBtl}CTG-C (12 mer)

MBS1com: C-TCAGTGTGTGAC-N (12 mer)

DNA1: 3'-CGCGTAGACTTCAGTGTGTGACATGTGAGCGC-5' (32 mer)

DNA2: 5'-GCGCATCTGAAGTCACACACTGTACACTCGCG-3' (32 mer)

The stock solution of a duplex DNA was prepared by mixing **DNA1** and **DNA2** at 1:1.1 ratio in 10 mM sodium phosphate buffer pH 7.0 at a very high concentration (100 μM). The melting temperature of this solution was measured at a lower concentration (3.0 μM) to ensure the formation of the DNA duplex. The

sigmoidal curve obtained with a T_m of 66.4 ^oC confirmed that the DNA duplex had formed. A control hybridization experiment of **MBS1** with **DNA1** was also performed. The results showed that **MBS1** could form a hybrid with **DNA1**, giving a switching ratio of 5.2 (at 1:1 ratio) (**Figure 3.12C**). In the single duplex invasion experiment, the fluorescence of single strand **MBS1** was measured, then the prepared DNA duplex was added while keeping the volume change minimum. The fluorescence spectra were measured again until a stable value was obtained. According to the results, the fluorescence signal of the excimer was slowly decreased, while that of the monomer was almost unchanged. We interpreted this as an evidence for the DNA duplex invasion by acpcPNA. The absence of the increase in monomer emission was explained by the quenching of the monomer by the nearby DNA strand. However, significant excimer emission was still observed after the fluorescence signal was stable. This meant that the **MBS1** could not completely invade into the duplex DNA strand. To solve this problem, 1 equiv. of another unlabeled acpcPNA strand **MBS1com** was added. After adding the **MBS1com** into the system, the signal of the excimer was further decreased, while that of the monomer remains the same (**Figure 3.12A** and **B**). These results confirm that the acpcPNA could invade the DNA duplex by the duplex invasion and double duplex invasion modes. The latter is more efficient, but it was difficult to quantitate the extent of the invasion because of the interference of the other DNA strand on the monomer emission. If one ignore the monomer emission, the invasion efficiency of around 60% by the duplex invasion and 88% by the double duplex invasion modes.

Calculated from;

$$\frac{\left(\frac{(\mathrm{F470})\mathrm{ds}-(\mathrm{F470})\mathrm{ss}}{(\mathrm{F470})\mathrm{ss}}\right)\mathrm{expt}}{\left(\frac{(\mathrm{F470})\mathrm{ds}-(\mathrm{F470})\mathrm{ss}}{(\mathrm{F470})\mathrm{ss}}\right)\mathrm{control}}$$

This experiment clearly demonstrates that DNA duplex invasion with acpcPNA is possible, and that the efficiency is increased in the double duplex invasion.

A)

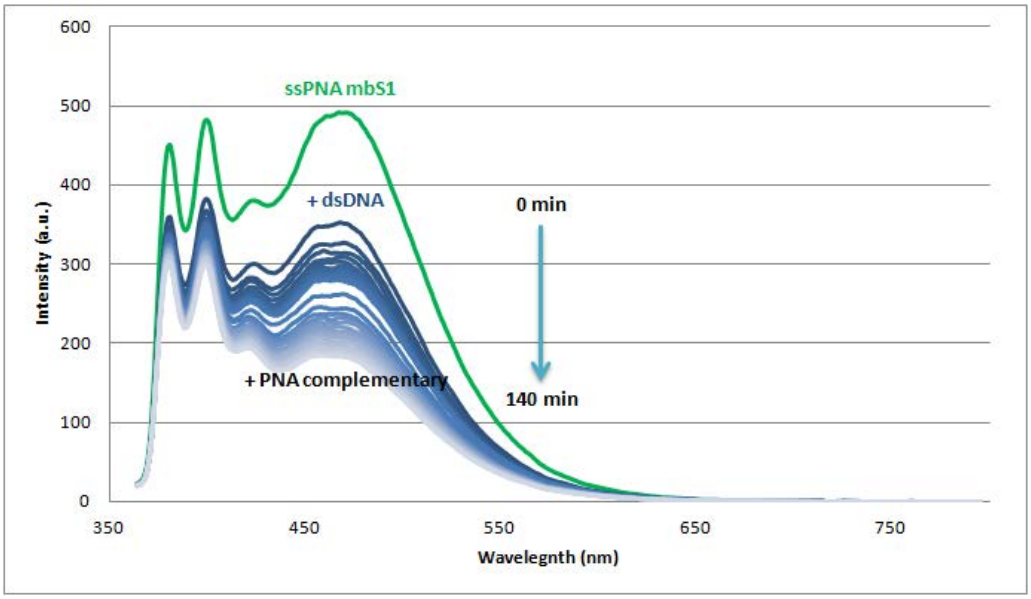
ssPNA mbS1
+ dsDNA
0 min
+ PNA complementary
140 min
Intensity (a.u.)
Wavelegnth (nm)
600
500
400
300
200
100
0
350
450
550
650
750

B)

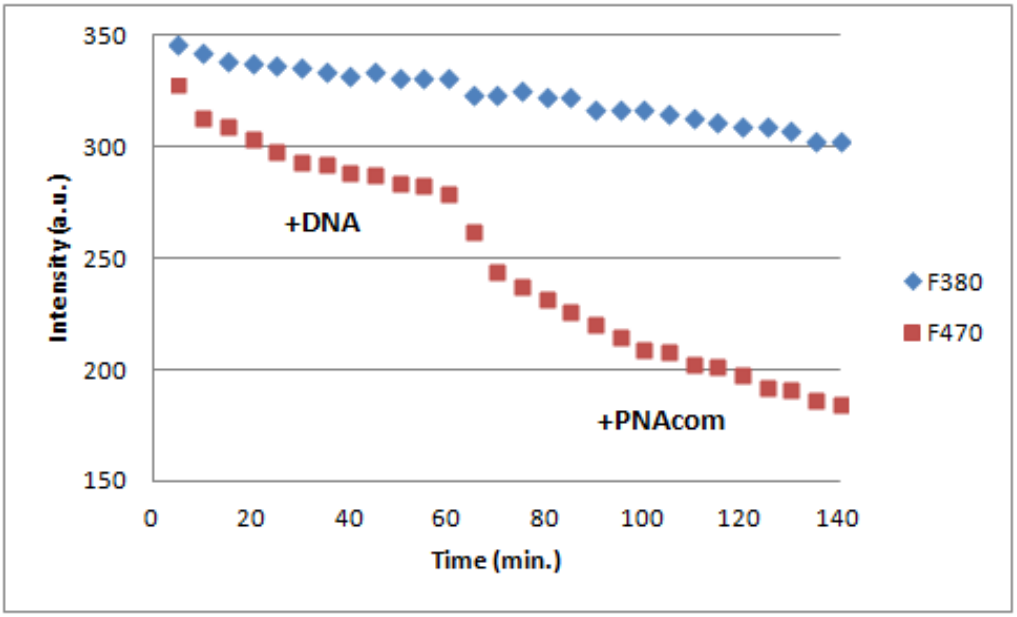
+DNA
+PNAcom
F380
F470
Intensity (a.u.)
Time (min.)
350
300
250
200
150
0
20
40
60
80
100
120
140

C)

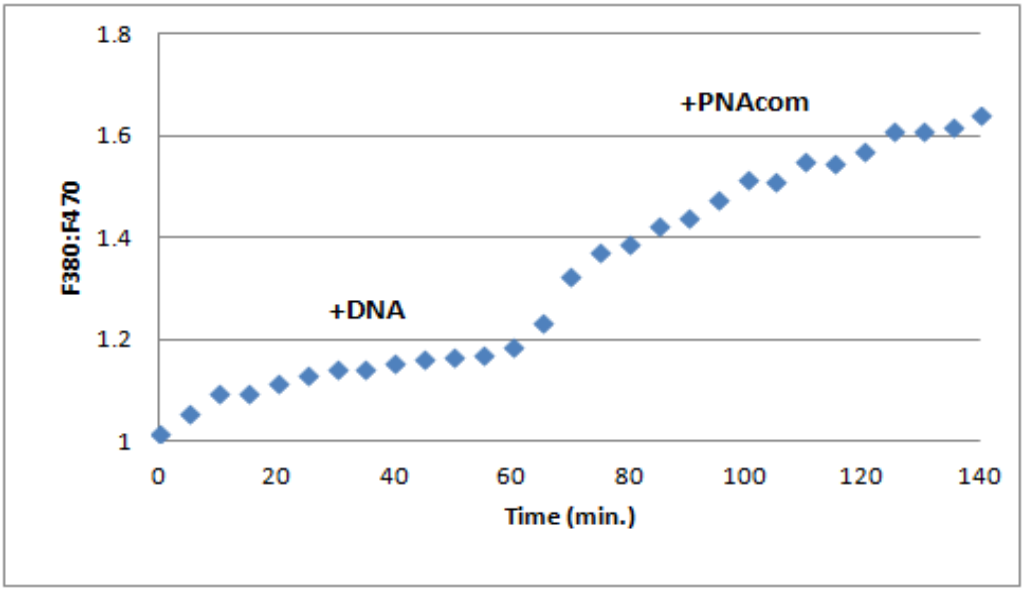

D)

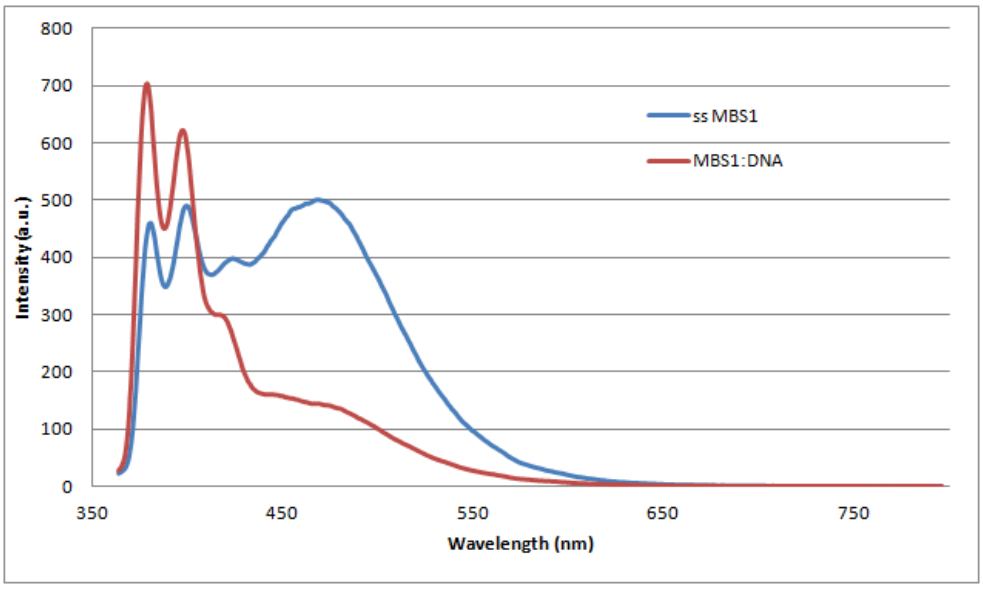

Figure 3.12 A) Fluorescent invasion was measured in 10 mM phosphate buffer pH 7.0, [**MBS1**] = 1.0 µM, ds[DNA] = 1.0 µM, **PNAcom** = 1.0 uM and λ_{excit} = 350 nm. **B)** Plots of F380 and F470 as a function of time (min). **C)** Plots of ratio F380:F470 as a function of time (min). **D)** Fluorescent control was measured in 10 mM phosphate buffer pH 7.0, [**MBS1**] = 1.0 µM, ds[DNA] = 1.0 µM, λ_{excit} = 350 nm.

CHAPTER IV
CONCLUSION

Dual pyrene-labeled acpcPNAs were designed as an excimer-monomer switching probe that can form pyrene excimer in the single stranded form and pyrene monomer after hybridization with DNA in duplex form. Two pyrene labels were attached onto acpcPNA backbone at specific positions via acylation (pyrenecarboxylic acid derivatives) or reductive alkylation (pyrenealdehyde derivatives) of APC-modified acpcPNA. To optimize the probe, the effects of distance between the two pyrene labels and the type of pyrene labels were investigated. The switching ratio, as calculated by division of the monomer/excimer (M/E) ratio (F_{380}/F_{470}) of the duplex with the same ratio obtained for the single stranded form, was used as a key parameter. In single stranded probes, the excimer emission should dominate, therefore the M/E ratio should be <1. In complementary DNA hybrids, the excimer emission should decrease and the monomer emission should increase, therefore the M/E ratio should increase, resulting in a switching ratio of greater than unity. Larger switching ratios indicate greater ability of the probe to switch from excimer to monomer upon hybridization with DNA. Starting with a simple homothymine system (T_9) with different types of labels at a fix distance, the more flexible pyrenebutyl label showed a better performance than pyrenecarboxyl, pyreneacetyl and pyrenebutyryl labels. Next the distance between the two pyrenebutyl labels were optimized and the best switching ratio of 30.8 was obtained at 5-base separation. The study was extended to three mix-base acpcPNA sequences, whereby switching ratios around 5-8 were observed. Attempts to improve the ratio by the addition of γ-cyclodextrin to stabilize the pyrene excimer failed. Nevertheless, the switching ratio of 5 was sufficient to be observed by naked eyes under UV light. Furthermore, the switching behavior was very specific for complementary DNA target as shown by switching ratios around 1 of most single mismatched targets. As a result, the dual pyrene-labeled acpcPNA probes should be a useful as a probe for DNA sequence detection. In addition, an application of the current excimer-monomer

switching probe as a tool to monitor the duplex invasion of duplex DNA by acpcPNA was also demonstrated.

REFERENCES

[1] Nielsen, P. E., Egholm, M., Berg, R. H., Buchardt**.** Sequence selective recognition of DNA by strand displacement with a thymine substituted polyamide**.** Science 254 (1991) : 1497-1500.

[2] Hyrup, B., Nielsen, P. E. Peptide nucleic acids (PNA): Synthesis, properties and potential applications. Bioorganic & Medicinal Chemistry 4 (1996) : 5-23.

[3] Suparpprom, C., Srisuwannaket, C., Sangvanich, P., Vilaivan, T. Synthesis and oligodeoxynucleotide binding properties of pyrrolidinyl peptide nucleic acids bearing prolyl-2-aminocyclopentanecarboxylic acid (ACPC) backbones. Tetrahedron Letters 46 (2005) : 2833-2837.

[4] Vilaivan, T., Srisuwannaket, C. Hybridization of pyrrolidinyl peptide nucleic acids and DNA: selectivity, base-pairing specificity and direction of binding**.** Organic Letters 8 (2006) : 1897-1900.

[5] Sahu, B. , Sacui, I., Rapireddy, S., Zanotti, K. J., Bahal, R., Armitage, B. A., Ly, D.H. Synthesis and characterization of conformationally preorganized, (R)-diethylene glycol-containing γ-peptide nucleic acids with superior hybridization properties and water solubility. Journal of Organic Chemistry 76 (2011) : 5614-5627.

[6] Rapireddy, S., He, G., Roy, S., Armitage, B. A., Ly, D. H. Strand invasion of mixed-sequence B-DNA by acridine-linked, γ-peptide nucleic acids (γ-PNA). Journal of the American Chemical Society 129 (2007) : 15596-15600.

[7] Tan, W., Wang, K. Drake, T. J. Molecular beacon. Current Opinion in Chemical Biology 8 (2004) : 547-553.

[8] Yesilkaya, H., Meacci, F., Niemann, S., Hillemann, D., Rüsch-Gerdes, S. Evaluation of molecular-beacon, taq man, and fluorescence resonance energy transfer probes for detection of antibiotic resistance-conferring

single nucleotide polymorphisms in mixed *Mycobacterium tuberculosis* DNA extracts. Journal of Clinical Microbiology 44 (2006) : 3826-3829.

[9] Clegg, R. M. Fluorescence resonance energy transfer and nucleic acids. Methods in Enzymology 211 (1992) : 353-388.

[10] Lilley, D. M. J., Wilson, T. J. Fluorescence resonance energy transfer as a structural tool for nucleic acids. Current Opinion in Chemical Biology 4 (2000) : 507-517.

[11] Tong, A. K., Li, Z., Jones, G. S., Russo, J. J., Ju, J. Fluorescence energy transfer tags for multiplex biological assays. Nature Biotechnology 19 (2001) : 756-759.

[12] Matsumoto, K., Shinohara, Y., Bag, S. S., Takeushi, Y., Morii, T., Saito, Y., Saito, I. Pyrene-labeled deoxyguanosine as a fluorescence sensor to discriminate single and double stranded DNA structures: Design of ends free molecular beacons. Bioorganic & Medicinal Chemistry Letters 19 (2009) : 6392-6395.

[13] Heinlein, T., Knemeyer, J., Piestert, O., Sauer, M. Photoinduced electron transfer between fluorescent dyes and guanosine residues in DNA-hairpins. Journal of Physical Chemistry 107 (2003) : 7957-7964.

[14] Kolpashchikov, D. M. Binary probes for nucleic acid analysis. Chemical Reviews 110 (2010) : 4709-4723.

[15] Masuko, M., Ohuchi, S., Sode, K., Ohtani, H., Shimadzu, A. Fluorescence resonance energy transfer from pyrene to perylene labels for nucleic acid hybridization assays under homogeneous solution conditions. Nucleic Acids Research 28 (2000) : 8.

[16] Varghese, R., Wagenknecht, H. A. Red-white-blue emission switching molecular beacons: Ratiometric multicolour DNA hybridization probes. Organic and Biomolecular Chemistry 8 (2010) : 526-528.

[17] Winnik, F. M. Photophysics of preassociated pyrenes in aqueous polymer solutions and in other organized media. Chemical Reviews 93 (1993) : 587-614.

[18] Ostergaard, M. E., Hrdlicka, P. J. Pyrene-functionalized oligonucleotides and locked nucleic acids (LNAs): Tools for fundamental research, diagnostics, and nanotechnology. Chemical Society Reviews 40 (2011) : 4877-5208.

[19] Dioubankova, N. N., Malakhov, A. D., Stetsenko, D. A., Gait, M. J., Volynsky, P. E., Efremov, R. G., Korshun, V. A. Pyrenemethyl *ara*-uridine-2′-carbamate: A strong interstrand excimer in the major groove of a DNA duplex. ChemBioChem 4 (2003) : 841-847.

[20] Fujimoto, K., Shimizu, H., Inouye, M. Unambiguoous detection of target DNAs by excimer-monomer switching molecular beacons. Journal of Organic Chemistry 69 (2004) : 3271-3275.

[21] Paris, P. L., Langehan, J. M., Kool, E. T. Probing DNA sequences in solution with a monomer-excimer fluorescence color change. Nucleic Acids Research 26 (1998) : 3789-3793.

[22] Tong, G., lawlor, J. M., Tregear, G. W., Haralambidis, J. Oligonucleotide-polyamide hybrid molecules containing multiple pyrene residues exhibit significant excimer fluorescence. Journal of the American Chemical Society 117 (1995) : 12151-12158.

[23] Yamana, K., Iwai, T., Ohtani, Y., Sato, S., Nakamura, M., Nakano, H. Bis-pyrene-labeled oligonucleotide: Sequence specificity of excimer and monomer fluorescence changes upon hybridization with DNA. Bioconjugate Chemistry 13 (2002) : 1226-1273.

[24] Conlon, P., Yang, C. J., Wu, Y., Chen, Y., Martinez, K., Kim, Y., Stevens, N., Marti, A. A., Jockusch, S., Turro, N. J., Tan, W. Pyrene excimer signaling molecular beacons for probing nucleic acids. Journal of the American Chemical Society 130 (2008) : 336-342.

[25] Kuhn, H., Demidov, V. V., Coull, J. M., Fiandaca, M. J., Gildea, B.D., Kamenetskii, M. D. Hybridization of DNA and PNA molecular beacons to single-stranded and double-stranded DNA targets. Journal of the American Chemical Society 126 (2004) : 1097-1103.

[26] Reenabthue, N., Boonlua, C., Vilaivan, C., Vilaivan, T., Suparpprom, C. 3 Aminopyrrolidine-4-carboxylic acid as versatile handle for internal labeling of pyrrolidinyl PNA. Bioorganic & Medicinal Chemistry Letters 21 (2011) : 6465-6469.

[27] Ditmangklo, B., Boonlua, C., Suparpprom, C., Vilaivan, T. Reductive alkylation and sequential reductive alkylation-click chemistry for on-solid-support modification of pyrrolidinyl peptide nucleic acid. Bioconjugate Chemistry 24 (2013) : 614-625.

[28] Vanvik, N. Westman, G. Wang, D. Kubista. M. Light-up probes: Thiazole orange-conjugated peptide nucleic acid for detection of target nucleic acid in homogeneous solution. Analytical Biochemistry 281 (2000) : 26-35.

[29] Kuhn H., Demidov, V. V. Coull, J. M. Fiandaca, M. J. Gildea, B. D. Frank-Kamenetskii. M. D. Hybridization of DNA and PNA molecular beacons to single-stranded and double-stranded DNA targets Journal of the American Chemical Society 126 (2004) : 1097-1023.

[30] Boonlua, C., Vilaivan, C., Wagenknecht, H. A., Vilaivan, T. 5-(Pyren-1-yl)uracil as a base-discriminating fluorescent nucleobase in pyrrolidinyl peptide nucleic acids. Asian Journal of Chemistry 6 (2011) : 3251-3259.

[31] Zheng, J., Li, J., Gao, X., Jin, J., Wang, K., Tan, W., Yang, R. Modulating molecular level space proximity: A simple and efficient strategy to design structured DNA probes. Analytical Chemistry 82 (2010) : 3914-3921.

APPENDIX

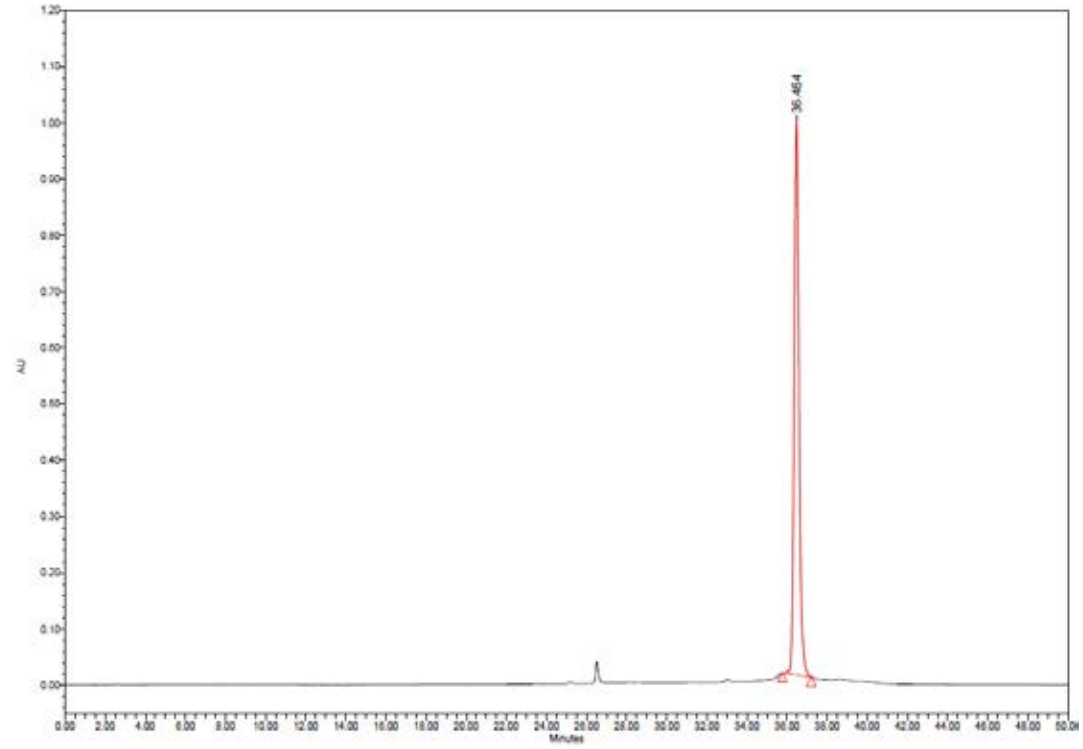

(a)

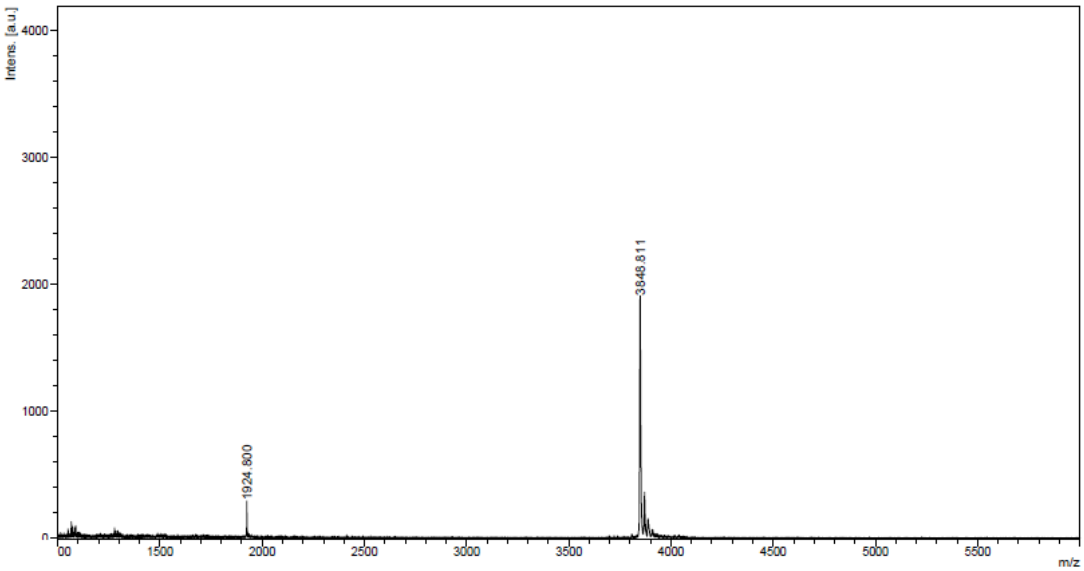

(b)

Figure A1 (a) Analytical HPLC chromatogram and (b) MALDI-TOF mass spectrum of **1BPBr** (calcd for $[M+H]^+$ = 3850.24)

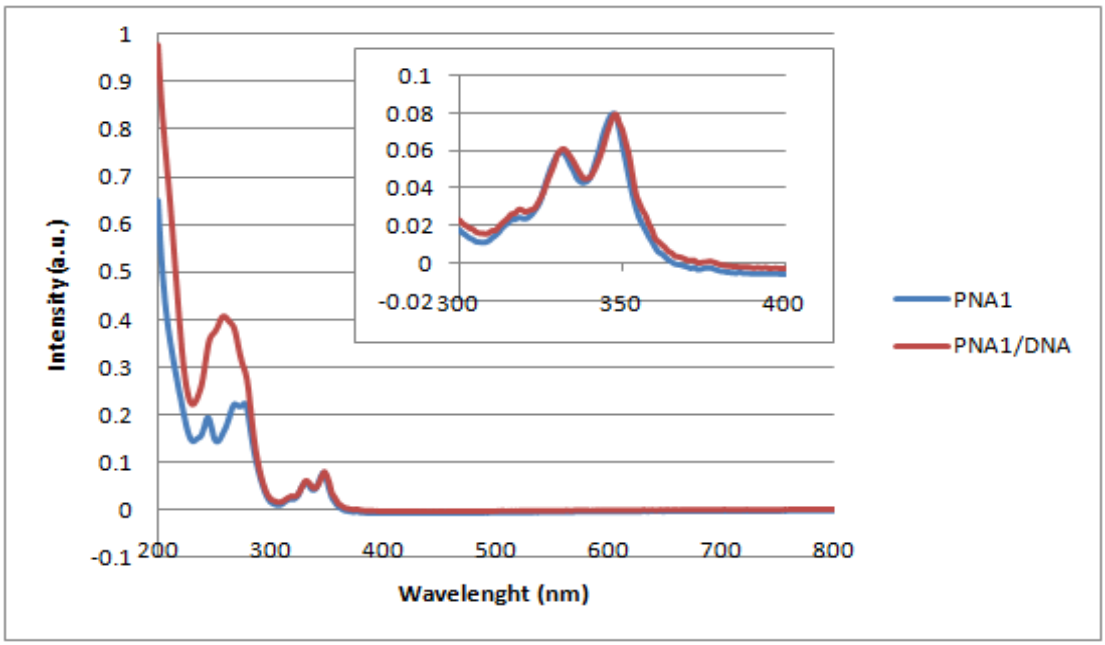

Figure A3 UV-Vis spectra of **1BPBr** in the absence and presence of DNA target in 10 mM phosphate buffer pH 7.0, [PNA] = 2.5 μM and [DNA] = 3.0 μM, λ_{excit} = 350 nm.

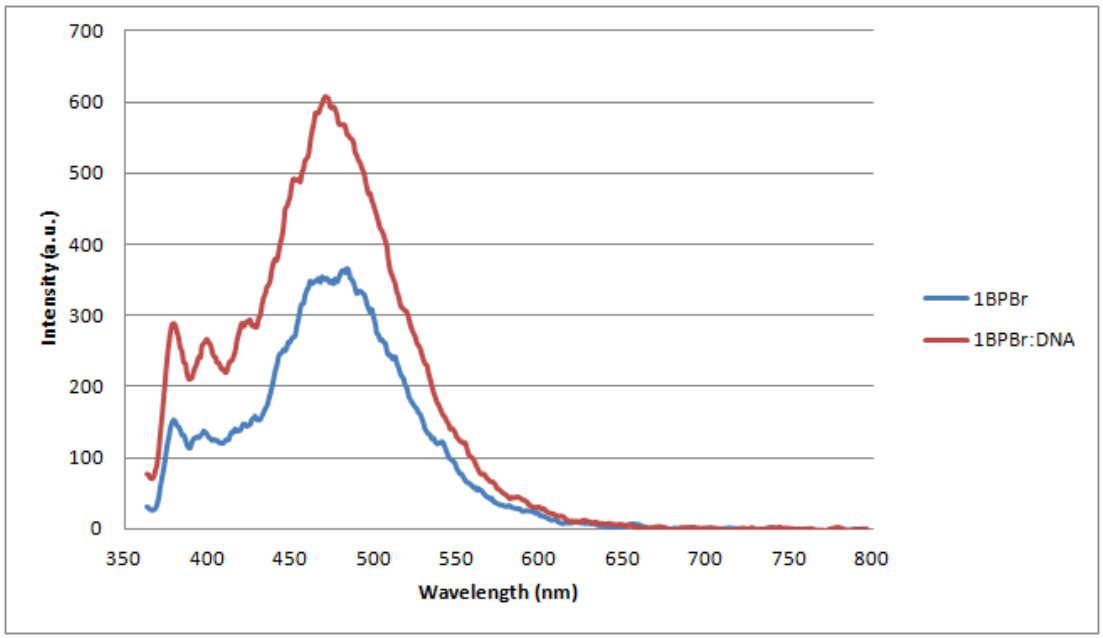

Figure A3 The fluorescence spectra of **1BPBr** in the absence and presence of DNA target in 10 mM phosphate buffer pH 7.0, [PNA] = 2.5 μM and [DNA] = 3.0 μM, λ_{excit} = 350 nm.

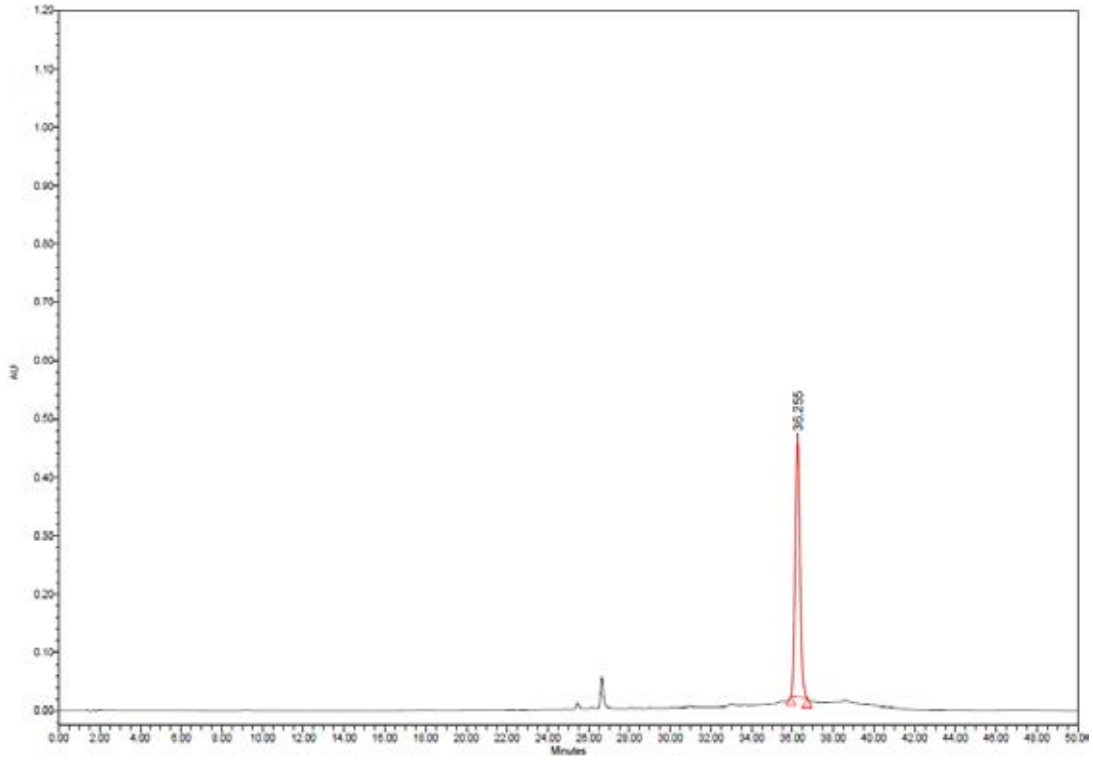

(a)

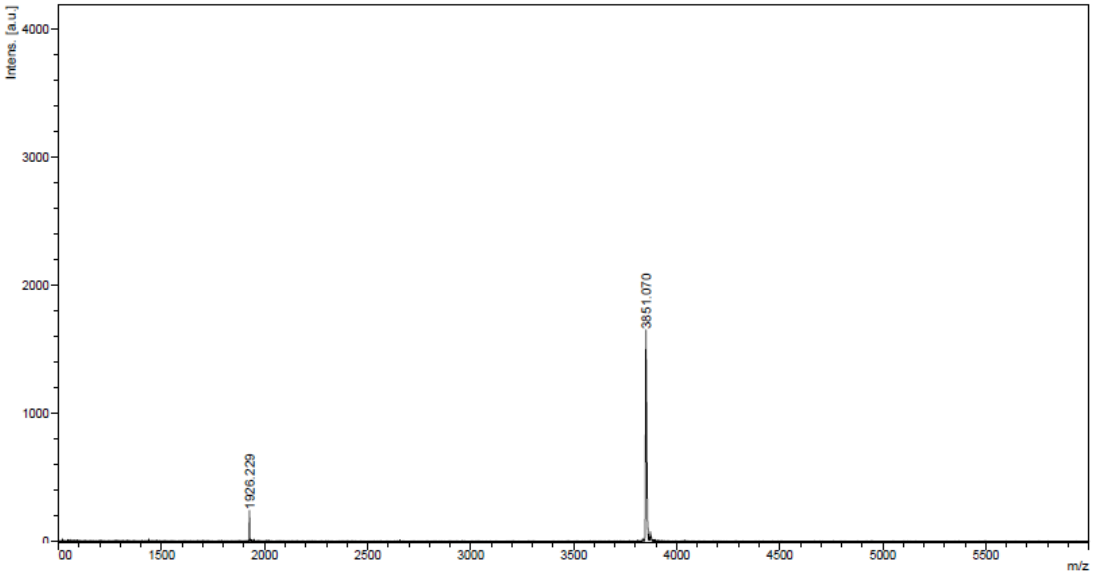

(b)

Figure A4 (a) Analytical HPLC chromatogram and (b) MALDI-TOF mass spectrum of **2BPBr** (calcd for $[M+H]^+ = 3850.24$)

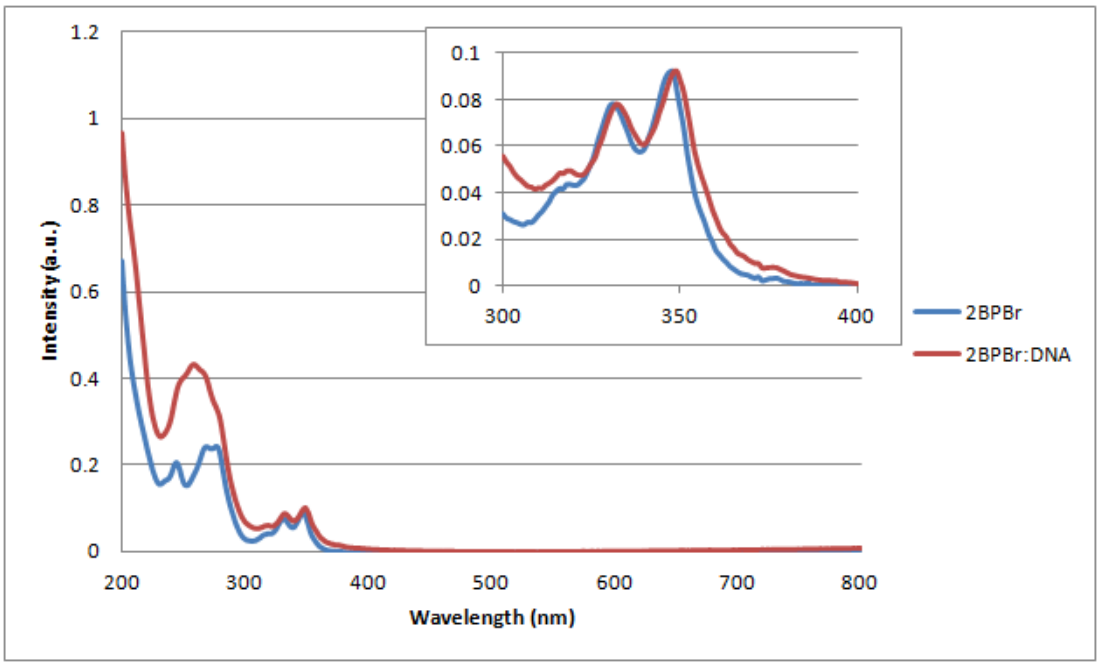

Figure A5 UV-Vis spectra of **2BPBr** in the absence and presence of DNA target in 10 mM phosphate buffer pH 7.0, [PNA] = 2.5 μM and [DNA] = 3.0 μM, λ_{excit} = 350 nm.

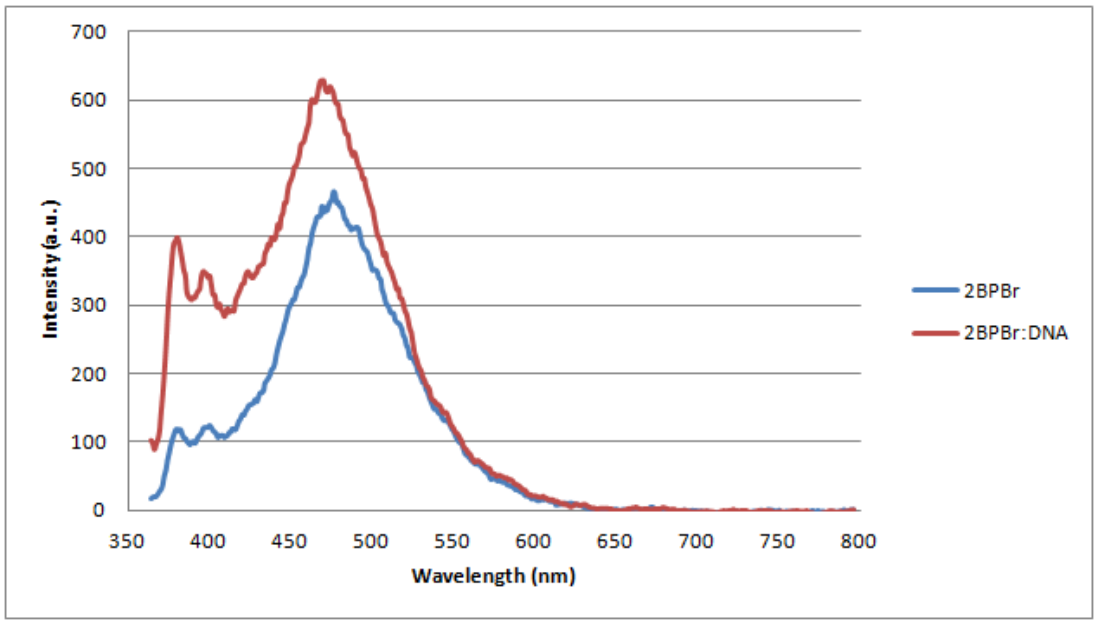

Figure A6 The fluorescence spectra of **2BPBr** in the absence and presence of DNA target in 10 mM phosphate buffer pH 7.0, [PNA] = 2.5 μM and [DNA] = 3.0 μM, λ_{excit} = 350 nm.

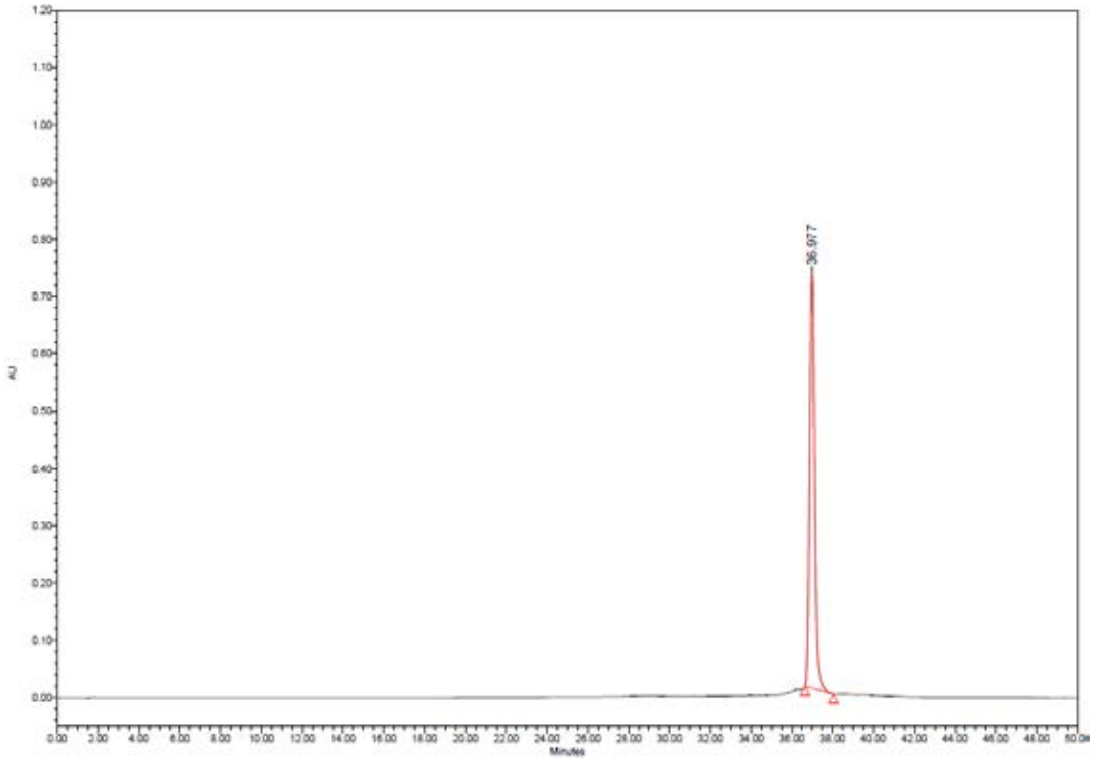

(a)

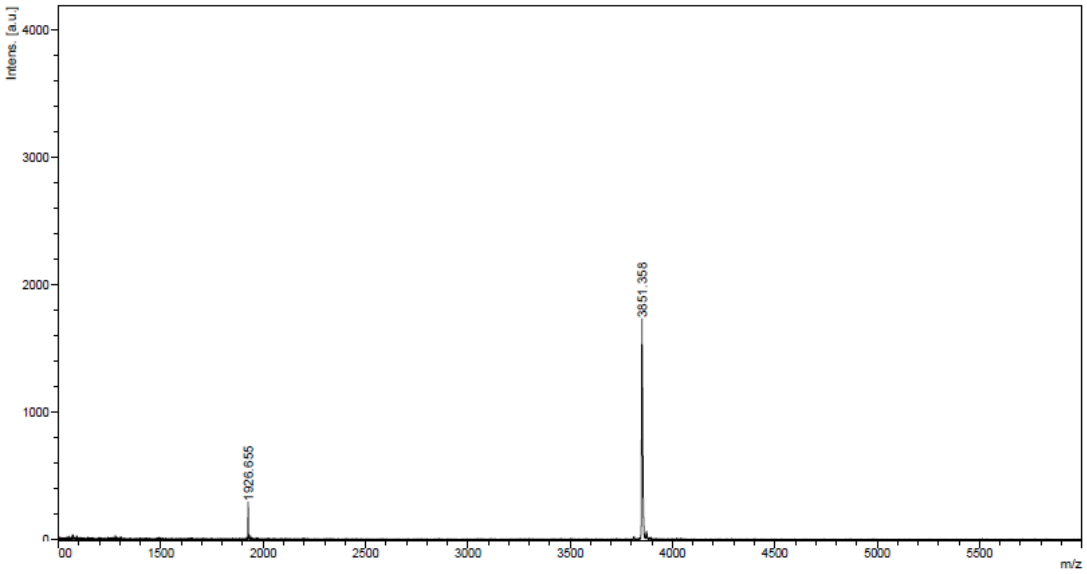

(b)

Figure A7 (a) Analytical HPLC chromatogram and (b) MALDI-TOF mass spectrum of **3BPBr** (calcd for $[M+H]^+$ = 3850.24)

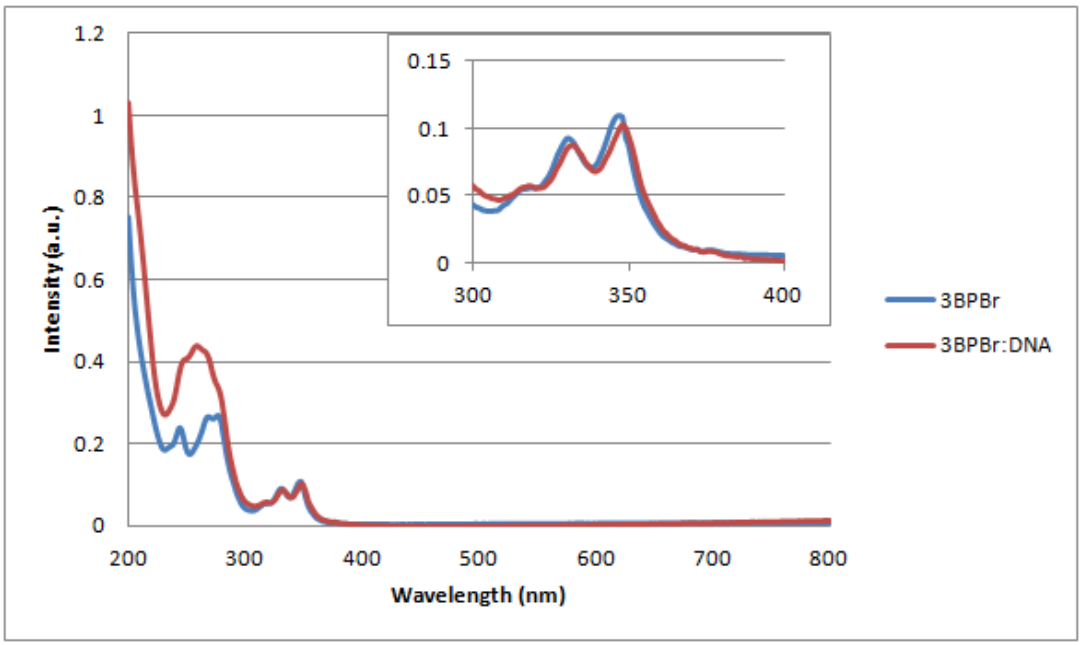

Figure A8 UV-Vis spectra of **3BPBr** in the absence and presence of DNA target in 10 mM phosphate buffer pH 7.0, [PNA] = 2.5 μM and [DNA] = 3.0 μM, λ_{excit} = 350 nm.

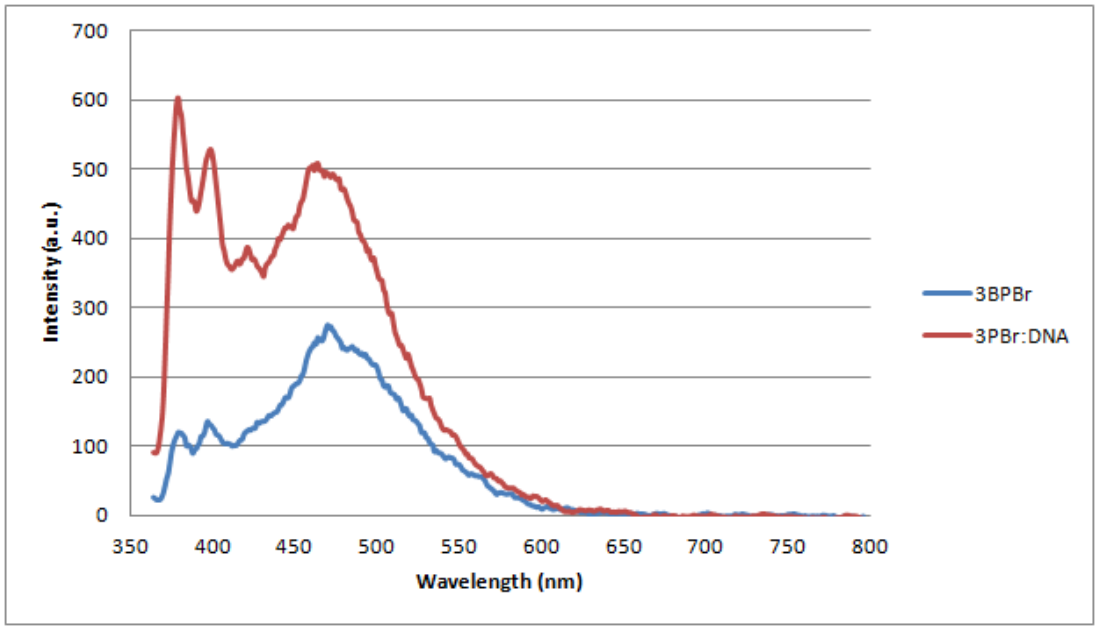

Figure A9 The fluorescence spectra of **3BPBr** in the absence and presence of DNA target in 10 mM phosphate buffer pH 7.0, [PNA] = 2.5 μM and [DNA] = 3.0 μM, λ_{excit} = 350 nm.

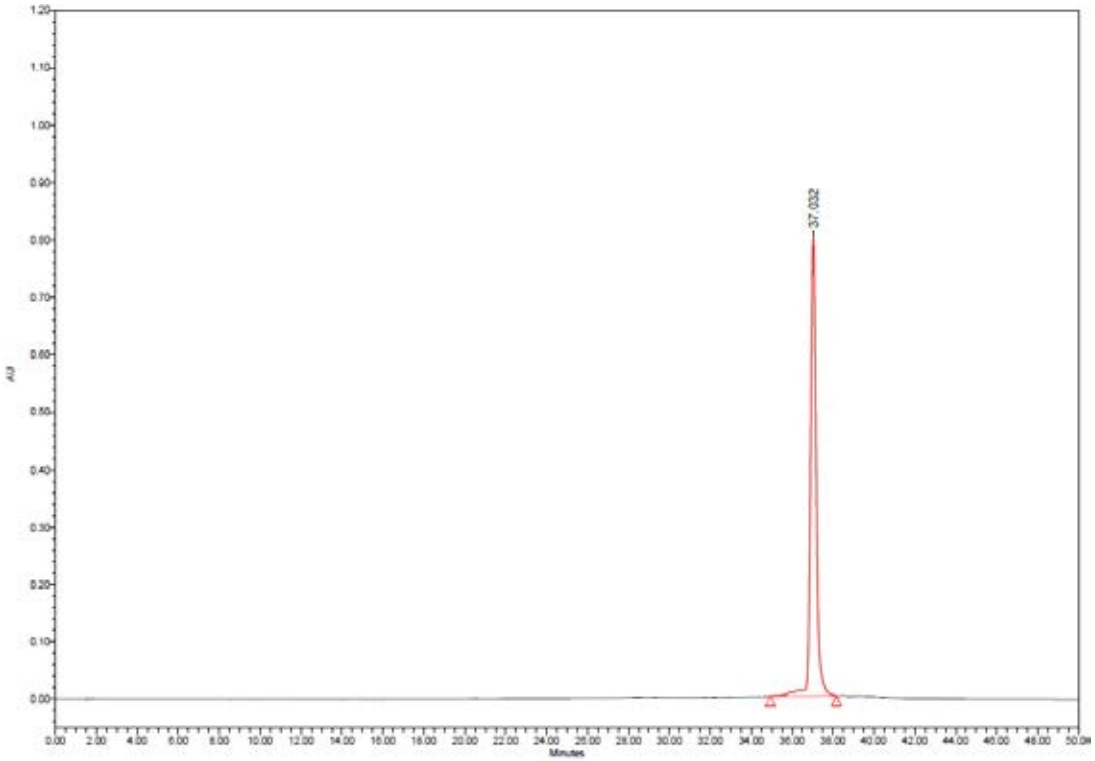

(a)

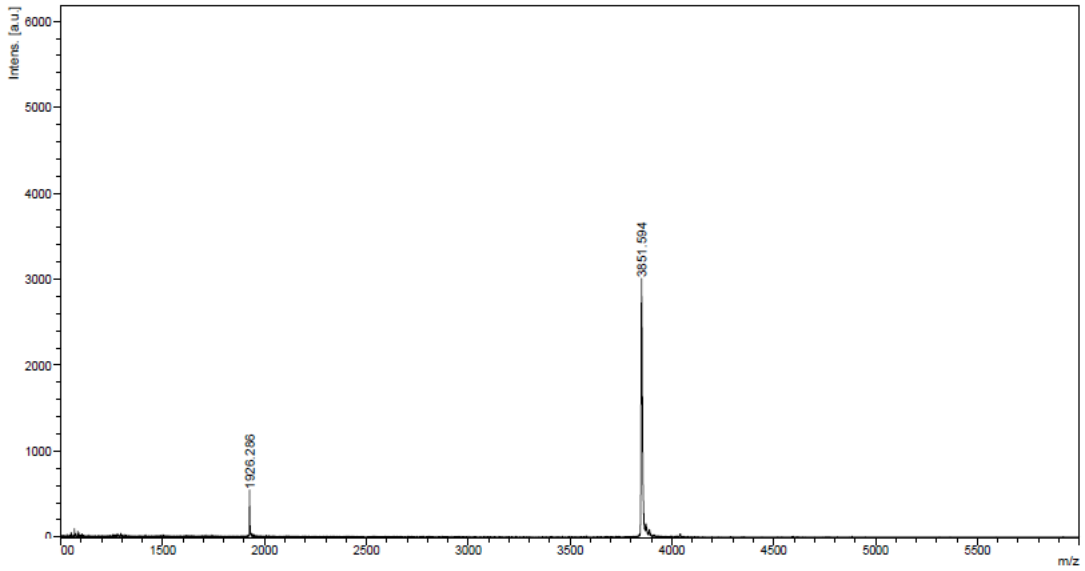

(b)

Figure A10 (a) Analytical HPLC chromatogram and (b) MALDI-TOF mass spectrum of **4BPBr** (calcd for $[M+H]^+ = 3850.24$)

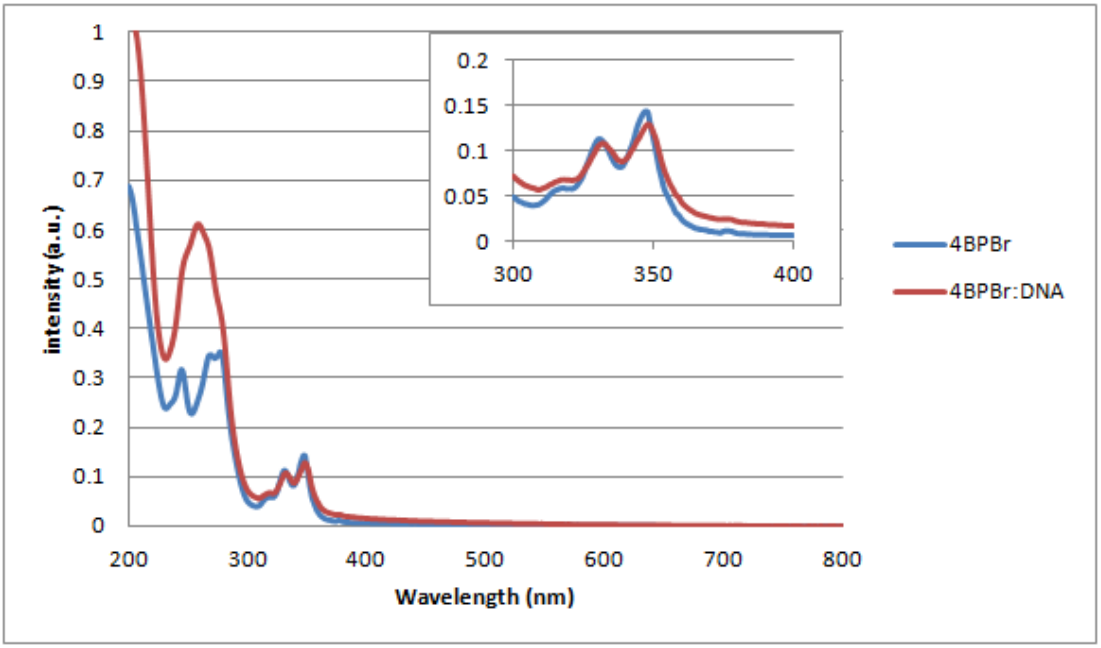

Figure A11 UV-Vis spectra of **4BPBr** in the absence and presence of DNA target in 10 mM phosphate buffer pH 7.0, [PNA] = 2.5 μM and [DNA] = 3.0 μM, λ_{excit} = 350 nm.

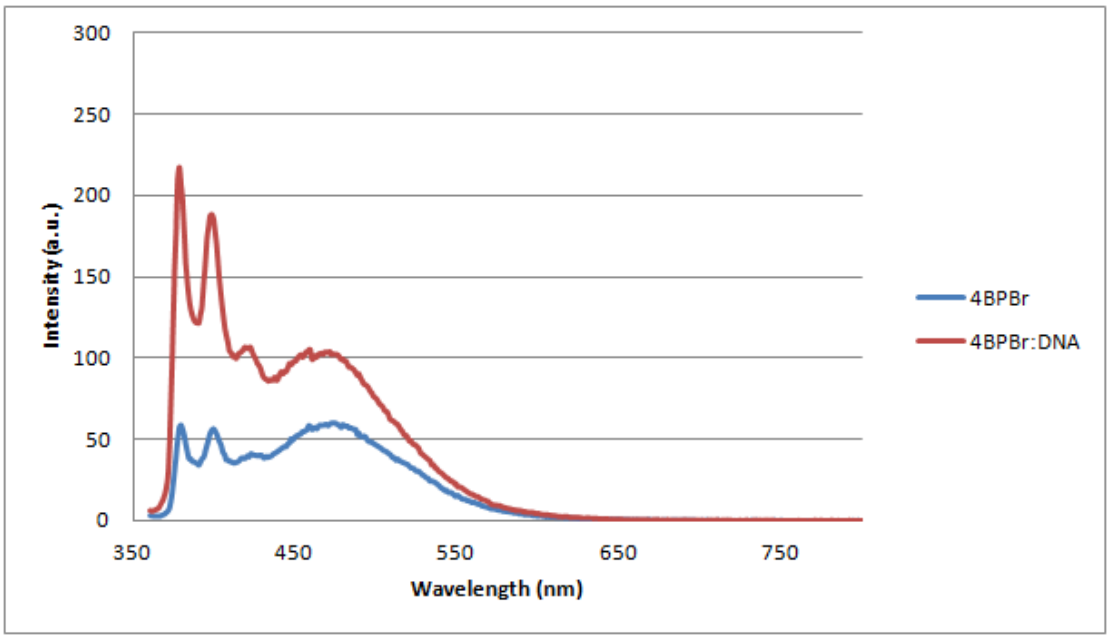

Figure A12 The fluorescence spectra of **4BPBr** in the absence and presence of DNA target in 10 mM phosphate buffer pH 7.0, [PNA] = 2.5 μM and [DNA] = 3.0 μM, λ_{excit} = 350 nm.

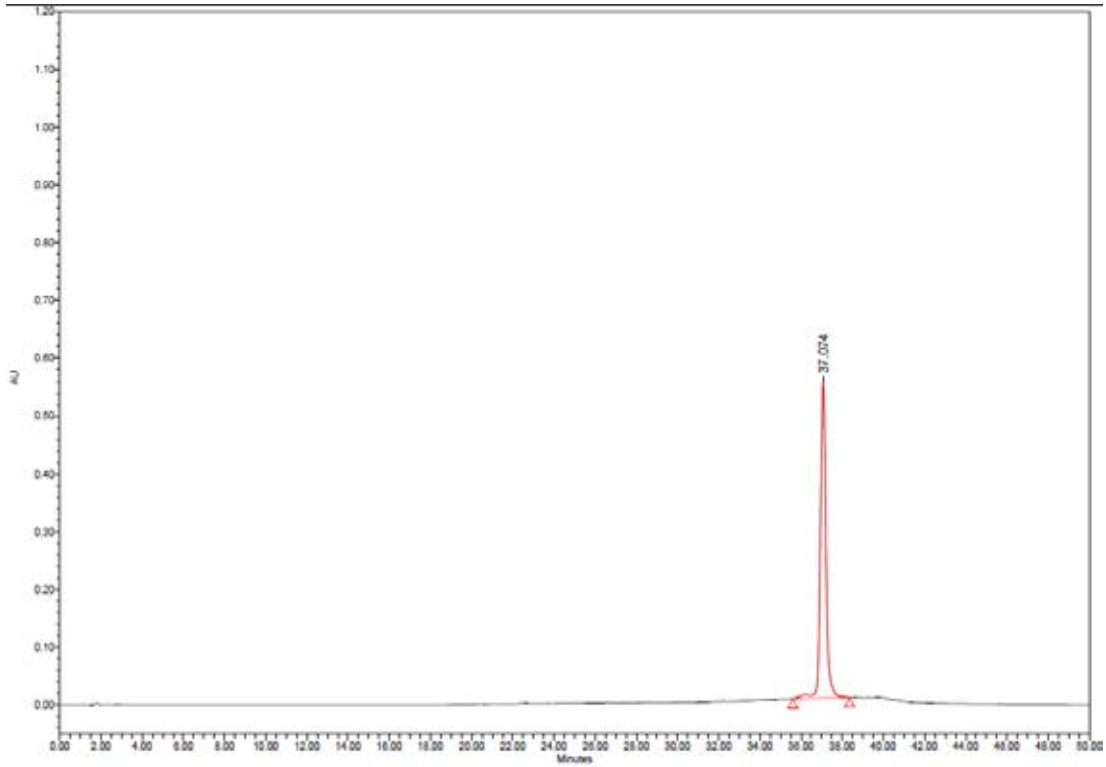

(a)

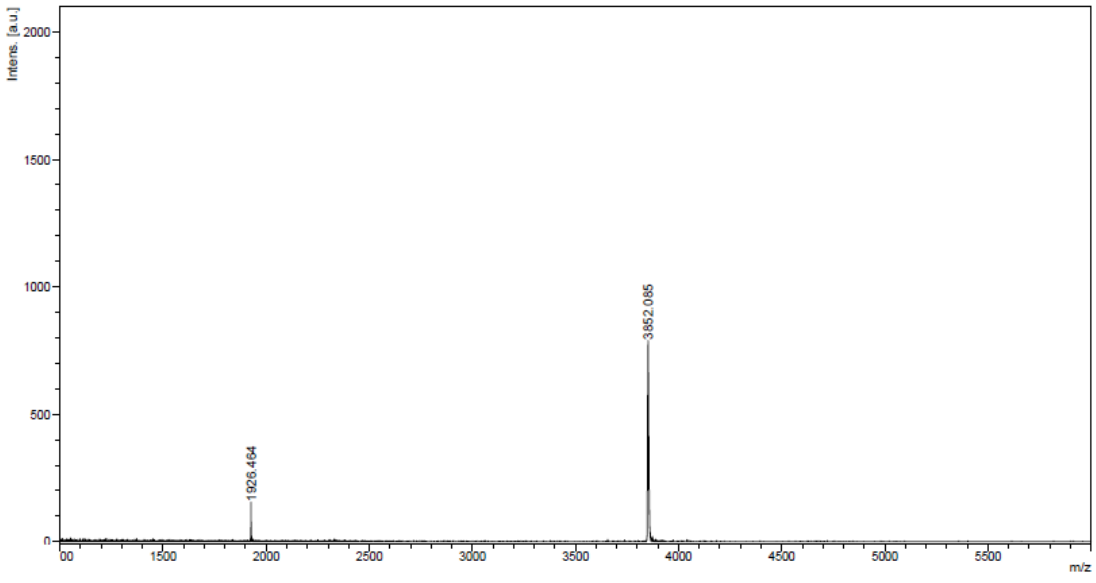

(b)

Figure A13 (a) Analytical HPLC chromatogram and (b) MALDI-TOF mass spectrum of **5BPBr** (calcd for $[M+H]^+$ = 3850.24)

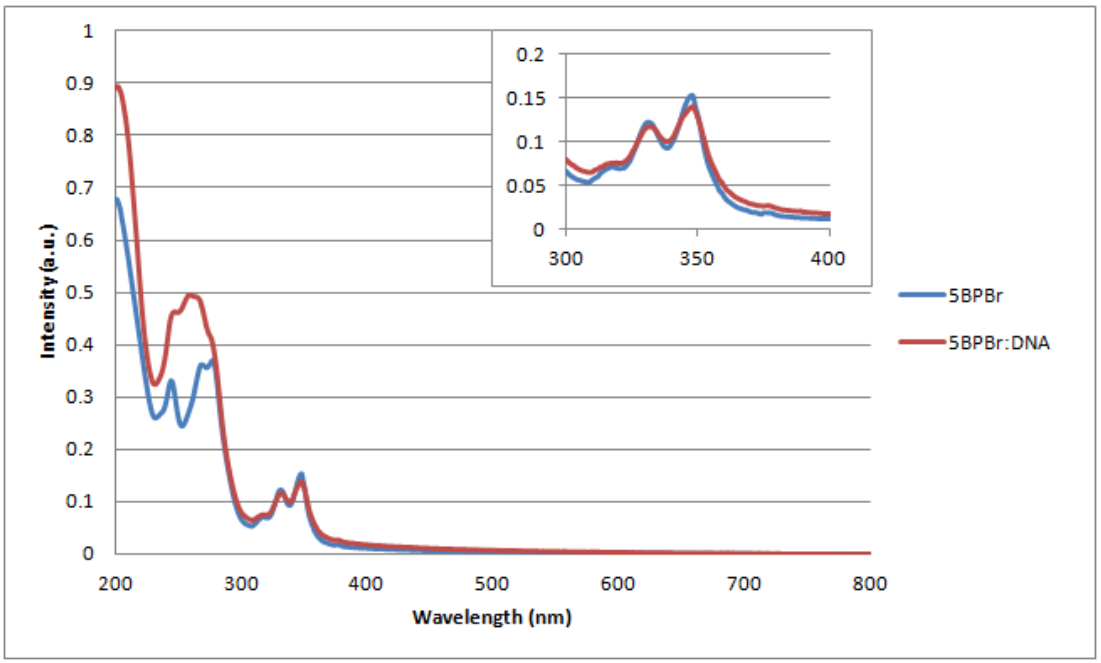

Figure A14 UV-Vis spectra of **5BPBr** in the absence and presence of DNA target in 10 mM phosphate buffer pH 7.0, [PNA] = 2.5 μM and [DNA] = 3.0 μM, λ_{excit} = 350 nm.

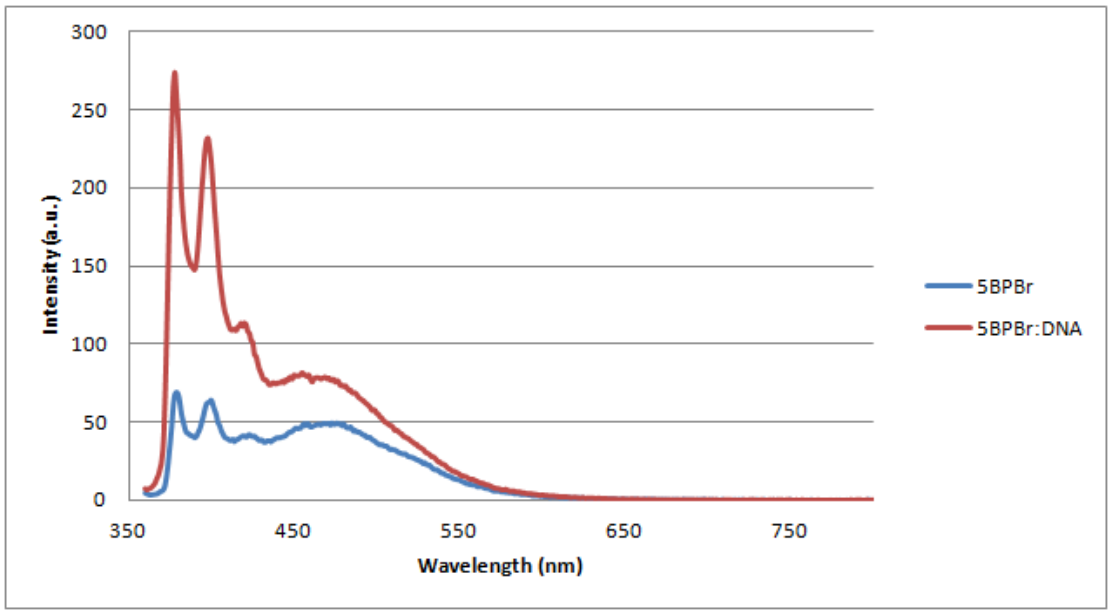

Figure A15 The fluorescence spectra of **5BPBr** in the absence and presence of DNA target in 10 mM phosphate buffer pH 7.0, [PNA] = 2.5 μM and [DNA] = 3.0 μM, λ_{excit} = 350 nm.

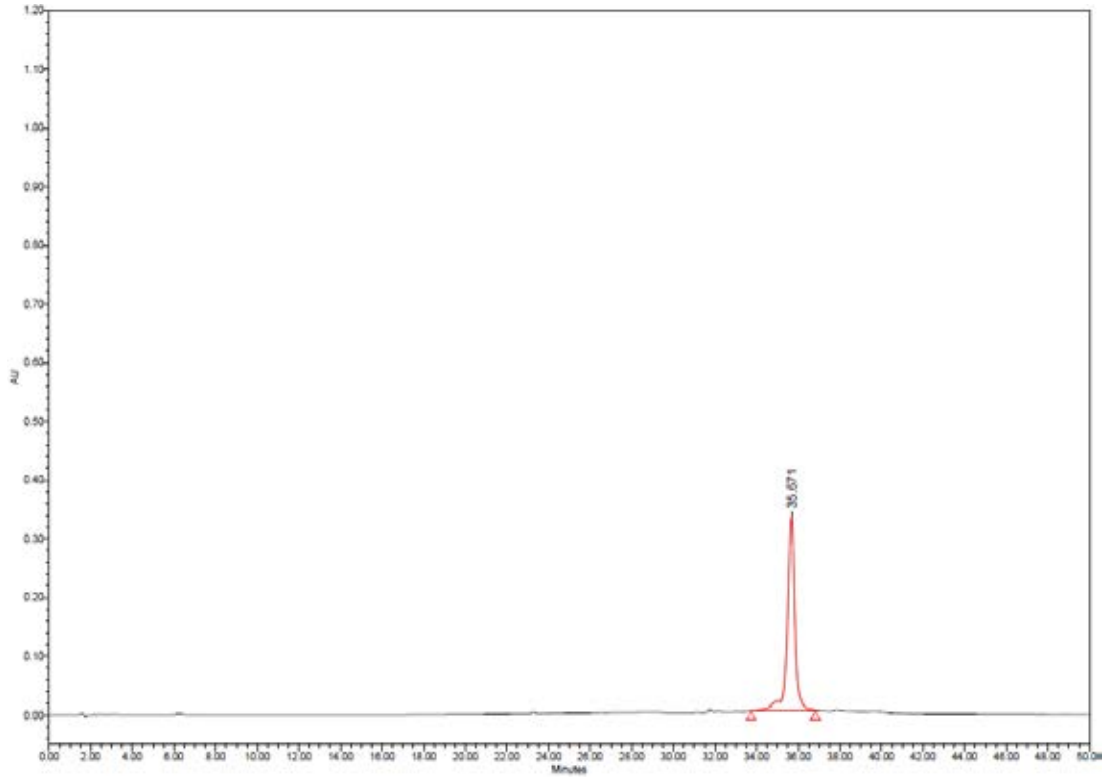

(a)

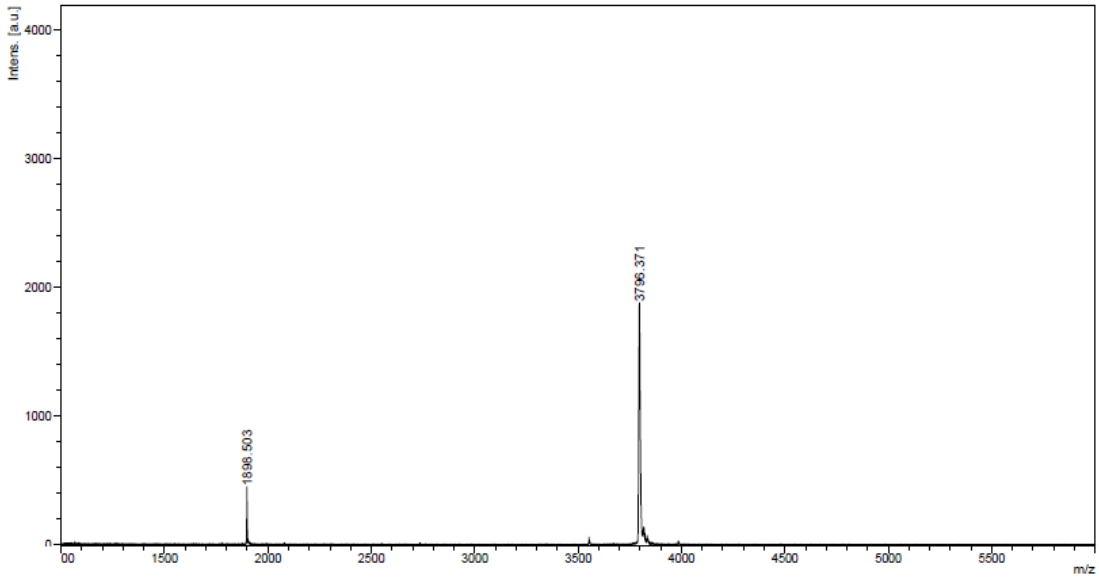

(b)

Figure A16 (a) Analytical HPLC chromatogram and (b) MALDI-TOF mass spectrum of **3BPAc** (calcd for $[M+H]^+ = 3794.08$)

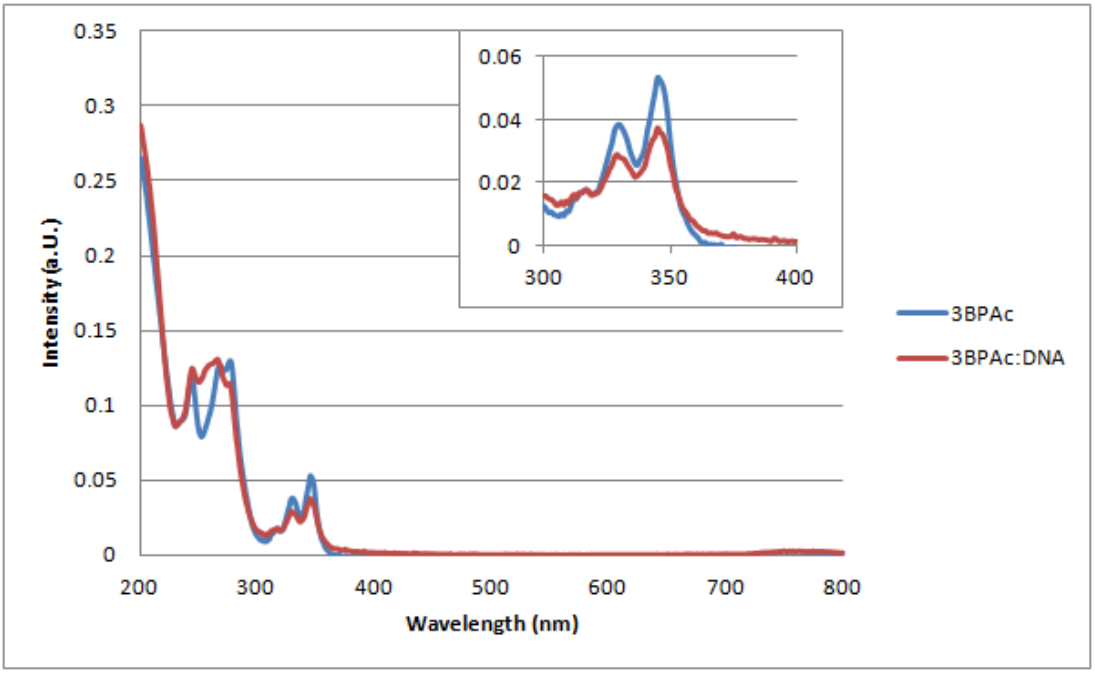

Figure A17 UV-Vis spectra of **3BPAc** in the absence and presence of DNA target in 10 mM phosphate buffer pH 7.0, [PNA] = 2.5 μM and [DNA] = 3.0 μM, λ_{excit} = 350 nm.

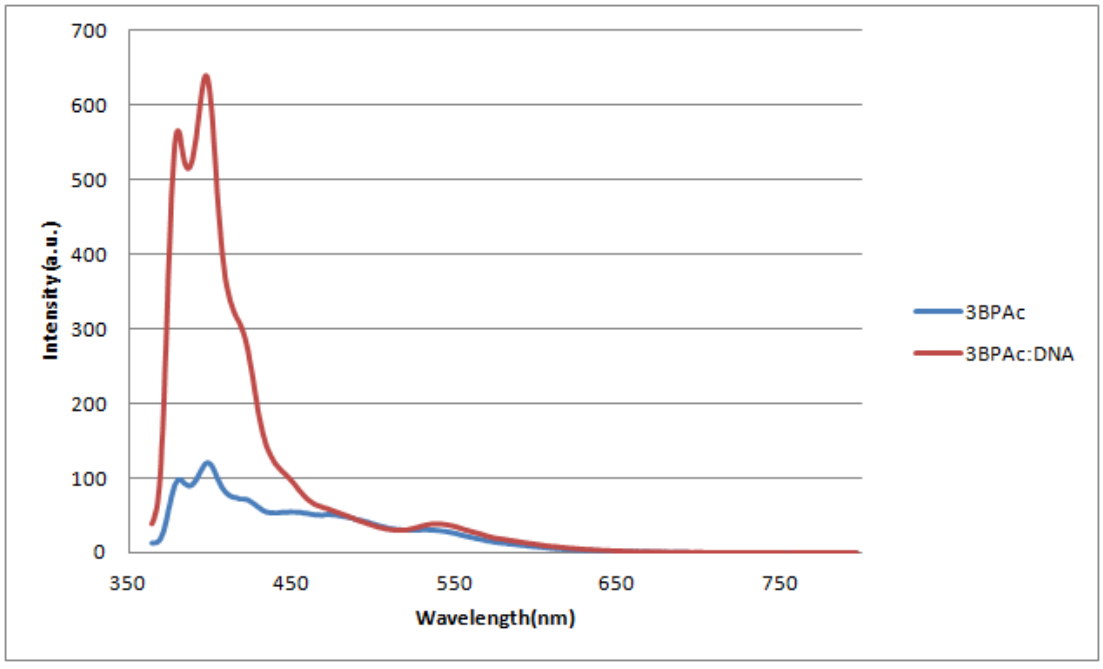

Figure A18 The fluorescence spectra of **3BPAc** in the absence and presence of DNA target in 10 mM phosphate buffer pH 7.0, [PNA] = 2.5 μM and [DNA] = 3.0 μM, λ_{excit} = 350 nm.

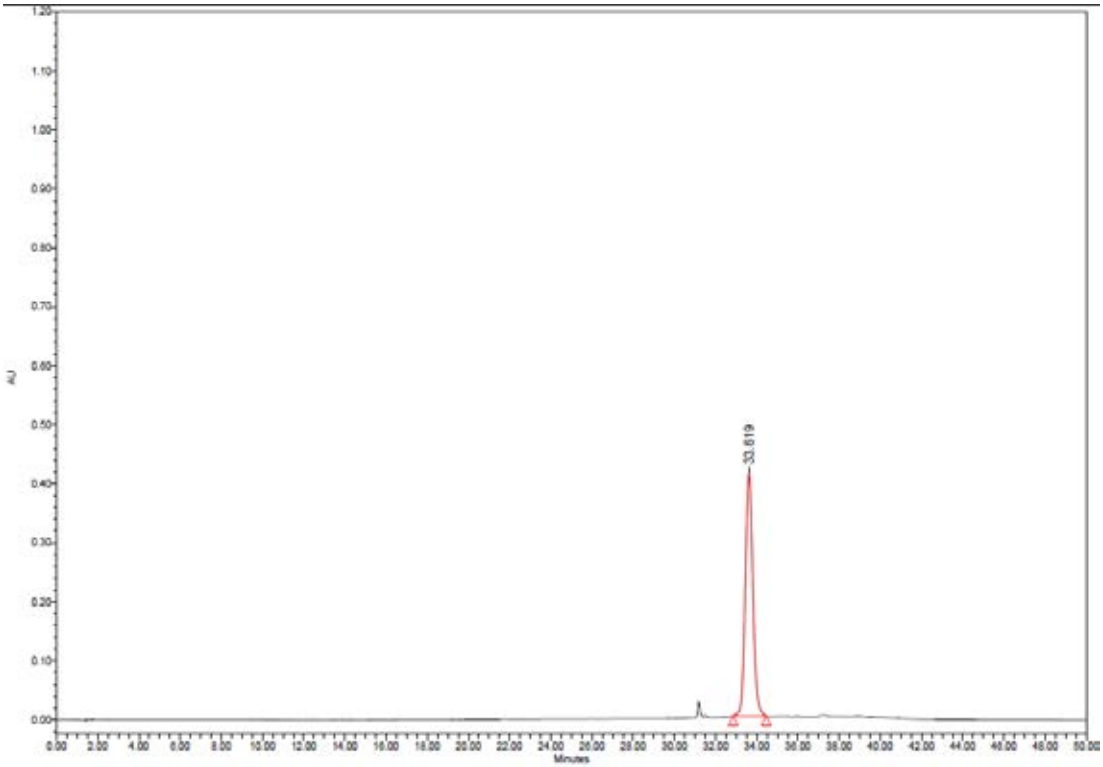

(a)

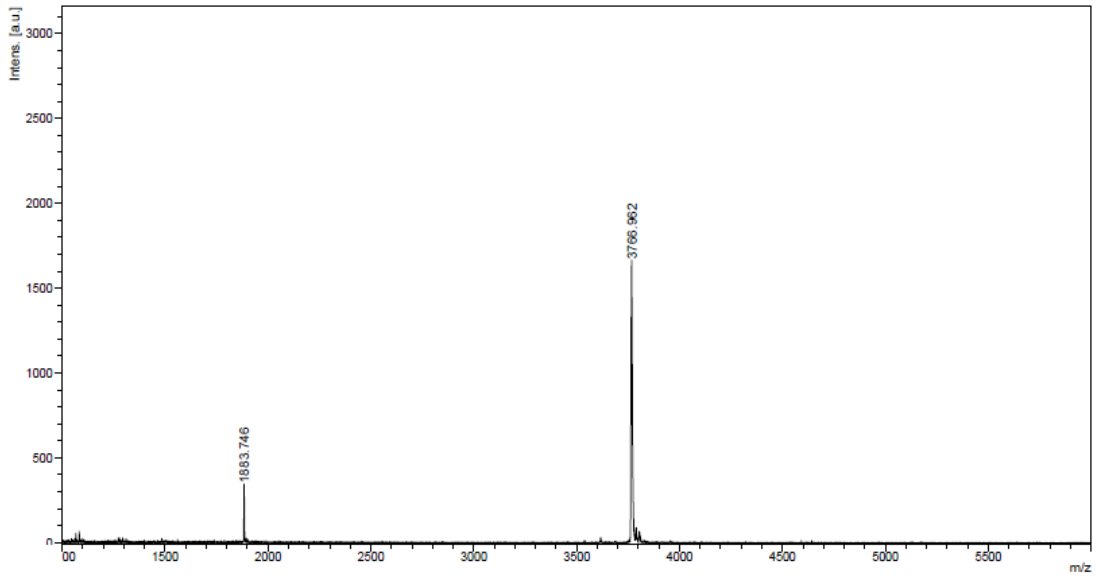

(b)

Figure A19 (a) Analytical HPLC chromatogram and (b) MALDI-TOF mass spectrum of **3BPCO** (calcd for $[M+H]^+$ = 3766.08)

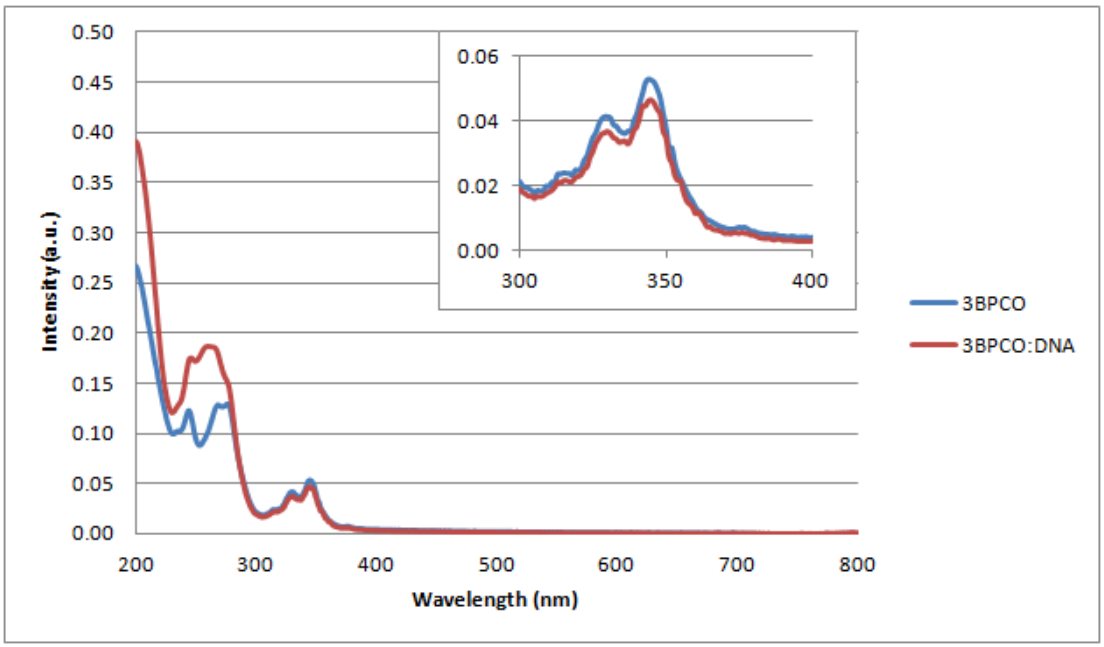

Figure A20 UV-Vis spectra of **3BPCO** in the absence and presence of DNA target in 10 mM phosphate buffer pH 7.0, [PNA] = 2.5 μM and [DNA] = 3.0 μM, λ_{excit} = 350 nm.

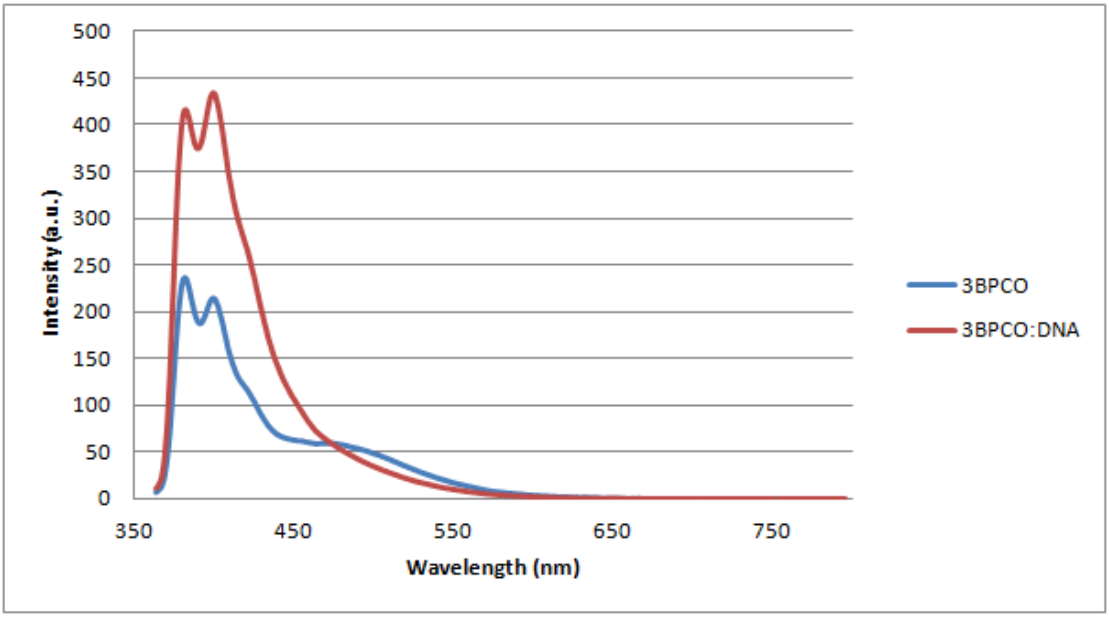

Figure A21 The fluorescence spectra of **1BPCO** in the absence and presence of DNA target in 10 mM phosphate buffer pH 7.0, [PNA] = 2.5 μM and [DNA] = 3.0 μM, λ_{excit} = 350 nm.

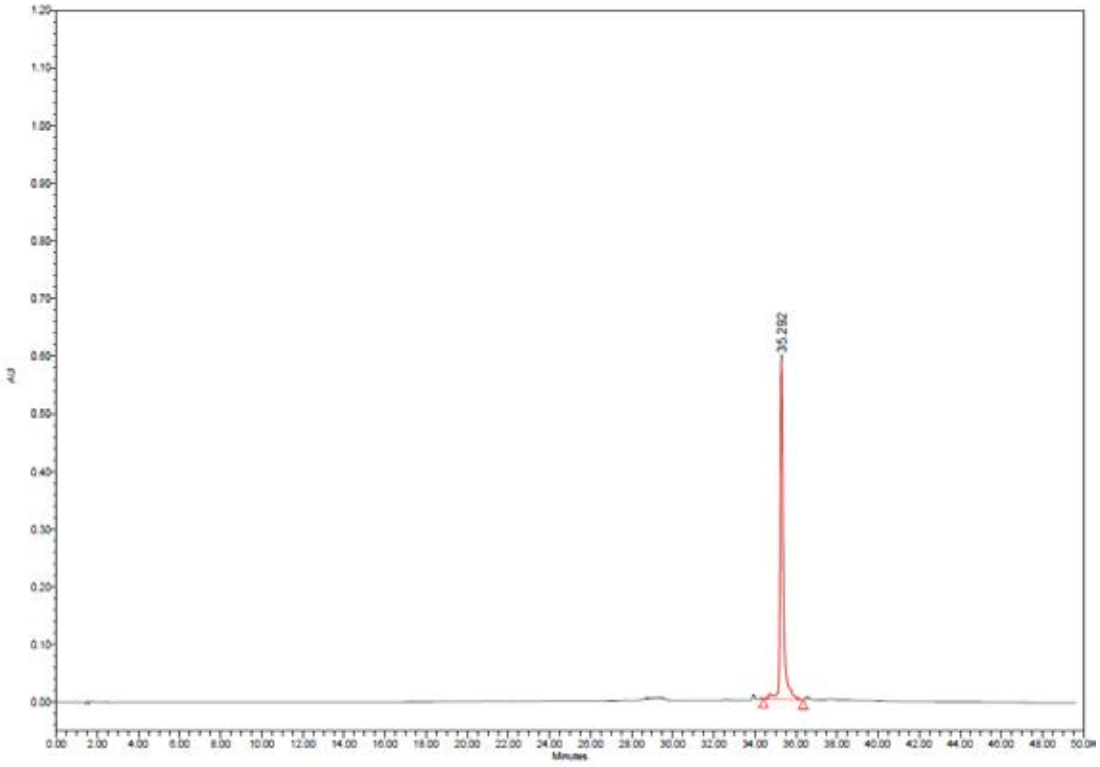

(a)

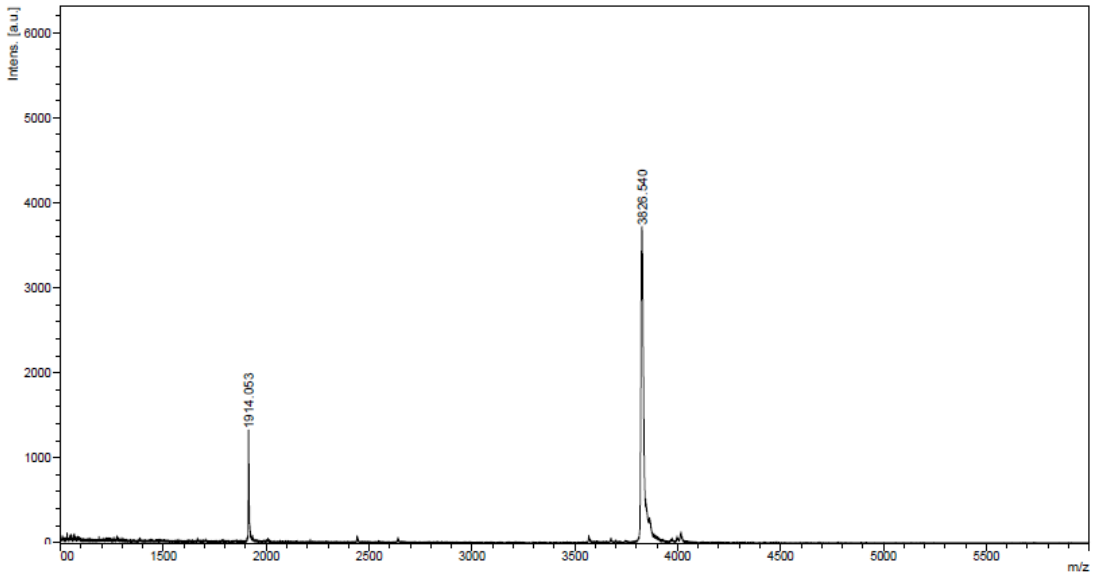

(b)

Figure A22 (a) Analytical HPLC chromatogram and (b) MALDI-TOF mass spectrum of **3BPBt** (calcd for $[M+H]^+$ = 3822.27)

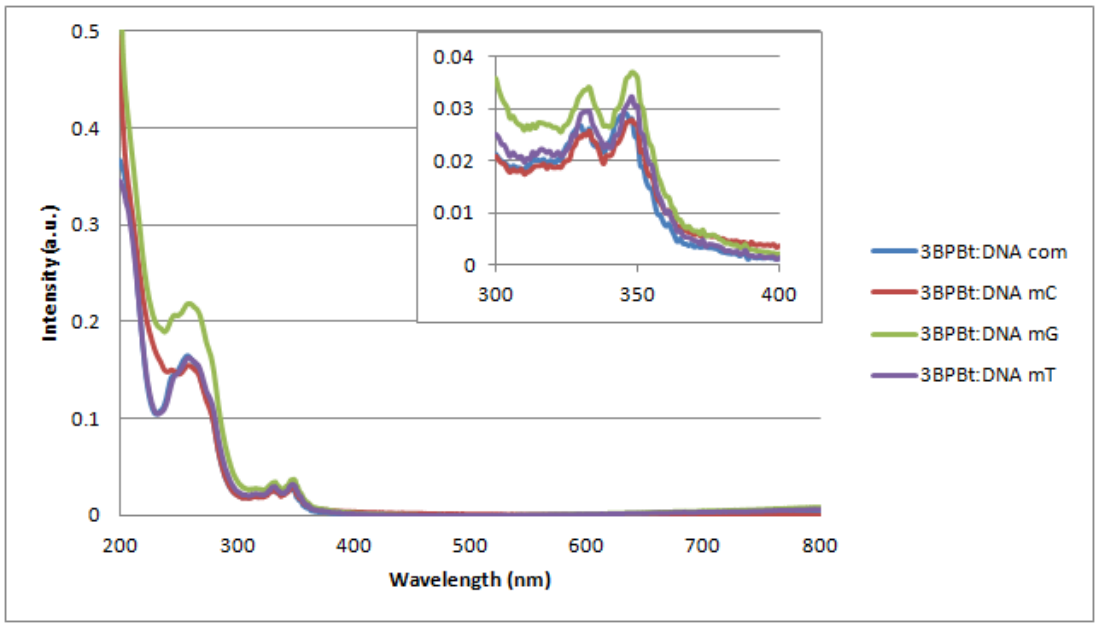

Figure A23 UV-Vis spectra of **3BPBt** in the absence and presence of DNA target in 10 mM phosphate buffer pH 7.0, [PNA] = 1.0 μM and [DNA] = 1.2 μM, λ_{excit} = 350 nm.

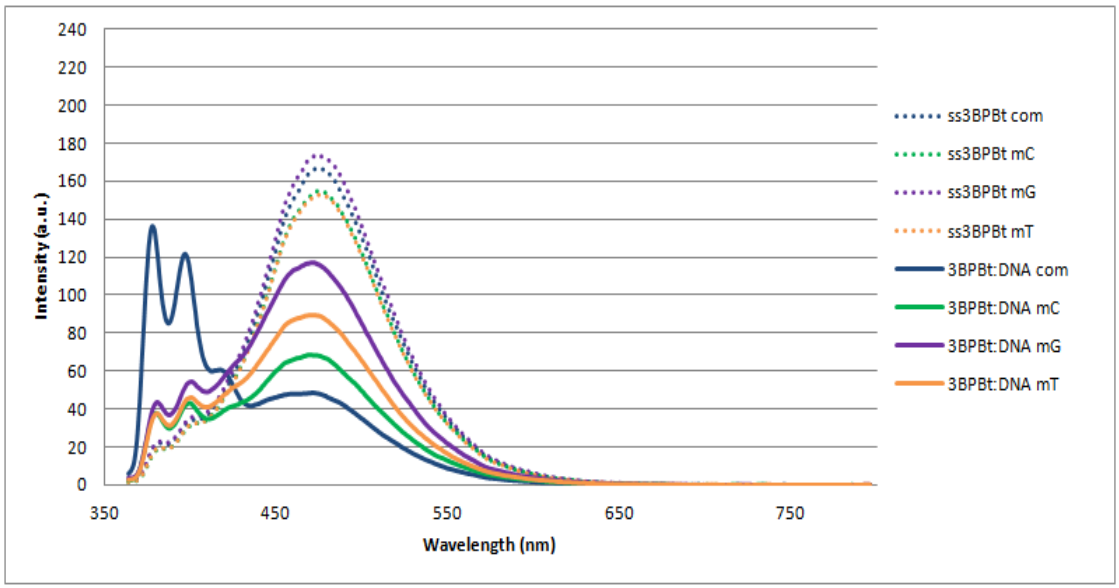

Figure A24 The fluorescence spectra of **3BPBt** in the absence and presence of complementary and mismatched DNA targets in 10 mM phosphate buffer pH 7.0, [PNA] = 1.0 μM and [DNA] = 1.2 μM, λ_{excit} = 350 nm.

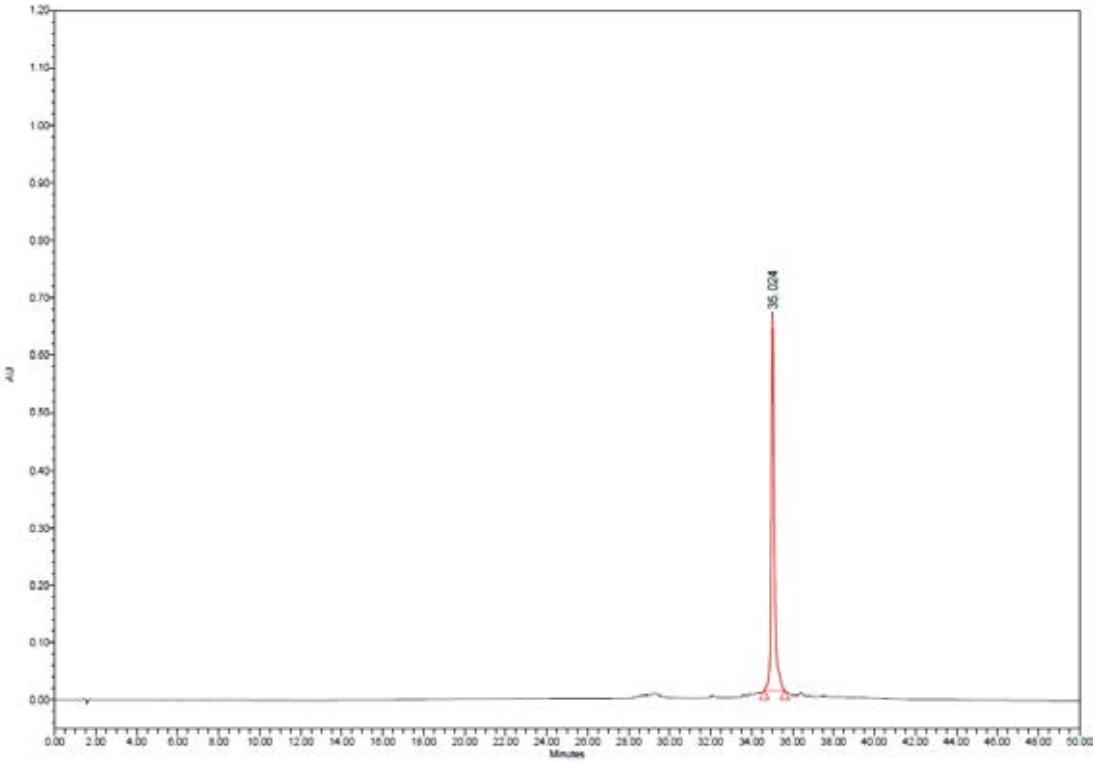

(a)

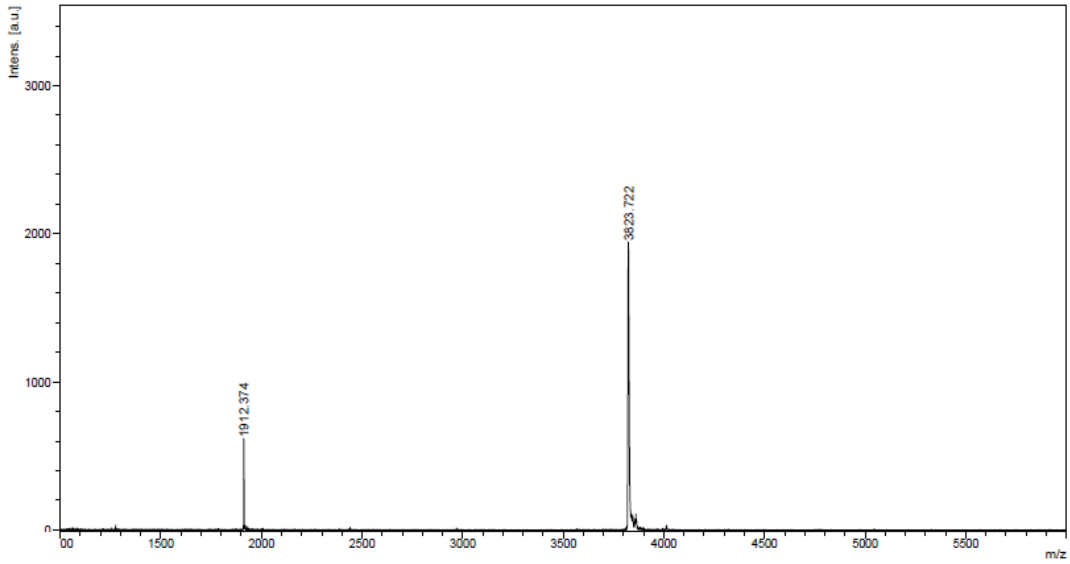

(b)

Figure A25 (a) Analytical HPLC chromatogram and (b) MALDI-TOF mass spectrum of **4BPBt** (calcd for $[M+H]^+$ = 3822.27)

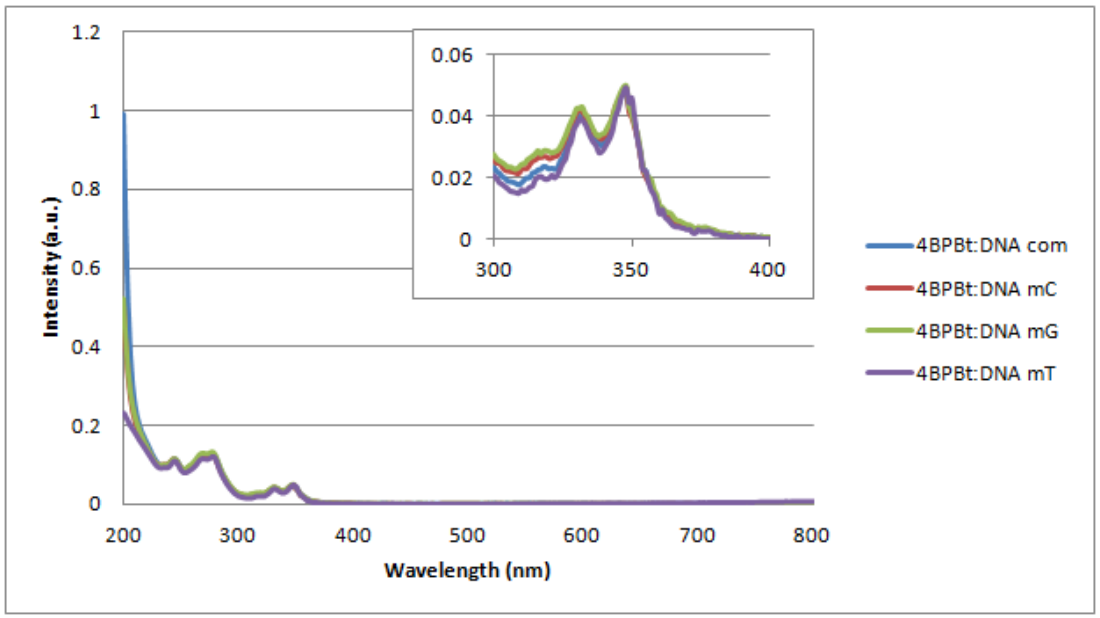

Figure A26 UV-Vis spectra of **4BPBt** in the absence and presence of DNA target in 10 mM phosphate buffer pH 7.0, [PNA] = 1.0 μM and [DNA] = 1.2 μM, λ_{excit} = 350 nm.

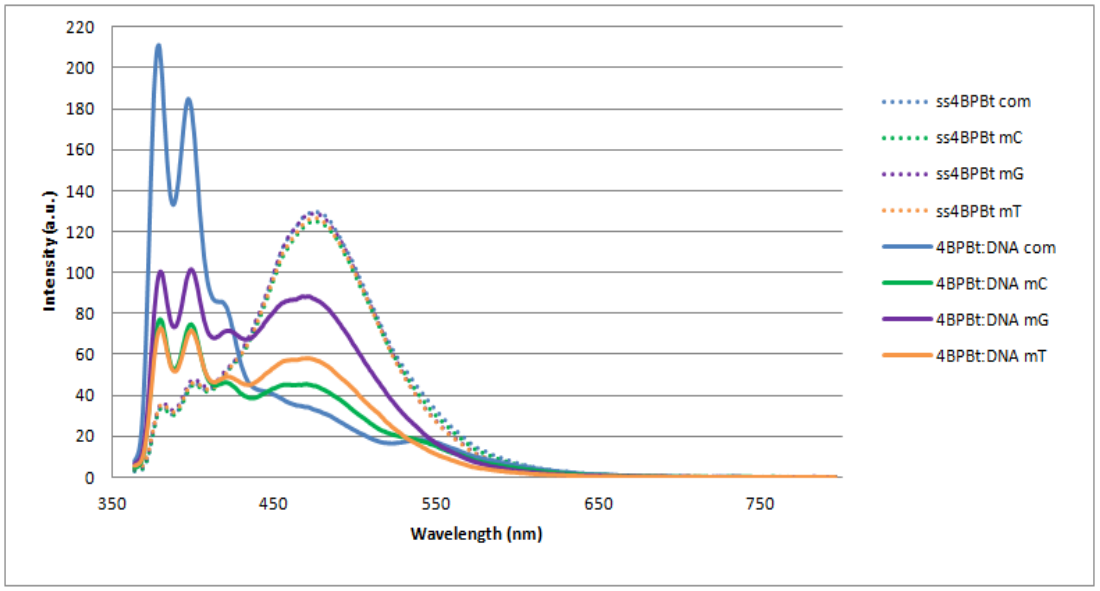

Figure A27 The fluorescence spectra of **4BPBt** in the absence and presence of complementary and mismatched DNA targets in 10 mM phosphate buffer pH 7.0, [PNA] = 1.0 μM and [DNA] = 1.2 μM, λ_{excit} = 350 nm.

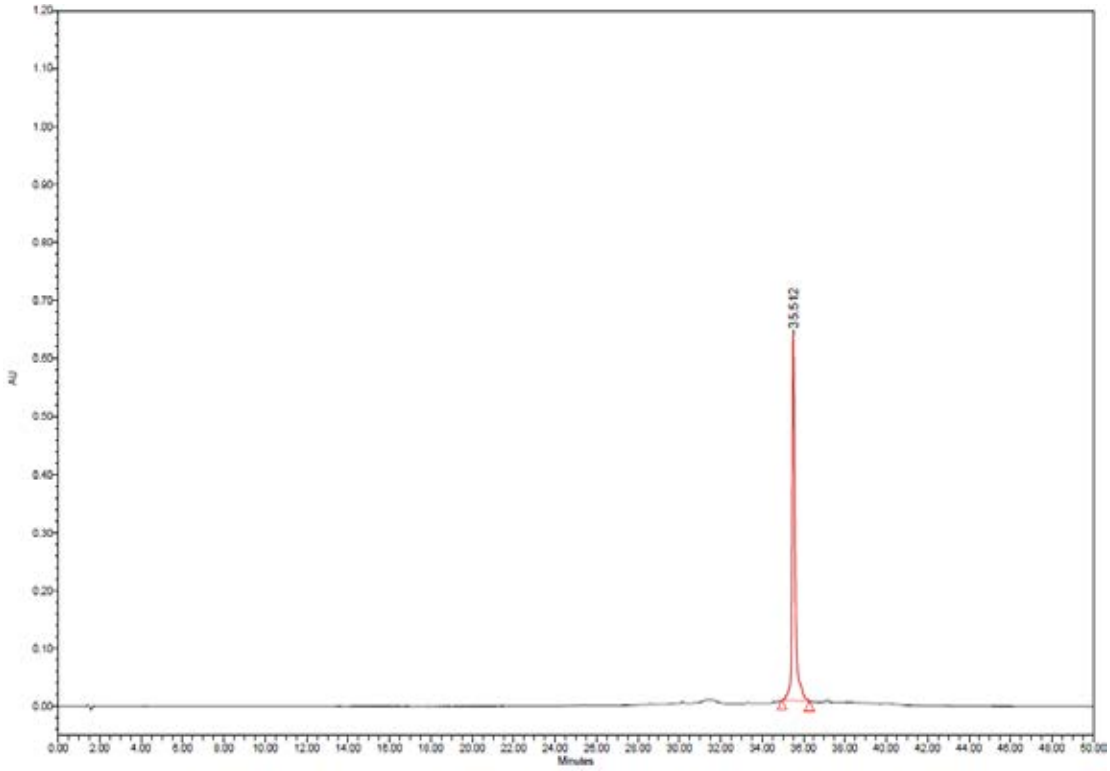

(a)

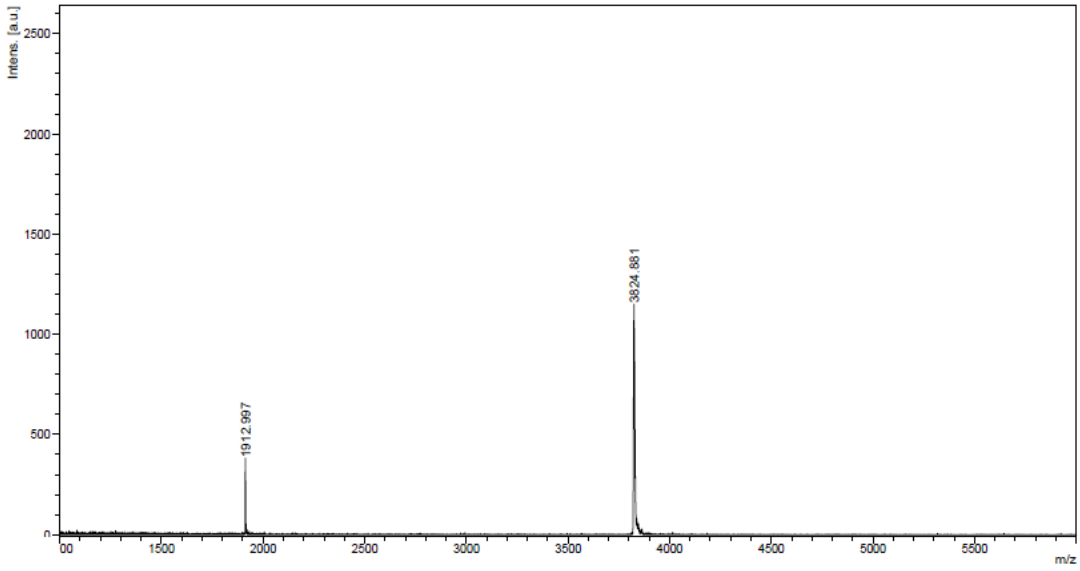

(b)

Figure A28 (a) Analytical HPLC chromatogram and (b) MALDI-TOF mass spectrum of **5BPBt** (calcd for $[M+H]^+$ = 3822.27)

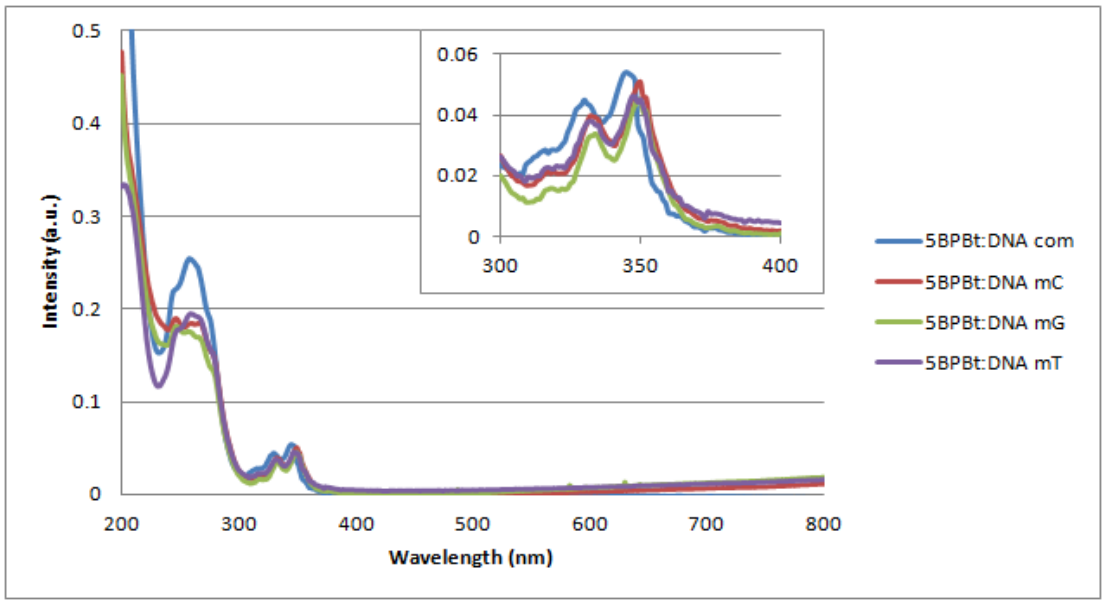

Figure A29 UV-Vis spectra of **5BPBt** in the absence and presence of complementary and mismatched DNA targets in 10 mM phosphate buffer pH 7.0, [PNA] = 1.0 μM and [DNA] = 1.2 μM, λ_{excit} = 350 nm.

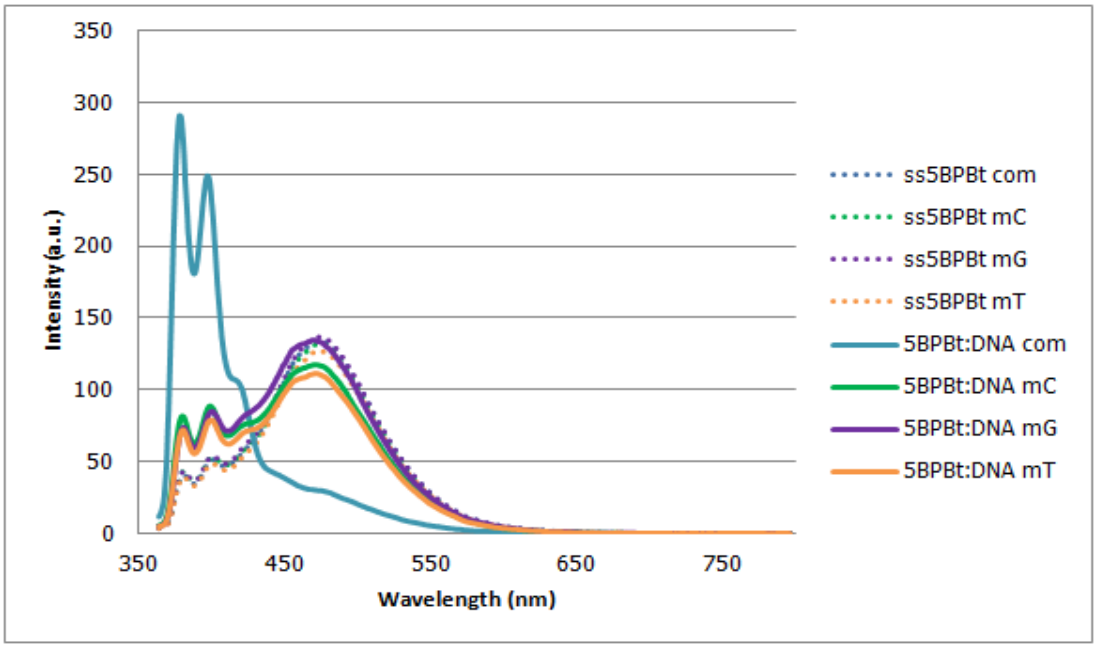

Figure A30 The fluorescence spectra of **5BPBt** in the absence and presence of complementary and mismatched DNA targets in 10 mM phosphate buffer pH 7.0, [PNA] = 1.0 μM and [DNA] = 1.2 μM, λ_{excit} = 350 nm.

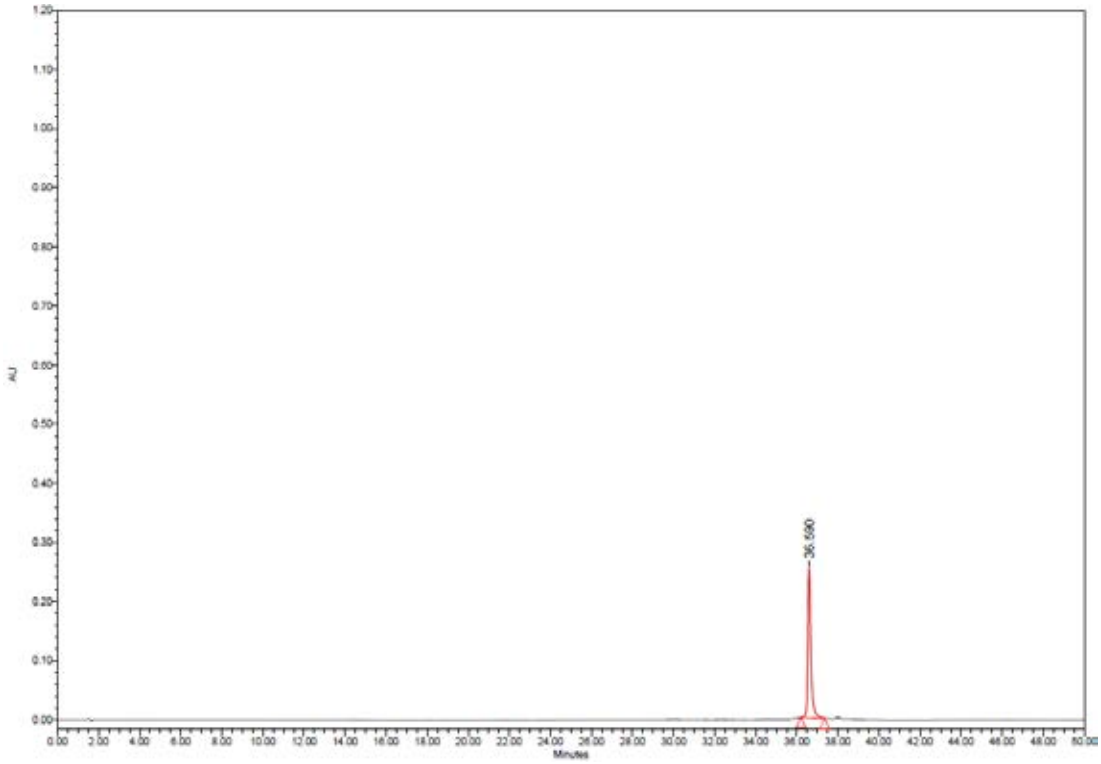

(a)

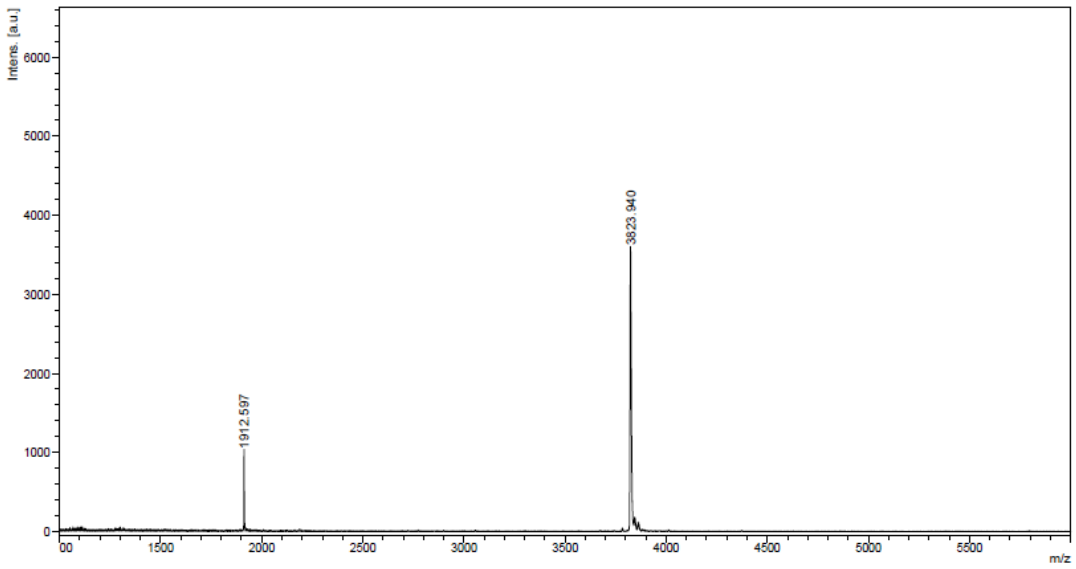

(b)

Figure A31 (a) Analytical HPLC chromatogram and (b) MALDI-TOF mass spectrum of **6BPBt** (calcd for $[M+H]^+$ = 3822.27)

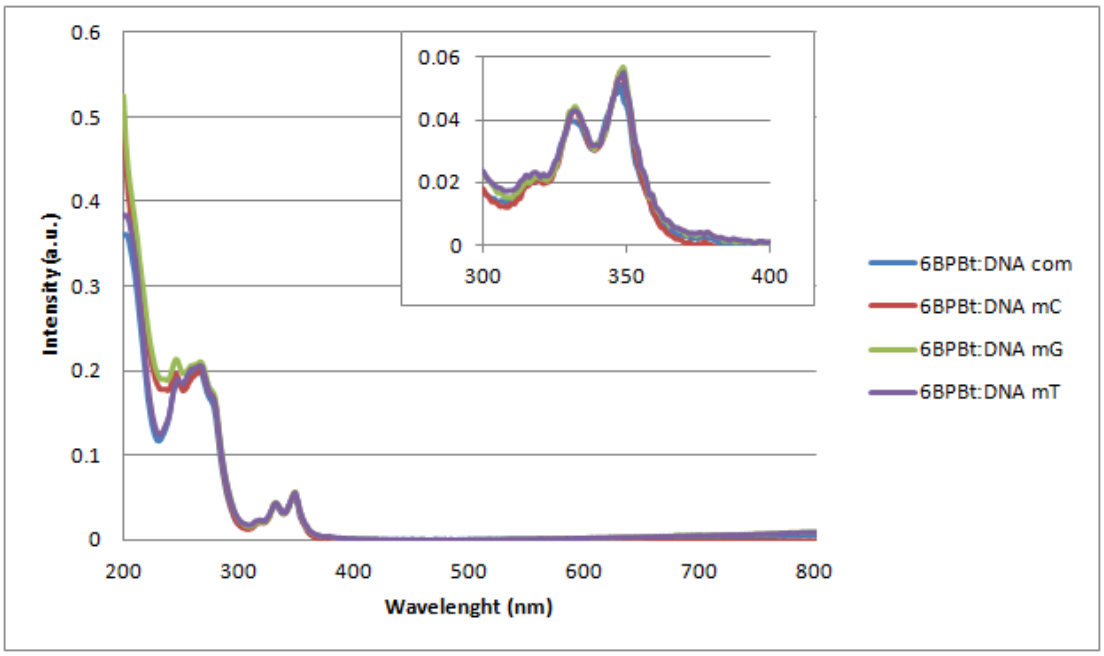

Figure A32 UV-Vis spectra of **6BPBt** in the absence and presence of DNA target in 10 mM phosphate buffer pH 7.0, [PNA] = 1.0 μM and [DNA] = 1.2 μM, λ_{excit} = 350 nm.

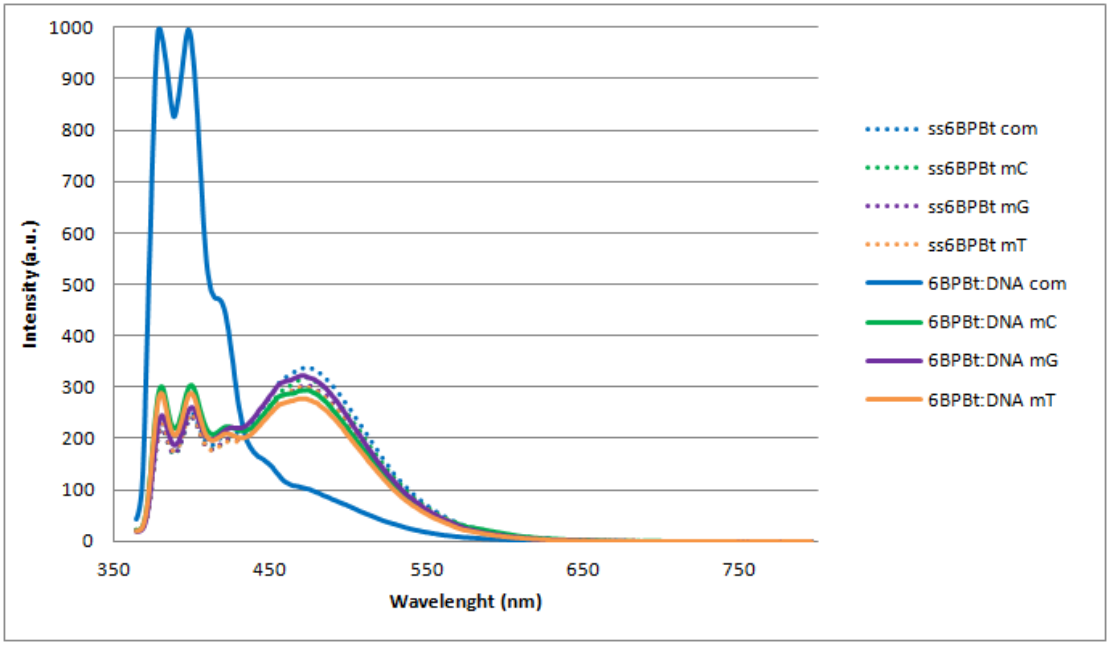

Figure A33 The fluorescence spectra of **6BPBt** in the absence and presence of complementary and mismatched DNA targets in 10 mM phosphate buffer pH 7.0, [PNA] = 1.0 μM and [DNA] = 1.2 μM, λ_{excit} = 350 nm.

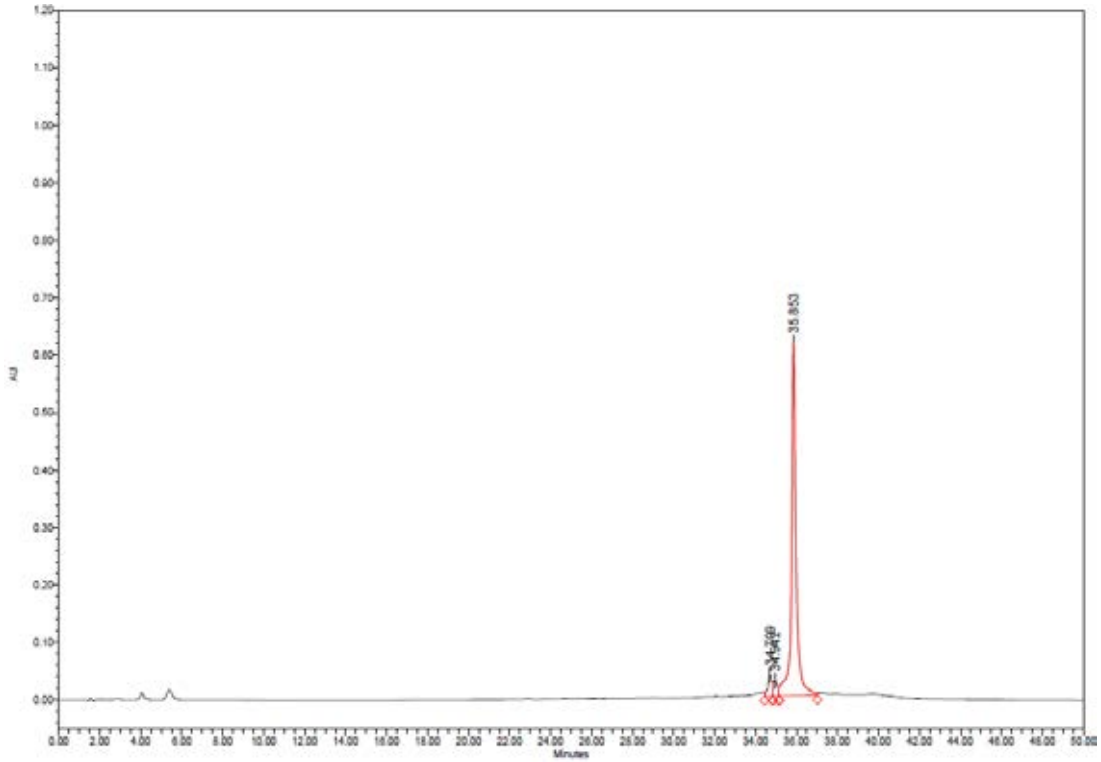

(a)

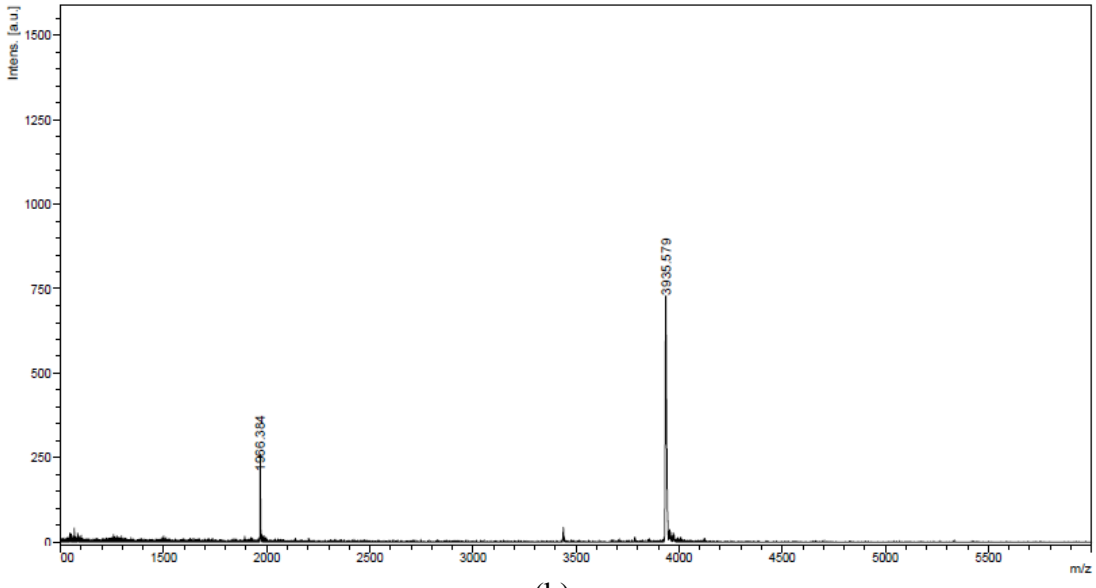

(b)

Figure A34 (a) Analytical HPLC chromatogram and (b) MALDI-TOF mass spectrum of **9BPBt** (calcd for $[M+H]^+$ = 3933.27)

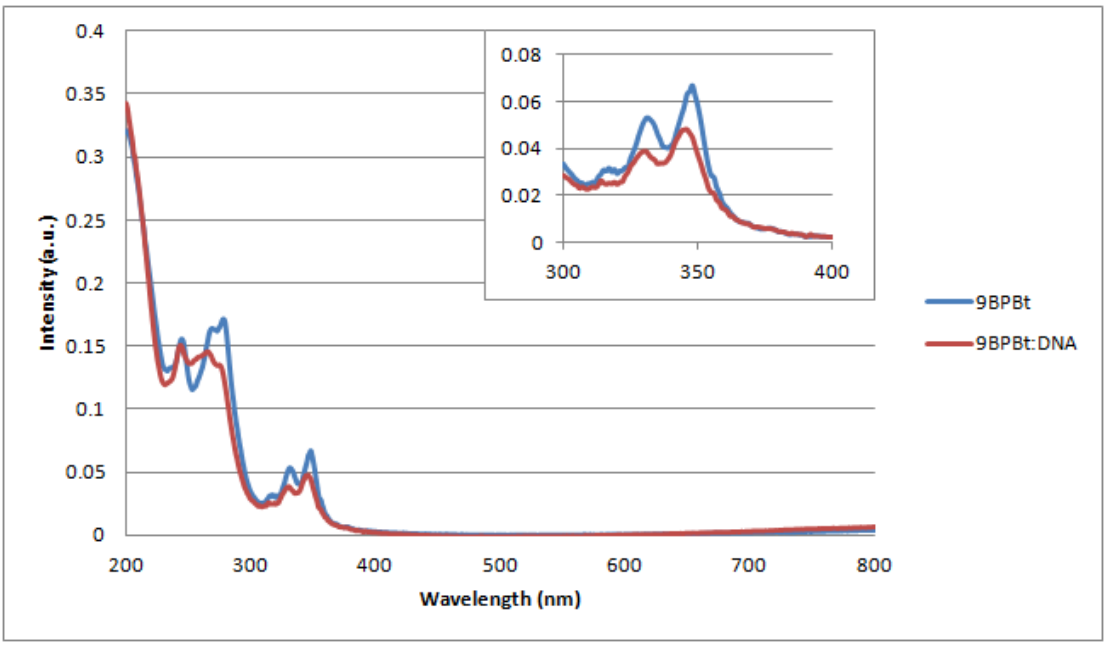

Figure A35 UV-Vis spectra of **9BPBt** in the absence and presence of DNA target in 10 mM phosphate buffer pH 7.0, [PNA] = 1.0 μM and [DNA] = 1.2 μM, λ_{excit} = 350 nm.

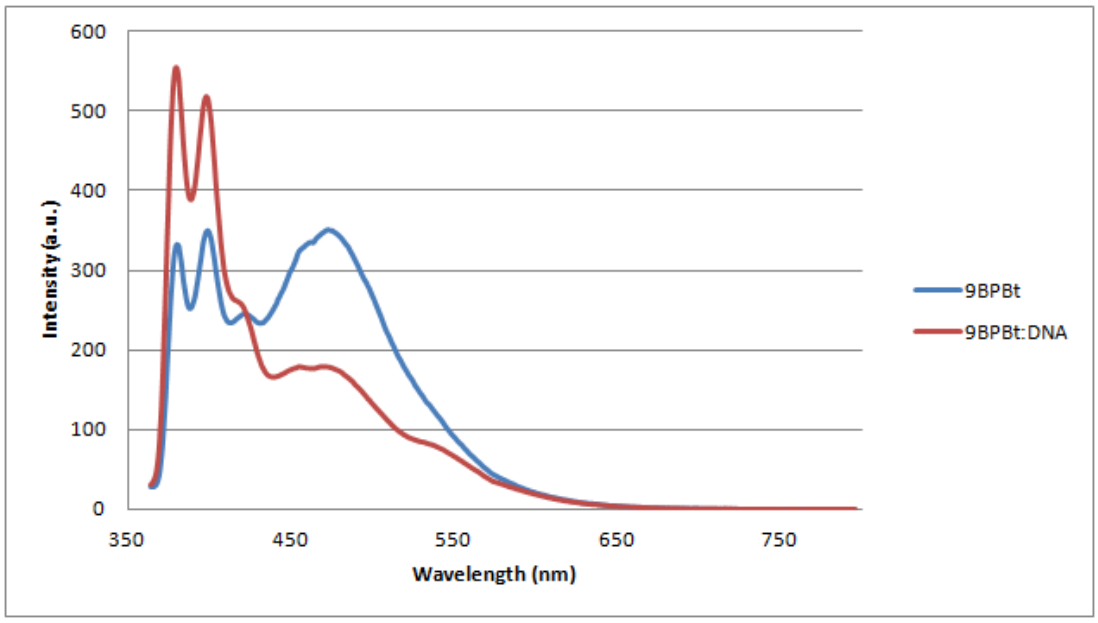

Figure A36 The fluorescence spectra of **9BPBt** in the absence and presence of DNA target in 10 mM phosphate buffer pH 7.0, [PNA] = 1.0 μM and [DNA] = 1.2 μM, λ_{excit} = 350 nm.

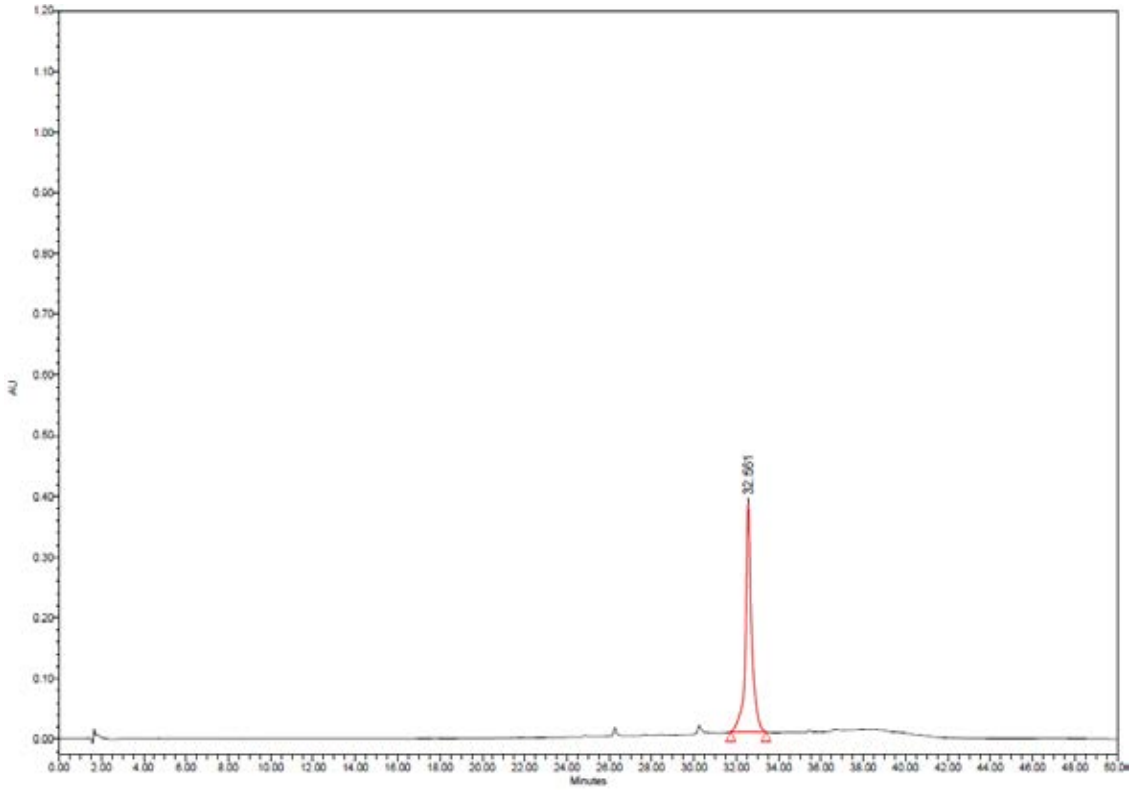

(a)

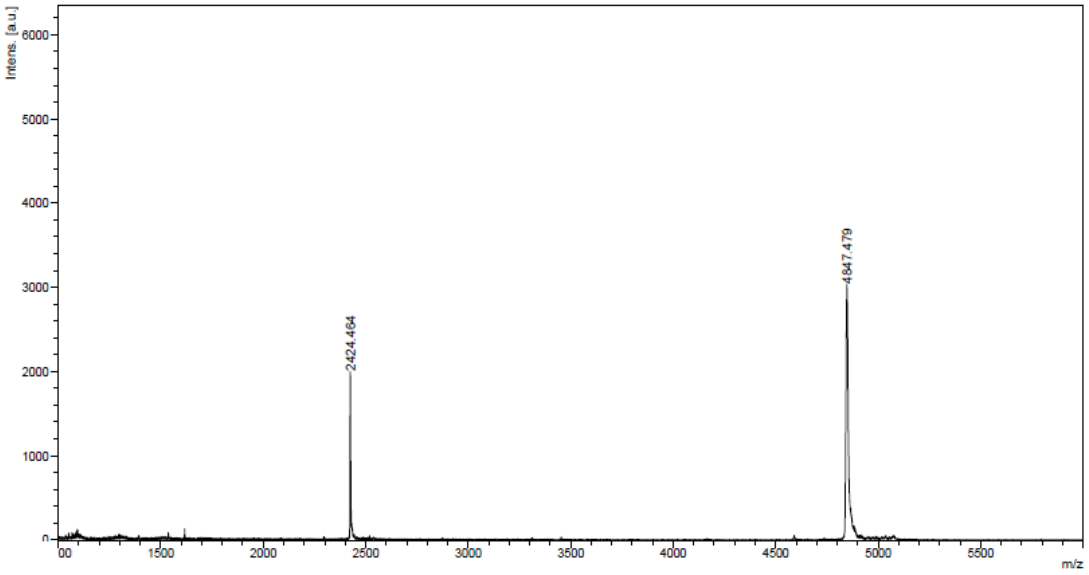

(b)

Figure A37 (a) Analytical HPLC chromatogram and (b) MALDI-TOF mass spectrum of **MBS1** (calcd for $[M+H]^+ = 4845.37$)

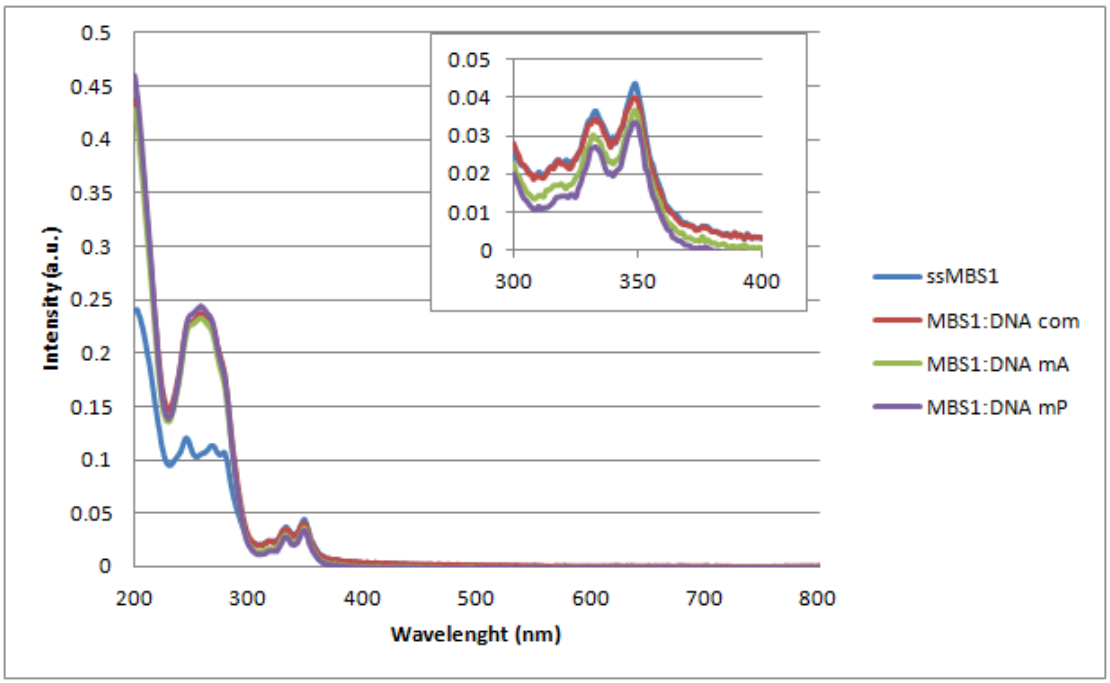

Figure A38 UV-Vis spectra of **MBS1** in the absence and presence of DNA target in 10 mM phosphate buffer pH 7.0, [PNA] = 1.0 μM and [DNA] = 1.2 μM, λ_{excit} = 350 nm.

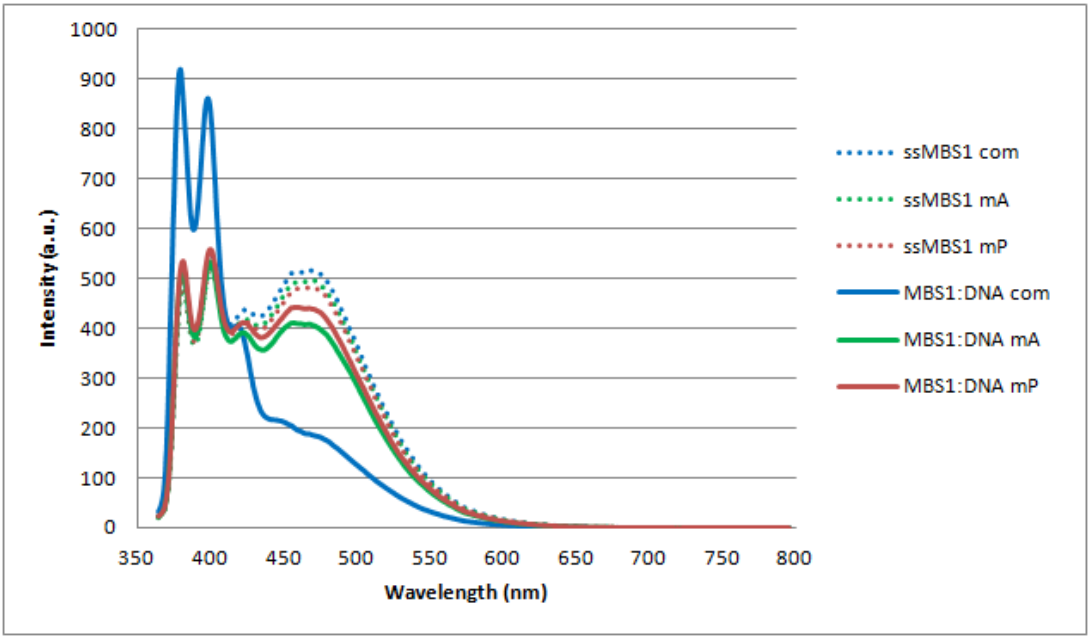

Figure A39 The fluorescence spectra of **MBS1** in the absence and presence of complementary and mismatched DNA targets in 10 mM phosphate buffer pH 7.0, [PNA] = 1.0 μM and [DNA] = 1.2 μM, λ_{excit} = 350 nm.

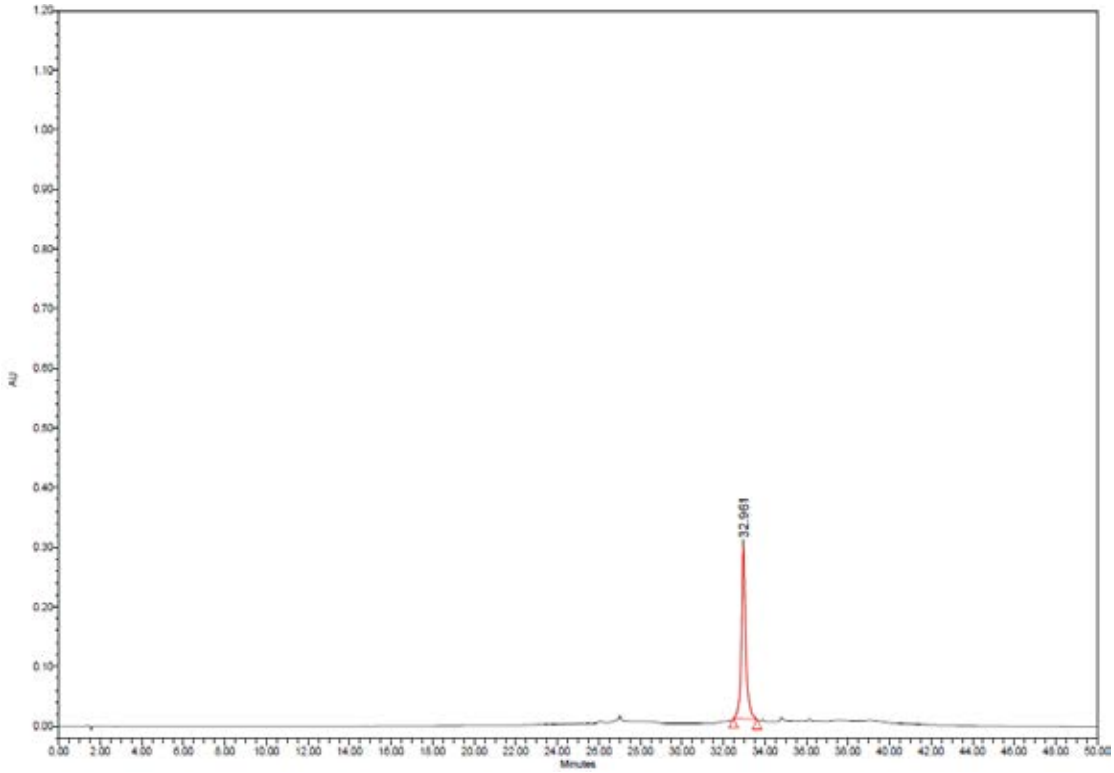

(a)

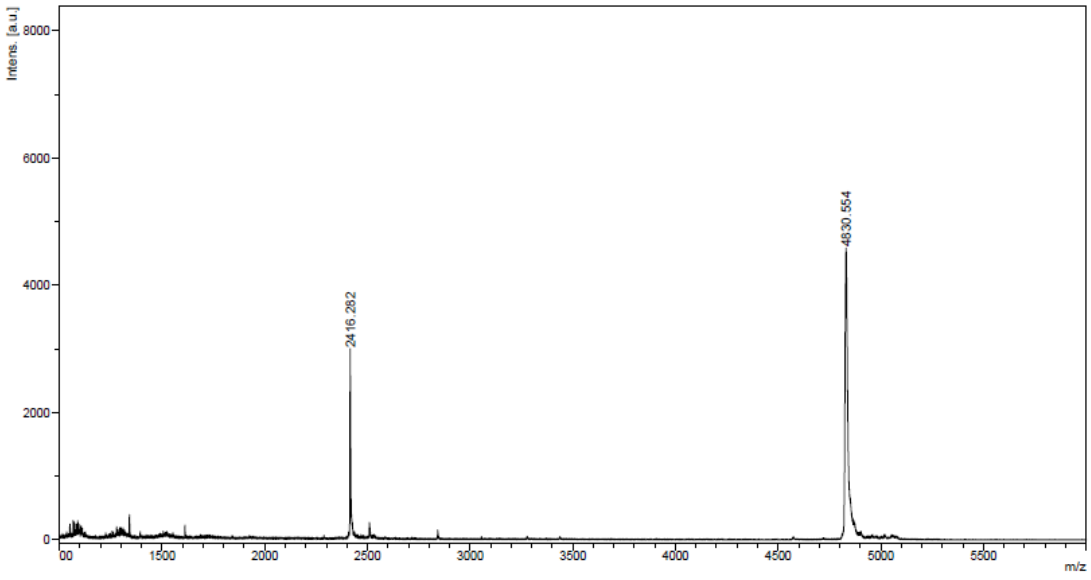

(b)

Figure A40 (a) Analytical HPLC chromatogram and (b) MALDI-TOF mass spectrum of **MBS2** (calcd for $[M+H]^+$ = 4827.34)

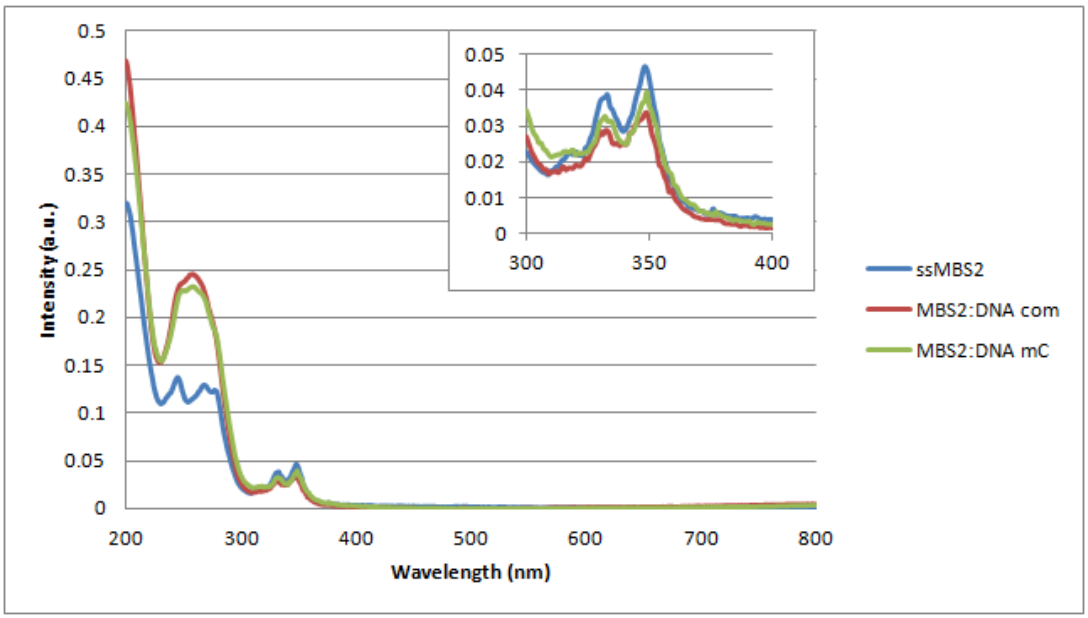

Figure A41 UV-Vis spectra of **MBS2** in the absence and presence of DNA target in 10 mM phosphate buffer pH 7.0, [PNA] = 1.0 μM and [DNA] = 1.2 μM, λ_{excit} = 350 nm.

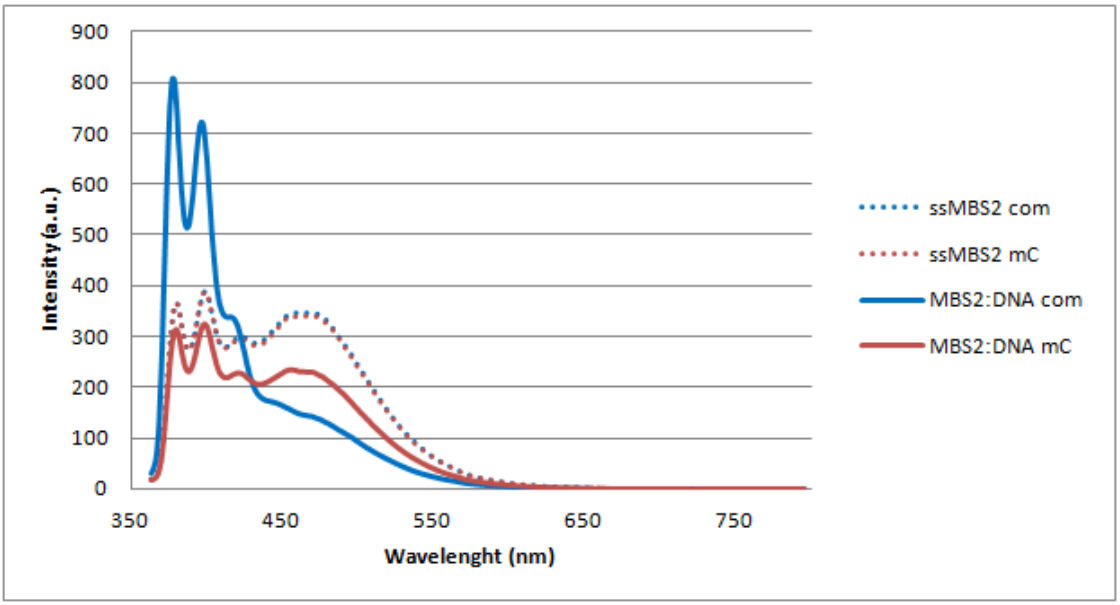

Figure A42 The fluorescence spectra of **MBS2** in the absence and presence of complementary and mismatched DNA targets in 10 mM phosphate buffer pH 7.0, [PNA] = 1.0 μM and [DNA] = 1.2 μM, λ_{excit} = 350 nm.

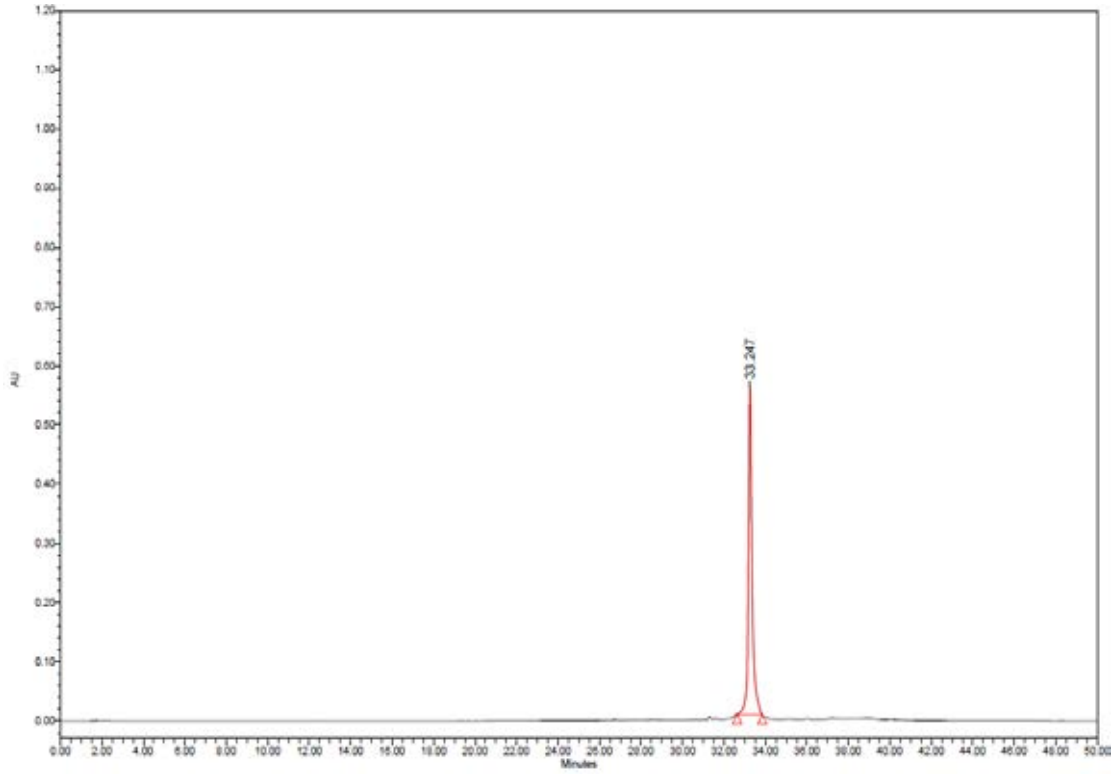

(a)

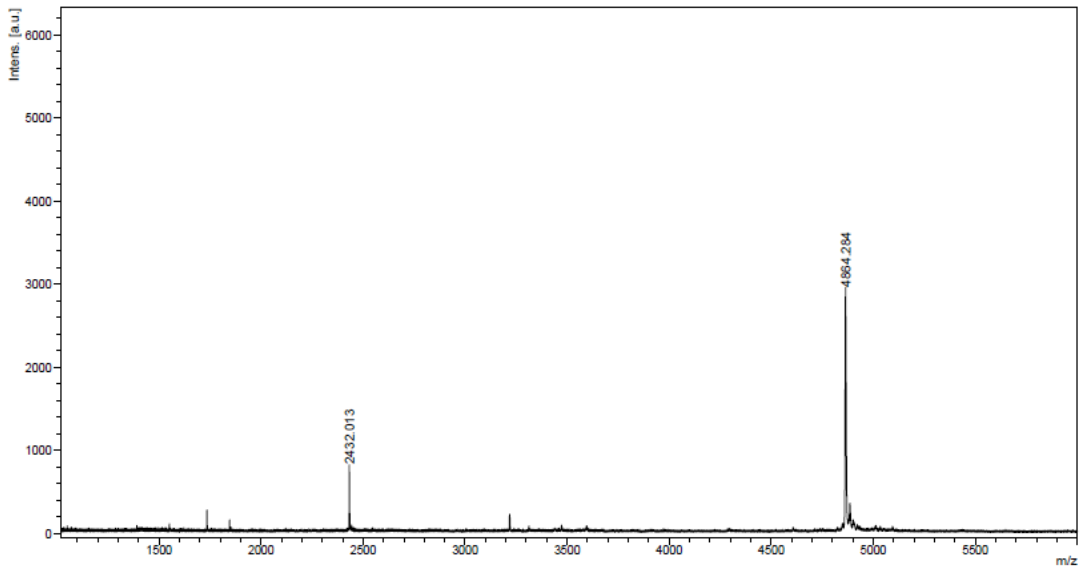

(b)

Figure A43 (a) Analytical HPLC chromatogram and (b) MALDI-TOF mass spectrum of **MBS3** (calcd for $[M+H]^+$ = 4865.39)

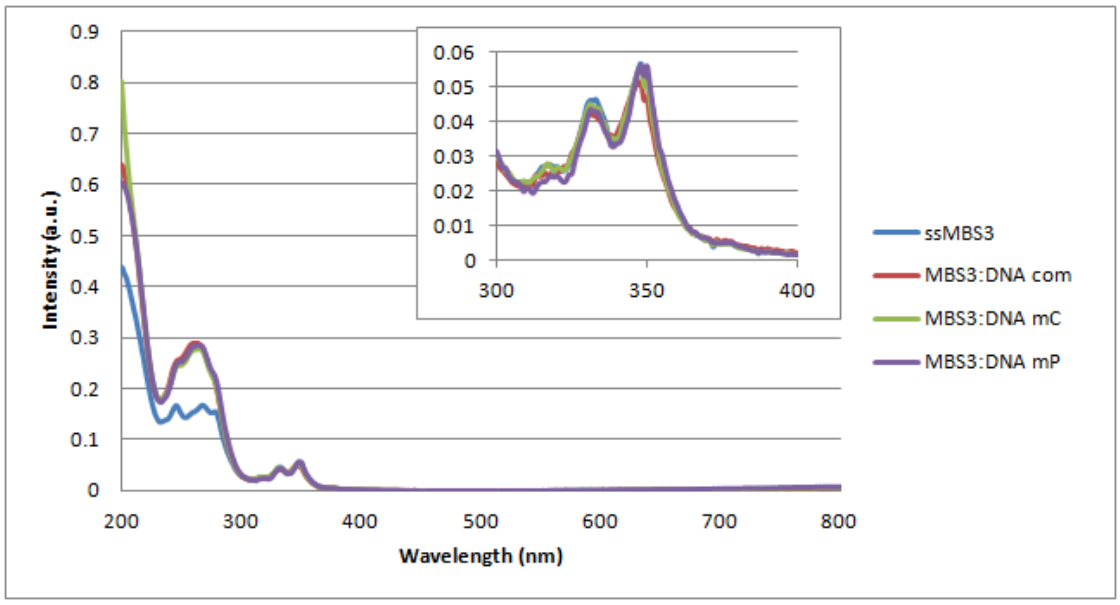

Figure A44 UV-Vis spectra of **MBS3** in the absence and presence of DNA target in 10 mM phosphate buffer pH 7.0, [PNA] = 1.0 μM and [DNA] = 1.2 μM, λ_{excit} = 350 nm.

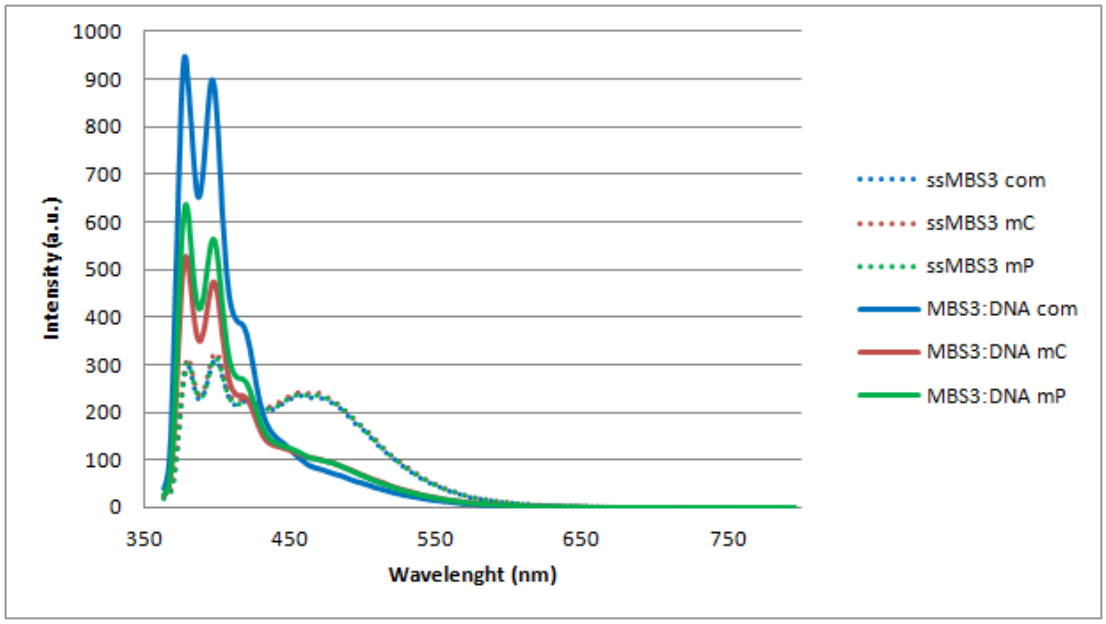

Figure A45 The fluorescence spectra of **MBS3** in the absence and presence of complementary and mismatched DNA targets in 10 mM phosphate buffer pH 7.0, [PNA] = 1.0 μM and [DNA] = 1.2 μM, λ_{excit} = 350 nm.

VITAE

Mr. Nattapon Maneelun was born on February 26th, 1988 in Nakornphanom, Thailand. He graduated Bachelor's Degree of Science, major in Chemistry from Faculty of Science, KhonKaen University, in 2009. He began studying his Master's degree at the Department of Chemistry, Facalty of Science, Chulalongkorn University in academic year of 2010.

His present address is 33 Moo 13, Tambon Thatphanom, Amphoe Thatphanom, Nakornphanom, Thailand, 48110, e – mail : maneelun_n@hotmail.com.

Awards and Experiences

2005 - Bronze medal from the 1st Chemistry Olypiad at Srinakharinwirot University.

2006-present - Received Development and Promotion of Science and Technology Talents Project (DPST) grant.

2010 - Poster and oral presentation in the 5th Congress on Science and Technology of Thailand for Youth.

2011 - Poster presentation in the 37th Congress on Science and Technology of Thailand (STT37).

- Poster presentation in Thailand research fund (RTA5280002) at Naresuan University.

2012 - Internship program at Pohang University of Science and Technology (POSTECH), South Korea, in the topic "Study for Nucleic Acid Recognition System" under supervision of Prof. Dr. Byeang Hyean Kim.

2013 - Poster and oral presentation in the 8th Congress on Science and Technology of Thailand for Youth.